The Development and Characterization of Epoxy-Silicone Blends as a Matrix for Antistatic Composites

Bc. Marek Jurča

Master's thesis
2017

Tomas Bata University in Zlín
Faculty of Technology

Univerzita Tomáše Bati ve Zlíně
Fakulta technologická
Ústav inženýrství polymerů
akademický rok: 2016/2017

ZADÁNÍ DIPLOMOVÉ PRÁCE
(PROJEKTU, UMĚLECKÉHO DÍLA, UMĚLECKÉHO VÝKONU)

Jméno a příjmení:	**Bc. Marek Jurča**
Osobní číslo:	**T15259**
Studijní program:	**N2808 Chemie a technologie materiálů**
Studijní obor:	**Inženýrství polymerů**
Forma studia:	**prezenční**
Téma práce:	**Vývoj a charakterizace epoxid-silikonové směsi jako matrice pro antistatické kompozity**

Zásady pro vypracování:

Vypracujte rešerši na zadané téma.
Připravte vzorky epoxid-silikonových směsí
Proveďte jejich analýzu pomocí DMA, DSC, SEM, reometru.
Optimalizovanou směs použijte jako matrici pro přípravu elektrovodivých kompozitů.
Proveďte měření elektrické vodivost a dielektrických parametrů kompozitů.
Dosažené výsledky graficky vyhodnoťte a proveďte závěr.

Rozsah diplomové práce:

Rozsah příloh:

Forma zpracování diplomové práce: **tištěná/elektronická**

Seznam odborné literatury:

Polymer Blends Handbook – L. A. Utracki
Epoxy Polymers: New Materials and Innovations – J.-P. Pascault, R. J. J. Williams
Cure kinetics, morphology and miscibility of modified DGEBA-based epoxy resin Effects of a liquid rubber inclusion – R. Thomas

Vedoucí diplomové práce: **doc. Ing. Jarmila Vilčáková, Ph.D.**
Centrum polymerních materiálů

Datum zadání diplomové práce: **2. ledna 2017**

Termín odevzdání diplomové práce: **10. května 2017**

Ve Zlíně dne 1. března 2017

L.S.

doc. Ing. František Buňka, Ph.D.
děkan

doc. Ing. Tomáš Sedláček, Ph.D.
ředitel ústavu

Příjmení a jméno: JURCA MAREK Obor: IP

PROHLÁŠENÍ

Prohlašuji, že

- beru na vědomí, že odevzdáním diplomové/bakalářské práce souhlasím se zveřejněním své práce podle zákona č. 111/1998 Sb. o vysokých školách a o změně a doplnění dalších zákonů (zákon o vysokých školách), ve znění pozdějších právních předpisů, bez ohledu na výsledek obhajoby [1];
- beru na vědomí, že diplomová/bakalářská práce bude uložena v elektronické podobě v univerzitním informačním systému dostupná k nahlédnutí, že jeden výtisk diplomové/bakalářské práce bude uložen na příslušném ústavu Fakulty technologické UTB ve Zlíně a jeden výtisk bude uložen u vedoucího práce;
- byl/a jsem seznámen/a s tím, že na moji diplomovou/bakalářskou práci se plně vztahuje zákon č. 121/2000 Sb. o právu autorském, o právech souvisejících s právem autorským a o změně některých zákonů (autorský zákon) ve znění pozdějších právních předpisů, zejm. § 35 odst. 3 [2];
- beru na vědomí, že podle § 60 [3] odst. 1 autorského zákona má UTB ve Zlíně právo na uzavření licenční smlouvy o užití školního díla v rozsahu § 12 odst. 4 autorského zákona;
- beru na vědomí, že podle § 60 [3] odst. 2 a 3 mohu užít své dílo – diplomovou/bakalářskou práci nebo poskytnout licenci k jejímu využití jen s předchozím písemným souhlasem Univerzity Tomáše Bati ve Zlíně, která je oprávněna v takovém případě ode mne požadovat přiměřený příspěvek na úhradu nákladů, které byly Univerzitou Tomáše Bati ve Zlíně na vytvoření díla vynaloženy (až do jejich skutečné výše);
- beru na vědomí, že pokud bylo k vypracování diplomové/bakalářské práce využito softwaru poskytnutého Univerzitou Tomáše Bati ve Zlíně nebo jinými subjekty pouze ke studijním a výzkumným účelům (tedy pouze k nekomerčnímu využití), nelze výsledky diplomové/bakalářské práce využít ke komerčním účelům;
- beru na vědomí, že pokud je výstupem diplomové/bakalářské práce jakýkoliv softwarový produkt, považují se za součást práce rovněž i zdrojové kódy, popř. soubory, ze kterých se projekt skládá. Neodevzdání této součásti může být důvodem k neobhájení práce.

Ve Zlíně 15.4.2017 .....

---

[1] zákon č. 111/1998 Sb. o vysokých školách a o změně a doplnění dalších zákonů (zákon o vysokých školách), ve znění pozdějších právních předpisů, § 47 Zveřejňování závěrečných prací:

(1) Vysoká škola nevýdělečně zveřejňuje disertační, diplomové, bakalářské a rigorózní práce, u kterých proběhla obhajoba, včetně posudků oponentů a výsledku obhajoby prostřednictvím databáze kvalifikačních prací, kterou spravuje. Způsob zveřejnění stanoví vnitřní předpis vysoké školy.

(2) Disertační, diplomové, bakalářské a rigorózní práce odevzdané uchazečem k obhajobě musí být též nejméně pět pracovních dnů před konáním obhajoby zveřejněny k nahlížení veřejnosti v místě určeném vnitřním předpisem vysoké školy nebo není-li tak určeno, v místě pracoviště vysoké školy, kde se má konat obhajoba práce. Každý si může ze zveřejněné práce pořizovat na své náklady výpisy, opisy nebo rozmnoženiny.

(3) Platí, že odevzdáním práce autor souhlasí se zveřejněním své práce podle tohoto zákona, bez ohledu na výsledek obhajoby.

[2] zákon č. 121/2000 Sb. o právu autorském, o právech souvisejících s právem autorským a o změně některých zákonů (autorský zákon) ve znění pozdějších právních předpisů, § 35 odst. 3:

(3) Do práva autorského také nezasahuje škola nebo školské či vzdělávací zařízení, užije-li nikoli za účelem přímého nebo nepřímého hospodářského nebo obchodního prospěchu k výuce nebo k vlastní potřebě dílo vytvořené žákem nebo studentem ke splnění školních nebo studijních povinností vyplývajících z jeho právního vztahu ke škole nebo školskému či vzdělávacího zařízení (školní dílo).

[3)] zákon č. 121/2000 Sb. o právu autorském, o právech souvisejících s právem autorským a o změně některých zákonů (autorský zákon) ve znění pozdějších právních předpisů, § 60 Školní dílo:

(1) Škola nebo školské či vzdělávací zařízení mají za obvyklých podmínek právo na uzavření licenční smlouvy o užití školního díla (§ 35 odst. 3). Odpírá-li autor takového díla udělit svolení bez vážného důvodu, mohou se tyto osoby domáhat nahrazení chybějícího projevu jeho vůle u soudu. Ustanovení § 35 odst. 3 zůstává nedotčeno.

(2) Není-li sjednáno jinak, může autor školního díla své dílo užít či poskytnout jinému licenci, není-li to v rozporu s oprávněnými zájmy školy nebo školského či vzdělávacího zařízení.

(3) Škola nebo školské či vzdělávací zařízení jsou oprávněny požadovat, aby jim autor školního díla z výdělku jím dosaženého v souvislosti s užitím díla či poskytnutím licence podle odstavce 2 přiměřeně přispěl na úhradu nákladů, které na vytvoření díla vynaložily, a to podle okolností až do jejich skutečné výše; přitom se přihlédne k výši výdělku dosaženého školou nebo školským či vzdělávacím zařízením z užití školního díla podle odstavce 1.

ABSTRAKT

Tato diplomová práce se zabývá modifikací epoxidové pryskyřice (ER) na bázi diglycidyl etheru bisfenolu A (DGEBA) polydimethylsiloxanem (PDMS). Epoxidový monomer byl vytvrzen diethylentriaminem (DETA) v přítomnosti dikumylperoxidu (DCP), který byl použit jako síťovadlo pro PDMS. Přidáním PDMS do ER vzniká fázově oddělená struktura tvořená elastomerními doménami dispergovanými v epoxidové fázi. Polymerní směsi byly studovány pomocí DMA, DSC, reologické analýzy, Charpyho rázového testu a rastrovací elektronové mikroskopie. DMA data a dosažená hodnota rázové pevnosti pro vzorky s PDMS (10 hm.%) za přítomnosti DCP (2 hm.%) v ER ukazují na nejvyšší mezifázovou kompatibilitu mezi PDMS a ER. Byly připraveny kompozity na bázi směsí ER/PDMS plněné vodivými plnivy (karbonylové železo a nikl). Dielektrická spektroskopie a měření elektrické vodivosti prokázalo významnou závislost elektrických vlastností těchto systémů jak na složení směsí tak typu a koncentraci plniv. Perkolačního prahu bylo dosaženo při 5 obj.% částic niklu (o průměru 3 μm) v polymerním kompozitu.

Klíčová slova: epoxidová pryskyřice, polymerní směs, houževnatost, elektrická vodivost

ABSTRACT

This diploma work deals with the modification of epoxy resin (ER) based on diglycidyl ether bisfenol A (DGEBA) by polydimethylsiloxane (PDMS). The epoxy monomer was cured with diethylentriamine (DETA) as a hardener in the presence of dicumyl peroxide (DCP) as a crosslinking agent of PDMS. The addition of PDMS to ER gives rise to a phase-separated structure consisting of elastomer domains dispersed in the epoxy phase. Methods as DMA, DSC, reological analysis, Charpy impact test and SEM were used for study of polymer blends. The DMA data and achieved value of impact strength for the samples with PDMS (10 wt.%) in the presence of DCP (2 wt.%) in ER indicate the highest interfacial compatibility between PDMS and ER. Composites on the basis of ER/PDMS blends filled with conductive filler (carbonyl iron and nickel) were prepared. Dielectric spectroscopy and electrical conductivity measurement have shown significant dependence of composites' electrical properties on both composition of blends as well as the type and concentration of fillers. Percolation threshold was reached at 5 vol.% for nickel particles (diameter 3 μm) in polymer composite.

Keywords: epoxy resin, polymer blend, toughness, electrical conductivity

ACKNOWLEDGEMENTS

I would like to thank my supervisor, assoc. prof. Jarmila Vilčáková, for guidance, support, and encouragement during the work on my master's thesis. My thanks also belong to assoc. prof. Natalia Kazantseva for proofreading.

Motto:

„Žijeme silou ducha, vše ostatní propadne smrti.“

Tycho Brahe

I hereby declare that the print version of my Master's thesis and the electronic version of my thesis deposited in the IS/STAG system are identical.

CONTENTS

INTRODUCTION

Polymers belong to the most widely used materials nowadays and their volume production overcomes traditional materials such as metal or glass. However, despite the large variability of offered polymers only a fraction of them have sufficient properties to meet our needs. Most of polymers require the use of additives to improve the mechanical, optical, aesthetic properties as well as resistance, durability and processability. The widely used additives include dyes, antioxidants, stabilizers, plasticizers and others. However, there are two separate categories of additives which have a completely dominant influence and are referred to by specific names. The first category is the addition of a polymer to other polymer, where the mixture is called a blend. The second category is called a polymer composite, where in a polymer matrix an inorganic filler (as carbon fibre, carbon black, glass fibre or metal particle) is dispersed. Both groups, blends and composites are widely used and therefore belong to very common objects of research.

Epoxy resins have unique properties, such as high strength, chemical and solvent resistance with very good adhesion not only to metal. Therefore they are very popular as a matrix for preparation of polymer composite materials and adhesives. However, their disadvantage is brittleness. Therefore, epoxy resins are often blended with rubbers. The addition of rubber, although resulting in reduction of strength and hardness, significantly improves the toughness of the blends. However, it is important to note that for the overall performance of the mixture compatibility between the epoxy resin and rubber is important. Without sufficient compatibility rubber will behave as an impurity, which will only lead to reduction in mechanical properties. In the case that the compatibility between polymers is small, additives called compatibilizers are used in order to increase the interaction between the two polymers and thereby improve toughness.

Polymers are known as dielectrics, what is very useful for applications such as cable coating, electrical devices, power switches, etc. However, the drawback of dielectrics is the ability to concentrate static electrical charge. It means that material allows the accumulation of electrostatic charge to up to 40 kV which might be destructive for some sensitive electronic devices. The other problem is the risk of spark during the discharge which might cause the ignition of flammable gases or liquids in industrial buildings or fuel tanks. In this case, it is necessary to increase the conductivity of polymers by incorporation of conductive fillers to prevent increase of charge to danger voltage levels. These materials are called electrical

discharged materials or also antistatic materials. In current work we introduce methodology that can significantly influence the electrical percolation threshold and simultaneously modify the brittle behaviour of epoxy resin by polydimethylsiloxane as well as develop conductive composites with two types of filler (carbonyl iron and carbonyl nickel).

I. THEORY

1 MATERIALS

1.1 Epoxy resin

Epoxy resins (ER) belong to group of thermosetting polymer cured by addition reaction. Typical for their monomers is epoxide function group. This group is quite reactive and can react with every compound containing a reactive hydrogen. Therefore in principal curing agents can be: amines, amides, imides, oximes, alcohols, phenols, acids, anhydrides, thiols. However, amines and anhydrides are usually used in practice.

The production of epoxy resin started in 1940s and it is still increasing. ER have tuneable properties because of the high variability of monomers. Both epoxy and hardener can contain aliphatic or aromatic as well as polar or nonpolar groups varying thermal and mechanical behaviour and chemical resistance of final product. However, all ER exhibit some common properties which make them unique among other thermoset resins. Firstly, cure shrinkage is low and therefore after curing low residual stress remain in product. Secondly, adjustable curing temperature and rate of reaction using different hardeners. And lastly, there is no need of solvents or other volatile substances. However, the drawback of ER is higher price in comparison with other thermosets [1].

1.1.1 Diglycidyl ether bisphenol A

Although there are hundreds of possible epoxides, the most 2 common epoxides are diglycidyl ether bispenol A (DGEBA) and novolac epoxy resin. Aliphatic epoxides are also produced in sizeable quantity, but they are usually used only as a modifiers. Novolac ER are based on phenol formaldehyde oligomers with additional epoxy group. Depending on molecular weight they behave as viscous liquids or solids. There is one epoxy group on each phenol unit providing high speed of curing. However, the system can be easily overheated and the product can be damaged. Therefore it is safer and easier to use DGEBA. Manufacturing of it is relatively simple and inexpensive and properties are decent. Two precursors are needed, bisphenol A which is synthesized from acetone and phenol catalysed by acids, and epichlorohydrin which is manufactured in two steps from allyl chloride by addition of hydrochlorous acid and elimination of hydrochloric acid. Those precursors are mixed in ratio 2:1 to form DGEBA. If the ratio of bisphenol A to epichlorohydrin is higher (up to 1:1), linear oligoethers are formed. Number of epoxy groups per molecule will stay two, but new hydroxyl groups which may undergo the cross-linking reactions will be formed

too. Epoxide oligomers are useful for industry because bigger molecules leads to shorter curing times.

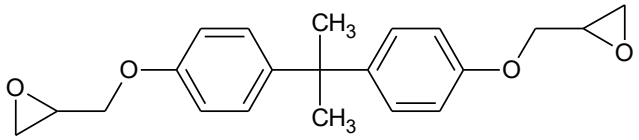

Scheme 1: Epoxy resin - DGEBA

Usually different curing agents are used for adjusting properties rather than different epoxides. Two basic systems are commercially available, i.e. amines and anhydrides. Generally, anhydrides have higher thermal resistance. On the other side, amines are cheaper and faster to process and do not need to use accelerators. They can be divided into 3 groups, i.e. aliphatic, cycloaliphatic and aromatic. Aliphatic amines are very reactive and they can be used at room temperature while aromatic amines need higher curing temperature or accelerators. Nevertheless, they provide higher stiffness and hardness as well as chemical and thermal resistance on the same or higher level as anhydrides. Therefore, aromatic amines were widely used in the past. However, there are health risks connected with their usage as well as problems with processing and higher price, thus are recently replaced with aliphatic and cycloaliphatic amines. If temperature of usage is not higher than 100 °C and demands on the mechanical properties are not very high, it is convenient to use cheaper aliphatic instead of cycloaliphatic amines [1].

1.1.2 Diethylenetriamine

Diethylenetriamine (DETA) is one of the commonly used aliphatic hardeners. This hardener is easy to process because of low viscosity and starts to react at room temperature. ER cured by DETA is not so stiff and hard but is more flexible compared to ER cured by other amine hardeners. The main drawback of amine hardeners is hygroscopicity.

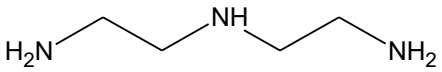

Scheme 2: Curing agent - DETA

ER are known for their excellent mechanical properties such as high strength and toughness. They are also very good adhesives and chemically are stable. On the other side, weak point is their price which is higher in comparison with other resins. Therefore they are predestined as a matrix for top composites and for low-amount application. Epoxide composites can be found in sport equipment, wind turbines [2], airplanes and ultralights, etc. The other common

applications of ER are universal glues and anticorrosive coatings not only in automotive [2]. ER have very good insulating properties and therefore they are widely used in electronics. Typical usages are components of electric circuits, LEDs or smartphones as well as solar panels and other devices [1].

1.2 Polydimethylsiloxane

Polydimethylsiloxane (PDMS) belongs to a class of polysiloxanes. The polysiloxanes are the oldest known group of organosilicon polymers, which are polymers where some carbon atoms are substituted with silicon. Although polysioxanes are the technically most important and widely used silicon-based polymers, several other classes exist, e.g. polysilazanes, polysilanes, polycarbosilanes. However, polysiloxanes will likely remain its primary position between organosilicon polymers in the future, because of their relatively low price, decent mechanical and heat resistance properties.

Each polymer material is as weak as its weakest bond is strong. At polymers is considered the strength of the bonds in the main chain as it can be found in tables that the strongest bond possibly forming polymer chain is Si-O (C-F is stronger but cannot form a polymer chain) with bond enthalpy 368 kJ/mol. Therefore, the thermal stability of siloxanes is high. On the other side, the Si-O has also very high conformational flexibility which leads to very low glass transition temperatures. The other advantages of polysiloxanes are uniform mechanical properties over a wide temperature range, chemical stability and low friction. The polysiloxane properties can be easily modified by usage of different side groups. The effect of short alkanes like methyl or ethyl, benzene rings and perfluorated alkanes on temperature dependent properties and chemical resistance of polysiloxane are different [3].

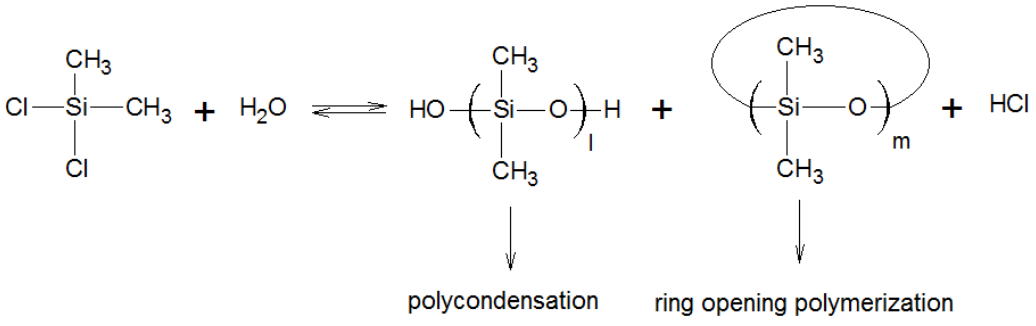

Scheme 3: Synthesis of PDMS prepolymers

PDMS is synthesized in 2 steps from dimethyldichlorosilane and water (Scheme 3) which is exothermic reaction. The products of reaction strongly depends on the synthesis conditions and used catalyst. Moreover it is also reversible, therefore only oligomers can be obtained. Hydroxyl ended dimethylsiloxane oligomers than undergo polycondensation reaction in oil-in-water emulsion stabilised by sulfonic acid surfactants. By those process can be obtained polymers with $M_n = 10^6$.

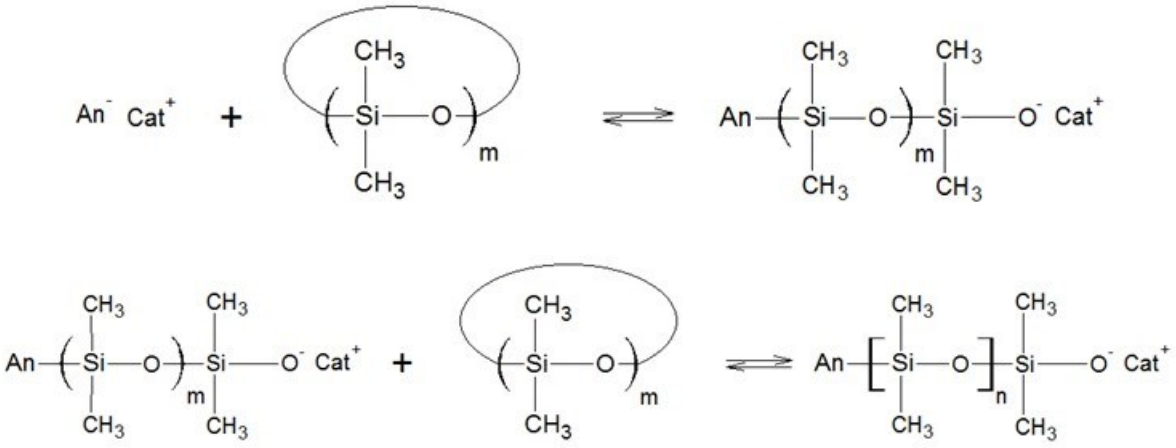

Scheme 4: Ring opening polymerization of PDMS

On the other side, the ring opening polymerization, usually anionic catalyzed, provides much better control of the process enabling control of PDI (Scheme 4). Commonly used monomers are octamethylcyclotetrasiloxane and hexamethylcyclotrisiloxane. As the base can be also used oligosiloxanolate providing preparation of telechelic polymers.

Utilization of the siloxane polymers is very broad. Low molecular weight polymers can be used as surfactants, antifoaming agents or lubricants and oils depending on side groups and size of molecules. Higher molecular weights with reactive groups can be used as glues or sealants with low stiffness but high thermal and chemical stability and good tenacity. Siloxane elastomers can be also used for good thermal and chemical stability in rubber industry for tubes or o-rings in automotive or for household goods. Moreover, polysiloxanes are nontoxic and biocompatible and therefore they are highly used in medicine for syringe pistons, respiratory masks, implantable chambers, etc. As a minor component they may also appear in the cosmetics or food processing industry as an ingredient of oils. PDMS is also used in soft lithography for stamps in micro or nanometer scale [3]. Another extraordinary potential field of use may be biomedical micro/nano sensors [4] or selective membranes [5].

1.3 Peroxides

Dicumyl peroxide (DCP) belongs to a class of organic peroxides which are compounds containing oxygen – oxygen bond. Those compounds are not very stable and can be easily decomposed to free radicals (Scheme 5).

Scheme 5: Decomposition of peroxide

The dissociation energy for homolytic dissociation can be acquired from heat or electromagnetic radiation (UV). It can be also catalysed by ions of metals (Fe^{2+}, Cu^{+}) at room temperature. Therefore lots of peroxides is unstable and only rarely can be any found in nature. However, they are very useful in many chemical synthesis and processes and people accomplished to find some stable structures which can be kept for long time in controlled environment. Also by varying R^1, R^2 is possible to adjust decomposition temperature (50–250 °C) and rate for needed application.

One of the most important fields of peroxide usage is polymer processing. Free radicals are used for polymerization, cross-linking of rubber (and some thermoplastic) and interfacial grafting of polymer blends. All vinyl polymers are synthesized via chain growth polymerisation. It can be done via ionic or coordination polymerisations which are developed and very selective. Free radical polymerization is still very often used due to low price, simplicity and low requirements for purity of monomer. Free radicals can be produced by azo compounds or more often by peroxides. Most of rubbers are vulcanized by sulphur (or sulphur containing compounds), however, some rubbers do not have double bonds essential for reaction with sulphur. Those rubbers have to be cross-linked by peroxides. And lastly, lots of immiscible polymers have low adhesion in interphase. This problem can be solved by introducing graft copolymer or organosilane, by addition of reactive group to one or both polymers, or interfacial grafting. Last method requires usage of free radicals which create graft copolymers during the blending [6].

1.3.1 Dicumyl peroxide

DCP is synthesized from dimethylbenzyl hydroperoxide with dimethyl phenyl carbinol catalysed by phosphorus halide (Scheme 6) [7].

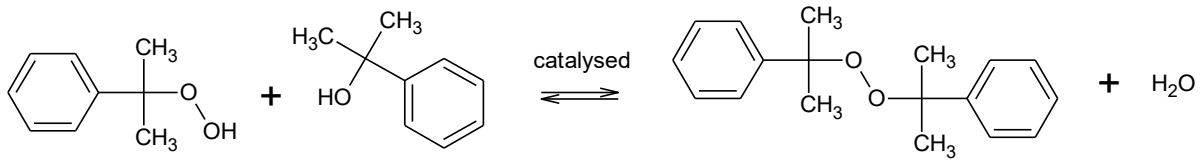

Scheme 6: Synthesis of DCP

The decomposition temperature of DCP is above 110 °C with half-life 1 hour at 135 °C [8]. Therefore, belongs to peroxides with a moderate decomposition temperature, suitable e.g. for interfacial grafting of polyethylene blends [9] or for cross-linking of PDMS [10].

1.4 Electroconductive fillers

1.4.1 Carbonyl iron

Carbonyl iron (CI) are highly pure spherical iron particles (±98 % Fe). CI is produced by thermal decomposition of iron pentacarbonyl ($Fe(CO)_5$). There are two grades of CI: "hard" grades and "soft" grades. *Hard grades* are primary products of thermal decomposition without any further chemical purification. They are typically mechanically hard with onion like (multi-layer) structure. On the other side, *soft grades* are annealed in hydrogen atmosphere after thermal decomposition. This process leads to higher purity of particles and transformation from onion-like to polycrystalline structure. Used type of CI in this work was soft grade SL from company BASF with diameter d_{50} = 9 μm. [11][12]

CI is relatively inexpensive easily processed filler. Important benefit is the possibility to prepare particles with different size, microstructure, composition and electromagnetic properties by varying the preparation process [12][13].

1.4.2 Nickel particles

Nickel powders (Ni) are highly pure hedgehog-like nickel particles (99,99 % Ni). Ni particles are similarly as carbonyl iron produced by thermal decomposition of nickel tetracarbonyl ($Ni(CO)_4$). Due to three-dimensional hedgehog-like exterior structure of Ni, polymer composites filled with hedgehog-like nickel particles exhibit low percolation

threshold which effectively means that lower amount of filler can be used and polymer composites with Ni are lighter. Besides other application, Ni is used as a filler for shielded polymeric materials [14][15].

2 POLYMER BLENDS

Although polymers are highly variable there are always new requirements that cannot be met using only one polymer. These requirements can include mechanical, optical and safety requirements as well as requirements for durability and price. From this reason polymers are often blended together to balance properties. This mixture of polymers is called blend. However, it was found that most of the polymers are not miscible even if their monomers are miscible. Many theories were developed to explain this phenomenon. Among the most important are Flory-Huggins and Flory equation of state theory. Flory-Huggins theory is a mathematical model calculating Gibbs free energy of mixing from heat of mixing and entropy. Although for many polymer systems gives good predictions of miscibility it cannot explain the lower critical solution temperature (LCST) which can be explained only by equation of state theory [16].

2.1 Flory-Huggins theory

Flory-Huggins theory as a thermodynamic process is derived directly from Gibbs free energy:

$$\Delta G_m = \Delta H_m - T\Delta S_m \quad (1)$$

where ΔG_m is change of the Gibbs energy of mixing, ΔH_m is change of the enthalpy of mixing, T is temperature and ΔS_m is change of the entropy of mixing. For miscibility must be satisfied:

$$\Delta G_m < 0 \quad (2)$$

As ΔH_m may be positive, zero or negative and ΔS_m positive small number, to satisfy previous condition the enthalpy must be small enough to be overcome by entropy. Theoretically it was derived for polymer 1 and polymer 2 interaction:

$$\Delta H_m = zN_1 r_1 v_2 \Delta\omega_{12} \quad (3)$$

where z is lattice coordinate number, N is number of macromolecules, r_1 is number of segments in polymer, v_2 is volume fraction and $\Delta\omega_{12}$ is change of internal energy. However it is not easy to use parameters z, r_1 and $\Delta\omega_{12}$ and it is convenient to use only one parameter:

$$\chi_{12} = \frac{zr_1\Delta\omega_{12}}{kT} \quad (4)$$

where χ_{12} is mixing parameter and k is Boltzmann constant. Combining 3 and 4 leads to:

$$\Delta H_m = kT\chi_{12}N_1v_2 \tag{5}$$

The entropy is derived directly from Boltzmann's relation:

$$\Delta S_m = k\ ln\Omega \tag{6}$$

where Ω is number of possible configurations. After a few adjustments and simplifications was derived following equation:

$$\Delta S_m = -\ k\ (N_1\ \ln v_1 + N_2\ \ln v_2) \tag{7}$$

where v is volume fraction. This equation clearly shows that polymer blends have a very low entropy, since the number of macromolecules in the volume is about 3 orders of magnitude lower than for the same volume of solvent. Combining 1, 5 and 7 leads to:

$$\Delta G_m = \ kT(\chi_{12}N_1v_2 + N_1\ \ln v_1 + N_2\ \ln v_2) \tag{8}$$

which is a key equation describing the mixture of both polymer – polymer and polymer – solvent independently derived by Flory and Huggins. Approximate parameter χ_{12} values can be calculated from the equation:

$$\chi_{12} = \beta + \frac{V_1}{RT}(\delta_1 - \delta_2)^2 \tag{9}$$

where V_1 is molar volume, δ is a solubility parameter and β is lattice constant of entropic origin which is a constant which has a value 0,35 for polymer – solvent interaction and 0 for polymer – polymer system. It can be seen that the key to understanding the enthalpy of mixing is just the difference of the solubility parameters, all other variables are just constants or selected quantities and ratios [16].

2.2 Solubility parameter

Also known as the Hildebrand solubility parameter provides a numerical estimate of the degree of interaction between materials. According to definition, it is square root of cohesive energy density:

$$\delta = \sqrt{\frac{\Delta E}{V}} \tag{10}$$

where ΔE is the energy of vaporization to a gas at zero pressure also known as cohesive energy and V is molar volume of the material. The quantity $\frac{\Delta E}{V}$ represents the energy of vaporization per unit volume. Which is not easy to know for polymers, which, due to their weight evaporate. Therefore, to determine solubility parameter for polymers is used swelling

test. The idea is straightforward since solvent with the nearest solubility parameter will swell the polymer. Before the measurement polymer is crosslinked to prevent dissolution and then exposed to various solvents. After sufficient time, the samples are weighed, the swelling coefficient is calculated and plotted against solvent's solubility parameter. Another possibility is to calculate the solubility parameter from knowledge of the chemical structure and the molar volume. This method was developed by Small, van Krevelen and others. The results of these calculations will then differ by less than 5 %, compared with the measured values.

There is a general rule that for solubility of the polymer in a solvent, the difference of solubility parameter should not be greater than 1. For miscibility of polymers is the maximum difference even far lower, due to low entropy of polymers. For the selected system of ER and PDMS are the parameter values 9,7 and 7,3 which predicts mutual immiscibility [16].

2.3 Immiscible polymer blends

When two immiscible polymers are blended together the phase separation will occur. Different morphologies can be reached by varying of volume ratio, viscosity and interactions between polymers. The two most common are dispersed spherical domains of polymer in continuous phase of other polymer (Figure 1A) and cocontinuous phases of both polymers (Figure 1B). [17]

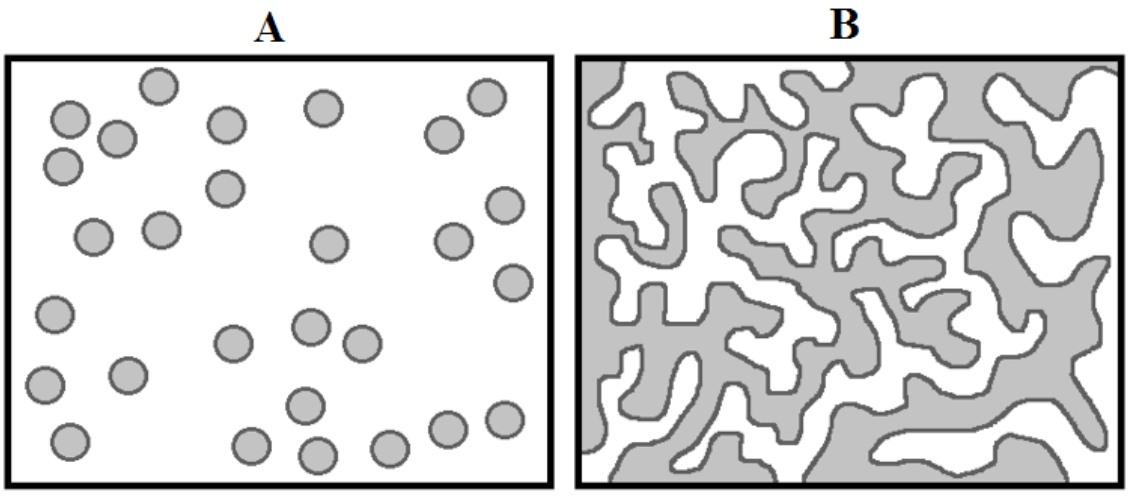

Figure 1: Illustration of morphologies of immiscible blends

Those morphologies can be used for various requirements but for some specialized it may not be enough and more complex morphologies e.g. nano-salami structure [18], gyroid or metastable perforated–lamellar morphology [19] may be demanded. But for all immiscible polymer systems is important the property of polymer – polymer interphase. The name interphase is used for the penetration zone whereas some chains penetrates from polymer A to the polymer B. The depth of penetration can be from a few Å up to a several nm. This area typically has different physical and mechanical properties than the either polymers. Although this zone is very small in comparison with polymer domains, it is crucial for overall performance of the polymer blend. Therefore it is important to have some bonds between the polymers. Usually weak Van der Walls forces does not give sufficient mechanic properties and it is favourable to use hydrogen or even covalent bond if possible. These bonds highly can reinforce interphase and improve material properties. Basically, the better system compatibility, the wider the interphase, the greater the number of bonds between the polymers and the superior mechanical properties. However, it is impossible to determine number of bonds or calculate the compatibility of the system and making and testing tons of samples is very time consuming. The only predictable is surface interphase. The thickness of the surface interphase can be calculated as:

$$S_{th} = \frac{2b}{(6\chi_{12})^{1/2}} \tag{11}$$

where b is statistical segment length.

One last important feature was not mentioned yet the surface tension. The surface tension can be also used for determination of miscibility or compatibility of blends. Simply said, the polymers with similar values of surface tension tend to have higher chance to be miscible or at least compatible.

The cohesive forces between molecules are responsible for surface tension. The molecules in the liquid are in equilibrium because they are equally attracted by other molecules from all sides, but the molecules at the surface do not have all neighbours and therefore it is energetically favourable for liquid to have as small surface as possible. In other words, energy is needed for creating new surface of the liquid:

$$\gamma = \frac{\Delta W}{\Delta A} \tag{12}$$

where γ is surface tension, ΔW is change of energy and ΔA is change of surface. This phenomenon can be also find at solids and is called surface energy. Since polymers are

blended in liquid state is preferably to use the term surface tension. However, it is inconvenient to use surface tension because it is not constant but a function:

$$\gamma = \gamma_D + \gamma_P \tag{13}$$

where γ_D is dispersive part of the surface tension and γ_P is polar part of the surface tension. It is important to know, that good compatibility in polymers not only requires similar surface tension values but also, polar and dispersion parts of surface tension. Surface tension is gaining importance at immiscible systems without any covalent bond between domains [17].

2.4 Epoxy resin – rubber polymer blends

Usage of rubber inclusion into epoxy resin was first proposed by McGarry, Willner and Sultan in the late 1960s and early 1970s. In their work, they used carboxyl-terminated acrylonitrile–butadiene rubber (CTBN) to enhance fracture toughness of DGEBA with negligible losses in thermal and other mechanical properties [20][21]. This was the origin of research of rubber-enhanced epoxy materials [22].

Since 1970s many blends with ER were proposed, for instance: hydroxyl-terminated butadiene rubber [23][24], CTBN [25][26][27], styrene-butadiene rubber [28], acrylic rubber [29], nature rubber [30][31][31], acrylonitrile–butadiene rubber [32], PDMS [33][34], PDMS copolymers [35][36] and also core-shell polysiloxane nanoparticles [37], poly(methyl methacrylate) [38] or methyl methacrylate-butadiene styrene [39] based. However some plastics were also used, for example: high impact polystyrene [40], triblockcopolymer of poly(methyl methacrylate) and poly(butyl acrylate) [41] or hydroxyl terminated poly(ether ether ketone) [42]. The percentage content of rubber/plastic inclusion vary from ones percent [23][43] up to 50 % [29] but commonly 10-20 % is used [26][30][31][37][44].

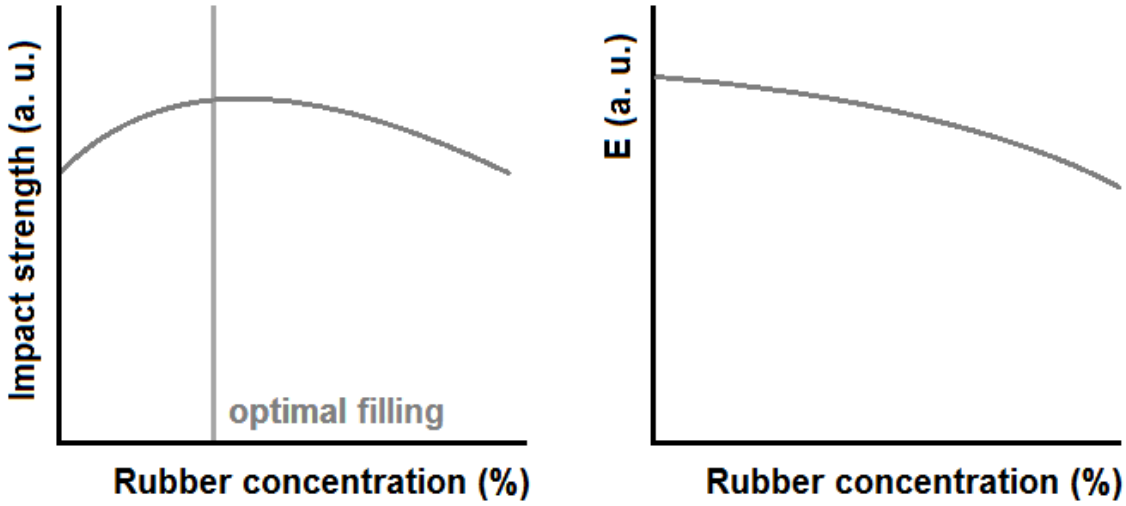

Figure 2: General illustration of rubber addition on mechanical properties of ER

However mechanical properties usually follow the trend (Figure 2), where impact strength as a function of weight/volume percentage has a local maximum and Young modulus is decreasing slightly at low concentrations and significantly at higher concentrations. Therefore optimal content is found [33][35][44]. Increase at impact resistance might be 10 % [44], 80 % [35] and even 110 % [45] depending on types of materials and compatibility between ER and rubber. Considering high initial gap between solubility parameters the only possibility is covalent bond. Some studies apply reactive blending which requires telechelic [30][31][33][46] or side chain groups [47] reacting with epoxy groups. Other common practice is usage of organosilanes [23] and peroxides [45].

3 COMPOSITE MATERIALS WITH A COMPLEX OF ELECTRICAL, MAGNETIC AND ELECTROMAGNETIC PROPERTIES

Most of the polymers are dielectrics which mean that if the electric field is applied they behave as insulators. Every rule has an exception and electroconductive polymers such as polyacetylene, PANI (polyaniline) [48][49], PPy (polypyrrol) [50][51] and PEDOT (poly(3,4-ethylenedioxythiophene)) [52][53] exist and are widely used in practice. However, at some application is needed to use plastics and rubbers with specific electric or electromagnetic properties. For this purpose are used different, usually conductive, fillers. They can be divided into the several groups:

a) Organic conductive fillers [53]

b) Metallic and ceramic fillers with electrical, magnetic and electromagnetic properties [54]

c) Antistatic agents [55]

Organic conductive fillers are carbon materials including carbon black, carbon fibres, graphite, etc. Main advantages of this group is low density and price. Carbon materials provide electrical conductivity through the π bonding system caused by sp^2 hybridisation that exists between adjacent carbon atoms. They are relatively easy to process with good adhesion to almost all polymers. Although their influence on mechanical properties is not negligible, considering electrical properties, the main purpose is the improvement of volume conductivity [56].

Metallic and ceramic fillers such as carbonyl iron, Ni powder, ferrites (NiZn, MnZn, Co_2Zn, Ni_2W etc.) exhibit complex of electrical, magnetic and electromagnetic properties, whereas other metallic fillers such as Al powder, TiO_2, etc. may have influence only on electrical (dielectric) properties [54].

Antistatic agents are compounds used in order to reduce or eliminate accrual of static electricity. They utilize the facts that in our environment is relatively high humidity and water is more conductive than plastics. Therefore antistatic agents are humectants containing hydrophilic and hydrophobic parts. Hydrophobic part provide good miscibility with plastics and hydrophilic part interact with air moisture. This cause the creation of thin layer of water on the surface which will discharge any static electricity. The advantage of antistatic agent

is the need of very low amount of this additive but on the other side the disadvantage is dependence of performance on the air humidity. With regard to the electromagnetic properties, the effect of antistatic agent is indirect increase of surface conductivity [55][56].

3.1 Electrostatic charge

As mentioned before, most of the polymers are dielectrics. Therefore their attribute is to concentrate electrostatic charge. This charge might have high voltage and thus in some application is necessary to gradually discharge it [56]. There are different levels of materials for electrostatic discharge according to reached conductivity as can be seen in Table 1.

Table 1: Sorting of materials according electric conductivity [57]

Material	Metals		Carbon powders and fibres			Shielding composites			Conductive composites			
Sig/cm	10^{5}	10^{4}	10^{3}	10^{2}	10^{1}	10^{0}	10^{-1}	10^{-2}	10^{-3}	10^{-4}	10^{-5}	10^{-6}
Material	Static dissipative composites			Antistatic composites			Base polymers					
Sig/cm	10^{-7}	10^{-8}	10^{-9}	10^{-10}	10^{-11}	10^{-12}	10^{-13}	10^{-14}	10^{-15}	10^{-16}		

The antistatic materials suppress electrostatic charging. Some electrostatic charge might arise, however the charge is discharge at lower voltage than at dielectrics. Static dissipative composites allows to rise only low initial charges which slowly flow to the ground. The conductive materials have low electrical resistance. Electrons flow easily across the surface or volume to the ground or other conductive objects [57].

3.2 Percolation theory

Percolation theory is a mathematical theory describing behaviour of connected clusters in a randomly arranged system. Conductive filler in polymer matrix are also conductive clusters randomly dispersed in volume and therefore conductivity–concentration dependence can be described by this theory.

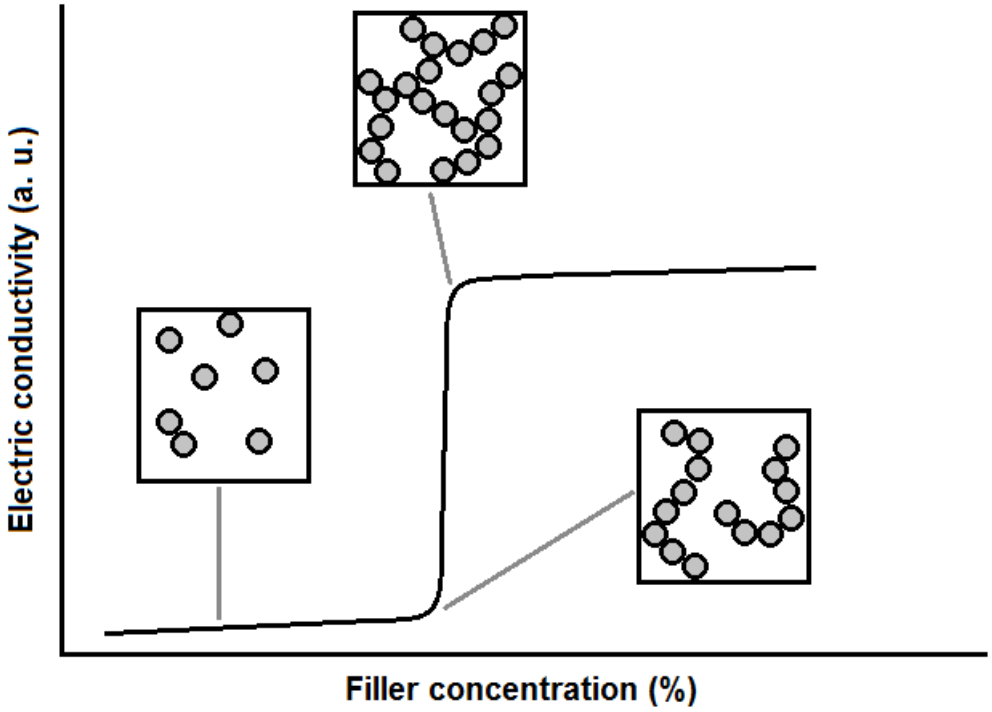

Figure 3: General illustration of percolation threshold

As can be seen at Figure 3, at low concentrations material behaves as a dielectric. Conductivity of composite bellow the percolation threshold can be mathematically described by following equation:

$$\sigma = \sigma_m (v_c - v)^{-q} \tag{14}$$

where σ is conductivity of composite, σ_m is conductivity of matrix, v_c is critical volume concentration of filler, v is volume concentration of filler and q is geometrical constant. The transfer of electrons in this region in caused mostly by tunnelling effect between isolated conductive particles. With increasing concentration is higher probability that some particles will touch, effectively making bigger clusters when suddenly one large cluster – a conductive path connecting both sides of the specimen is formed. When conductive path is formed, the conductivity of material suddenly increase by several orders of the magnitude. This critical concentration is called percolation threshold and highly depend on the size and shape of particles. The number of conductive paths is increased at higher concentrations and therefore a continuous increase at conductivity can be again observed. This is described by following equation:

$$\sigma = \sigma_0 (v - v_c)^t \tag{15}$$

where σ_0 is conductivity of filler and t is geometrical constant [58].

3.3 Electromagnetic wave absorbers

Interest about electromagnetic wave absorbers (EWAs) historically started during the World War II. The first application was camouflaging of submarines. Later interest with EWA was determined by the development of Stealth technology. Nowadays the renewed interest in the EWAs is caused by wide spread of wireless electronics and the need to shield some devices from external electromagnetic radiation in the radio and micro waves band. The frequency range 0,8–10 GHz is of particular importance here, since the majority of communication and information transfer systems operate in this frequency region.

Generally, EWAs materials can be classified from the viewpoint of complex permittivity and magnetic permeability into two groups as: dielectric and magnetodielectric types [59]. Since dielectric-type absorbers are nonmagnetic, their absorptive characteristic depends only on the frequency dispersion of the complex permittivity. This type of materials includes polymer composites filled with conductive filler such as (i) carbon-based materials (graphene, carbon black, carbon nanotubes, etc.), (ii) semiconductive materials ($BaTiO_3$, SiC, etc.) and (iii) conducting polymers (PANI, PPy, etc.). On the contrary, magnetodielectric type are characterized by frequency dependence of both complex permittivity and complex magnetic permeability. These types of materials includes polymer composites filled with different types of magnetic fillers, e.g. carbonyl iron powder (CI), ferrite powders, alloys, as well as multi-component fillers combining magnetic and conductive phases in their composition.

The efficiency of EWA is normally estimated by two parameters: the reflection coefficient and the operating frequency range (or bandwidth). The reflection coefficient (R) is a parameter that characterizes the absorbing ability of EWA in decibels (dB). The level of R equal to –10 dB which corresponds to 90 % absorption of incident energy (assuming that there is no transmitted energy); this can be considered as a standard level for usual EWA.

The standard objective of the design of EWA is to obtain an absorber of minimal thickness that has the lowest possible reflectance within the widest possible operating bandwidth. These requirements are contradictory to each other: real EWAs are known to have good performance only within a limited bandwidth. The application of magnetodielectric-type radio absorbers allows one to obtain broader operating bandwidths compared to dielectric-types absorbers. Nevertheless, the ratio of the edge frequencies of such absorbers (at the level of reflection coefficient equal to –10 dB) is in the range 1,5–1,8 [60]. One of the

beneficial properties of such absorbers is that the operating frequency range can be changed here by varying the particle size and their concentration in the polymer matrix.

One of efficient methods for expanding the range of operating frequencies of radar absorbers is the application of periodic patterns called frequency selective surfaces (FSSs). The application of an FSS allows one to increase the operating frequency bandwidth of magnetic-type EWAs by a factor of more than 1,5 virtually without increasing the thickness of the absorber [61].

4 METHODOLOGY

4.1 Differential scanning calorimetry

Differential scanning calorimetry (DSC) is used for measuring thermal processes in the sample. These processes include phase changes and chemical reactions. In terms of thermosets the most important processes are glass transition and crosslinking reaction. While crosslinking will be followed by a significant irreversible exothermic process, the glass transition temperature as a second order phase transition is usually identifiable by change of the heat capacity of the material. However some polymer glasses may exhibit endothermic peak particularly after having been aged [62][63][64]. This effect is explained by longer relaxation times of aged glass which shows delayed response to heating. Therefore specimen displays overshot when recovering to higher temperature equilibrium.

Crucial parts of DSC instrument are two measuring cells – for the sample and for the reference. Reference and holder for sample are typically aluminium pans. During the measurement both, sample and reference, maintain at same temperature and heat flux is measured. Difference between energetic requirements of pan with sample and empty pan is assigned to sample [65].

4.2 Charpy impact test

Impact strength is a material property, which represents the amount of energy that material is able to absorb before fracture occurs. One way to measure the impact strength is Charpy test. In this test the specimen is placed in the anvil of the instrument and broken by the hammer on a pendulum. The impact strength of the material can be determined from energy balance:

$$E_{k1} = E_{k2} + E_f + E_{ks} + Q \tag{16}$$

where E_{k1} is kinetic energy of hammer before impact, E_{k2} is kinetic energy of hammer after impact, E_f is energy needed for fracture, E_{ks} is kinetic energy of pieces of specimen after impact and Q is heat given by impact and friction of pendulum. The values of the last two energies is negligible. For the pendulum, the kinetic energy is fully converted into potential energy and vice versa. Therefore, the equation can be rewritten as:

$$E_{p1} = E_{p2} + E_f \tag{17}$$

where E_{p1} is potential energy of hammer at the start of test, E_{p2} is potential energy of hammer in highest deflection after impact. Using the equation:

$$E_{p1} - E_{p2} = \Delta E_p \tag{18}$$

where ΔE_p is difference between potential energies, equation 2 can be rewritten into:

$$\Delta E_p = E_f \tag{19}$$

It is important to note that potential energy can be directly determined from the angle of the arm of the pendulum and vertical line. According to definition, the impact strength is given by the following equation:

$$Impact\ strength = \frac{E_f}{A} \tag{20}$$

where A is area of the sample [66].

4.3 Dynamic mechanical analysis

Dynamic mechanical analysis (DMA) is a cyclical mechanical testing of materials for study of viscoelastic behaviour. In this measurement specimen is loaded in region of elastic deformation. Therefore the sample may undergo hundred thousands of cycles while the conditions are changing. Important changing parameters in terms of viscoelasticity are temperature and frequency. Generally at high frequencies specimen behaves more elastic and less viscous. On the other side at high temperature specimen is softer and may undergo several phase transitions. While semi-crystalline polymers exhibit melting (first-order phase transition), other polymers undergo glass transition, so called alpha transition. At glass transition large segments of main chain start freely moving. However there are two other second-order phase transition at lower temperatures. Namely beta and gamma transitions associated with movement of side groups respectively bond bending and stretching. Transition temperatures are easily determined from temperature profile of loss angle, which is given by equation:

$$tg\ \delta = \frac{E''}{E'} \tag{21}$$

where δ is a loss angle, E' is storage modulus and E'' is loss modulus. That modulus can by combined to:

$$E^* = E' + iE'' \tag{22}$$

where E^* is complex modulus and i is imaginary unit. Measurements of temperature or frequency dependencies are performed by using different mechanical stress. Used geometry should match the application usage of material. Different types of stress are according to used geometry tension, shear, bending etc. [67].

4.4 Rheological analysis

Rheological analysis is powerful technique for study curing reactions of thermosets. While the curing is time and temperature dependent, rotation viscometers are used, typically with parallel-plate geometry. This type of viscometer consists of two horizontally positioned circular plates. Between those plates is inserted sample. While the lower plate is static the upper plate oscillate with chosen frequency and amplitude. However oscillation movement is hindered by the presence of the sample. Therefore oscillator needs higher torque to move with upper plate. This torque is directly proportional to viscosity of sample, which undeniably arises from following equations:

$$\tau = c_1 . M \tag{23}$$

where τ is shear stress, c_1 is geometrical constant and M is torque,

$$\dot{\gamma} = c_2 . \omega \tag{24}$$

where $\dot{\gamma}$ is shear rate, c_2 is geometrical constant, ω is angular velocity,

$$\eta = \frac{\tau}{\dot{\gamma}} \tag{25}$$

where η is shear viscosity. During the curing reaction viscosity increases and also material becomes more elastic and less viscous. At one point there is an intersection between storage and loss modulus ($tg\ \delta$ = 45°). This point is called gelation point that corresponds to the formation of the first infinite macromolecule penetrating from one side of sample to the other side [68].

4.5 Scanning electron microscopy

Although there are many methods to examine the material characteristics, to understand some phenomena is necessary to identify the material morphology. One of the possibilities is scanning electron microscopy (SEM). This method is used for characterization of heterogeneous materials on nanometer and micrometer scale. Small area of sample is irradiated with focused electron beam. Those electrons interact with material and produce

secondary electrons which are collected, analysed and used for creating three-dimensional-like images of surface. Electrons are generated in electron gun and accelerated to an energy in range 0,1–50 keV. The beam of electron is then focused by electron lenses to a spot on a sample with a diameter usually smaller than 10 nm. This size defines the smallest point on the picture which can be obtained from SEM. The image is than created point by point. The lenses cause the beam to move along the line on a sample, than along the other line bellow the first line and so on, until a rectangular image of the sample is generated. To avoid interaction of electron with air, measurement is performed under high vacuum of about 10^{-4} Pa [69].

4.6 DC electric conductivity

Direct current (DC), unlike the alternating current (AC), is a flow of electric charge carries only in one direction. Simply said, materials can be divided into conductors and insulators depending if the current can flow through them or not. This can be mathematically described by equation:

$$G = \frac{I}{U} \tag{26}$$

where G is conductivity, I is electrical current and U is voltage. The conductivity is also geometrically dependent and therefore specific conductance is used:

$$\sigma = G\frac{l}{A} \tag{27}$$

where σ is specific conductance, l is length of conductor and A is its area. Conductivity can be easily measured just by connecting two electrodes with sample at opposite sides. However this might be problematic for characterization of dielectrics due to the presence of surface conductivity caused by thin layer of water conducting better than sample. Besides that, other problem is contact resistance. Therefore more sophisticated method was developed, i.e. four-point method.

A two-point method is based on standard measurement described above. The surface conductivity is eliminated by a guard ring placed around one electrode to absorb surface current. Therefore only the current flowing through the material is measured [70].

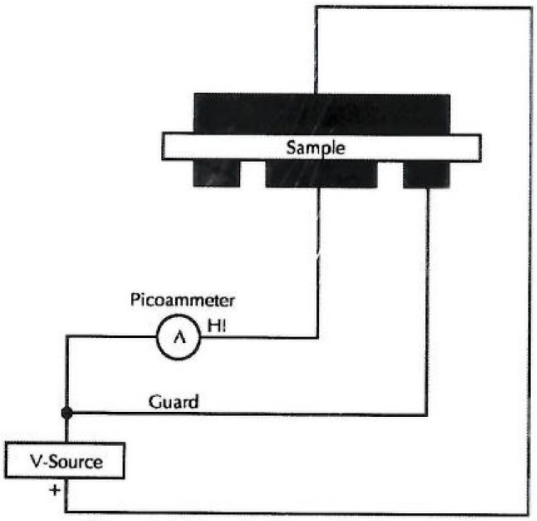

Scheme 7: Two-point method

A four-point method was proposed by Van der Pauw [71]. In this method, four probes are placed on one side of the sample. Current flows between two probes and the other two probes measure voltage. This effectively eliminates the effect of contact resistance and thus allows conductivity measurements of samples with low resistivity. This method is also suitable for measuring conductivity of thin films [70].

4.7 Dielectric spectroscopy

Dielectric spectroscopy (DS) is method based on the interaction of electromagnetic field with electric dipole moments. Behaviour of dipole moments in alternating current is expressed by permittivity (ε). Commonly used frequencies are lower than 10^{10} Hz, i.e. frequency region up to microwaves. At this frequency region significant decrease in permittivity (ε dispersion) for materials containing induced dipole moments is usually observed. On the other side the lower limit of DS is 10^{-6} Hz.

Dipole moments exist due to asymmetry of charges in molecules and atoms. There are several causes of this asymmetry. Electronic polarization arises from electrons orbiting atomic nucleus. Dipolar and ionic polarizations originate in asymmetrical molecules which turn according to the direction of the electric field. The response of material is described by complex permittivity:

$$\varepsilon^* = \varepsilon' + i\varepsilon'' \qquad (28)$$

where ε^* is complex permittivity, ε' is real part of permittivity, ε'' is imaginary part of permittivity and i is imaginary unit. It is useful to express ratio of imaginary and real permittivity as:

$$tg\ \delta_E = \frac{\varepsilon''}{\varepsilon'} \tag{29}$$

where δ_E is a dielectric loss angle. This can be used for classification of materials. The materials with $\frac{\varepsilon''}{\varepsilon'} \gg 1$ are referred as a conductors while $\frac{\varepsilon''}{\varepsilon'} \ll 1$ are dielectrics (insulators).

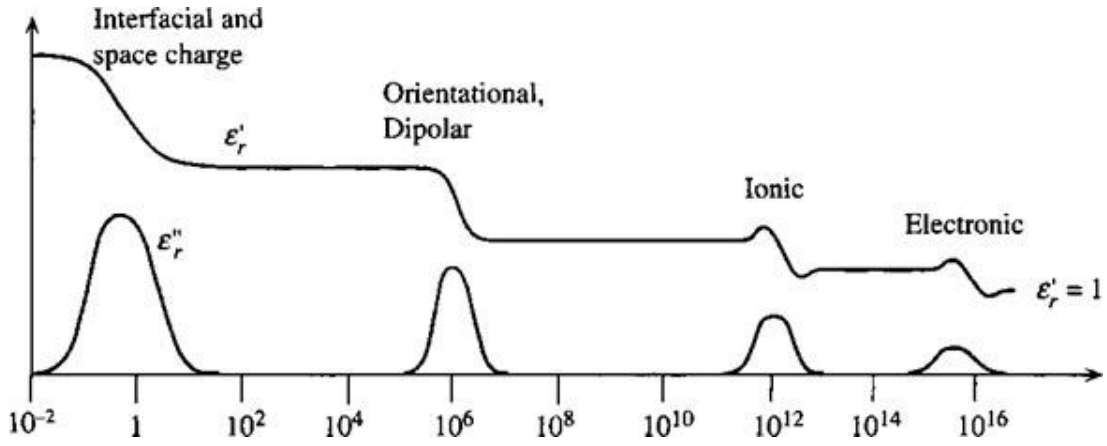

Figure 4: Frequency dependence of storage and loss permittivity for dielectrics [72]

Frequency dependence of real and loss permittivity for dielectrics is schematically illustrated in Figure 4. Permittivity is the ability of dipole moment to change orientation according to orientation of external electric field. At higher frequencies some dipoles might not be able to rotate as fast as the external field is changing and their contribution to real permittivity disappear.

Dielectric spectroscopy is used in polymer science with a goal to study structural transitions such as T_g or crystal transitions (for semi-crystalline polymers), as well as chemical changes of polymers as cross-linking or ageing. This method is also very sensitive to evaluate the quality of polymer surface for coating or gluing. This method is also useful for evaluating of polymer blends, composites and additives in polymers [73].

II. ANALYSIS

5 AIMS OF DIPLOMA THESIS

The aim of the work is to modify the brittle behaviour of epoxy resin by polydimethylsiloxane and to develop composites with controllable total conductivity.

The work that has been carried out within this diploma work entitled “The Development and Characterization of Epoxy-Silicone Blends as a Matrix for Antistatic Composites” can be summarized into following parts:

1. Development of technology for preparation of epoxy-silicone system with improved mechanical properties.

2. Development of homogeneous polymer composites based on epoxy-silicone systems filled with different types of conductive fillers (carbonyl iron and carbonyl nickel).

3. Characterization of structural, mechanical and electrical properties of polymer composites.

4. Optimization of polymer composites technology with a view to improve their toughness and electrical properties.

6 PREPARATION OF POLYMER BLENDS

In the first part of my work was goal to optimize of processes and properties of polymer blends based on epoxy resin (ER) and polydimethylsiloxane (PDMS) for use as a polymer matrix for antistatic and electromagneticshielding composites. ER was prepared from bisphenol A diglycidyl ether (DGEBA, D-3415, Sigma Aldrich, USA) cured by diethylenetriamine (DETA, D93856, Sigma Aldrich, USA). Dicumyl peroxide (DCP, Sigma Aldrich, USA) was used as free radical initiator. In my work were used two kinds of PDMS: vinyl-terminated polydimethylsiloxane (V, Sigma Aldrich, USA) and Sylgard 184 (S, Sylgard 184 – base A, Dow Corning, USA).

Blends were prepared by following procedure. DGEBA and DCP were put into the triple-neck round-bottom flask and stirred it half an hour at 80 °C. Than PDMS was added and stirred 30 minutes at 130 °C. After cooling to 50 °C, DETA was added and stirred another 10 minutes for pre-crosslinking. Prepared material was casted into the forms and air bubbles were removed in vacuum desiccator. Forms were closed and placed into the oven preheated on 100 °C and material was cured for 1 hours. After cooling, the sample was took out of the form and post-curing was performed at 130 °C for 1 hour. All stirring was performed under N_2 atmosphere and stirred at 300 rpm by MM-8000. If prepared blend did not contain DCP or/either PDMS, the processing of mixture remained same. Considered reaction mechanism for curing ER is:

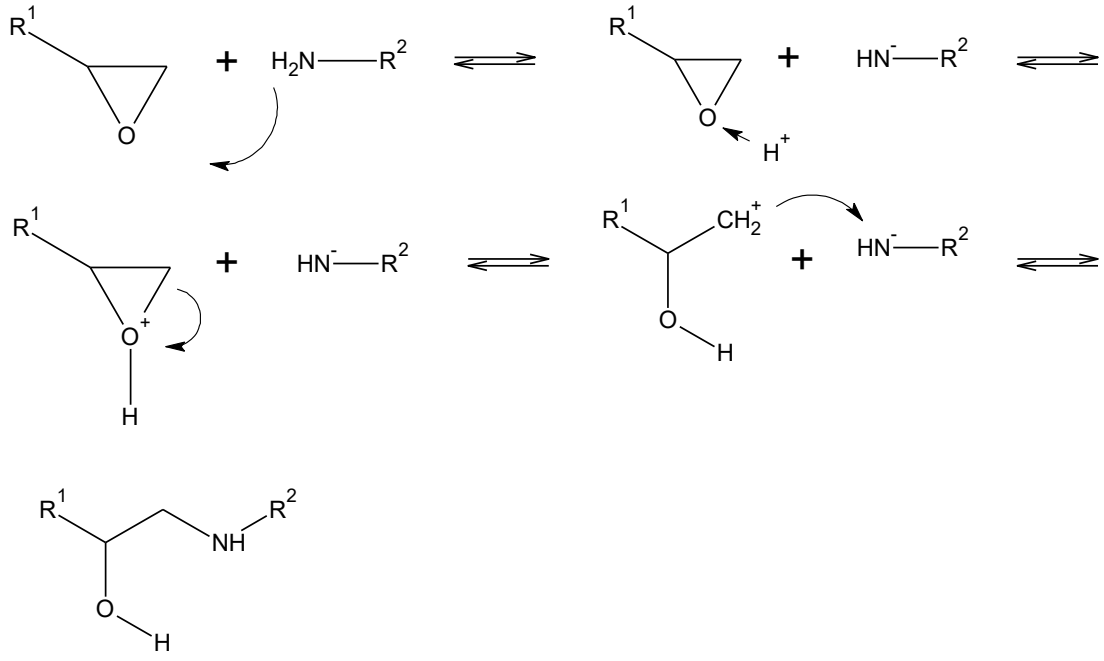

Scheme 8: Mechanism of cross-linking reaction of ER

As was shown before, active hydrogen is needed for opening oxirane ring. While DGEBA has 2 epoxy groups, DETA has 5 active hydrogens and therefore for full conversion is needed molar ratio DGEBA:DETA as 5:2.

I suppose that cross-linking via DCP begins with decomposition:

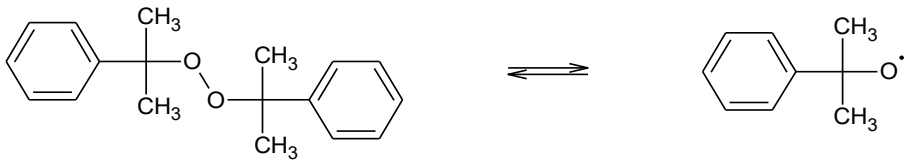

Scheme 9: Decomposition of DCP

followed by initiation:

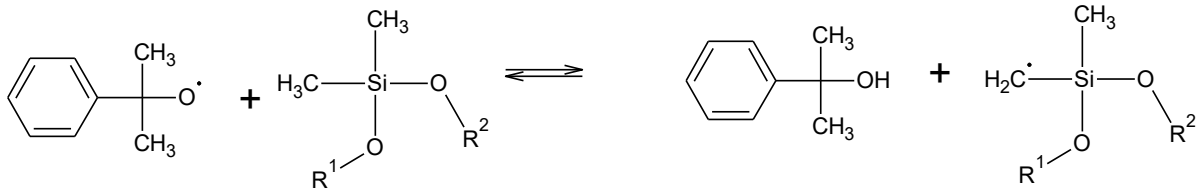

Scheme 10: Initiation of cross-linking of PDMS

There are different possible cross-linking reactions as well as other terminations, but two most important reactions are:

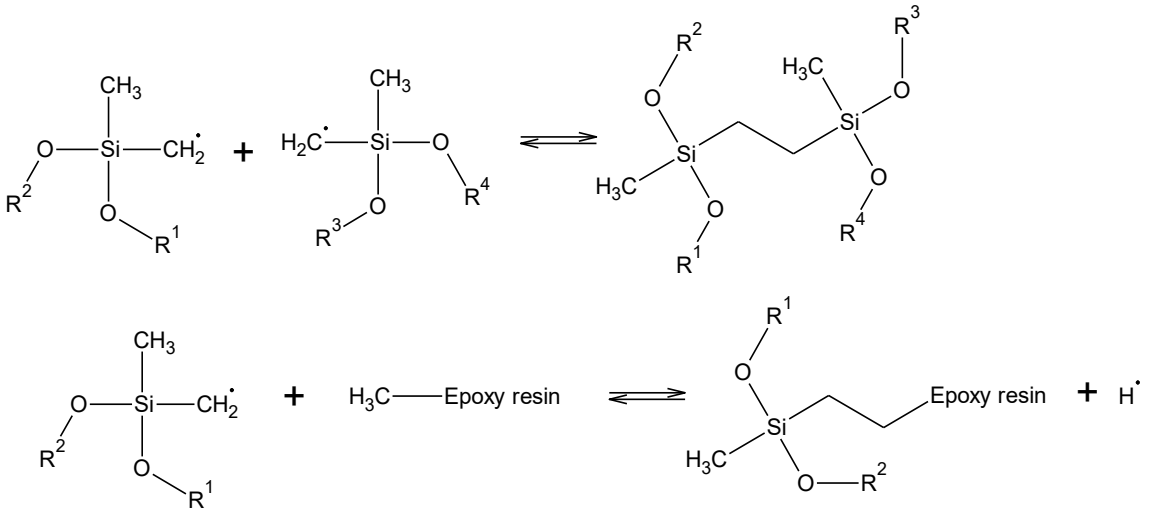

Scheme 11: Possible cross-linking reactions

First reaction leads to cross-linking of PDMS spheres giving them shape, size and mechanical properties. Second reaction improves interphase and prevents coalescence.

For better understanding of the influence of elastomer on mechanical properties of ER, 0–15 % weight concentrations of PDMS has been chosen. Weigh concentration of DCP was varied between 0–3 %. List of specimen with their composition and codes is presented in the Table 2.

Table 2: List of prepared blends ER/PDMS

Samples	DGEBA + DETA	PDMS-V	PDMS-S	DCP
	(wt.%)	(wt.%)	(wt.%)	(wt.%)
D0	100	-	-	-
Dd1	99	-	-	1
Dd2	98	-	-	2
Dd3	97	-	-	3
DV5	95	5	-	-
DV10	90	10	-	-
DV15	85	15	-	-
DV5d1	94	5	-	1
DV5d2	93	5	-	2
DV5d3	92	5	-	3
DV10d1	89	10	-	1
DV10d2	88	10	-	2
DV10d3	87	10	-	3
DV15d1	84	15	-	1
DV15d2	83	15	-	2
DV15d3	82	15	-	3
DS5	95	-	5	-
DS10	90	-	10	-
DS15	85	-	15	-
DS5d1	94	-	5	1
DS5d2	93	-	5	2
DS5d3	92	-	5	3
DS10d1	89	-	10	1
DS10d2	88	-	10	2
DS10d3	87	-	10	3
DS15d1	84	-	15	1
DS15d2	83	-	15	2
DS15d3	82	-	15	3

7 DIFFERENTIAL SCANNING CALORIMETRY

7.1 Determination of ratio of epoxy resin and curing agent

For creating of any epoxy resin with good mechanical properties is necessary to determine ratio of epoxy resin and curing agent. The exact ratio is required for the formation of the maximum possible number of bonds, leading to high network density. This ratio can be calculated using the following equations:

$$n_E = n_H \tag{29}$$

where n_E is number of epoxy groups and n_H is number of active hydrogens in curing agent. Equation 29 can be also written as:

$$\frac{z_E m_E}{M_E} = \frac{z_H m_H}{M_H} \tag{30}$$

where z_E is quantity of epoxy groups in molecule of epoxy resin, m_E is weight of epoxy resin, M_E is molar mass of epoxy resin, z_H is quantity of active hydrogens in molecul of curing agent, m_H is weight of used curing agent, M_H is molar mass of curing agent. This equation can be converted to:

$$\frac{m_E}{m_H} = \frac{z_H M_E}{z_E M_H} \tag{31}$$

Finally, substituting the values used for the system DGEBA and DETA gain ratio:

$$\frac{m_E}{m_H} = \frac{5 .340,4}{2 .103,2} = \frac{100}{12} \tag{32}$$

In many other works is eventually selected a lower ratio for easy processing. For DGEBA and DETA system the frequently used ratio 100:6,5. For comparison, there was chosen ratio 100:9. DSC method has been used to study curing reaction with a view to determine the optimal between DGEBA and DETA. The measurement was performed in the temperature range from -50 to 180 °C with a heating rate of 10 °C/min.

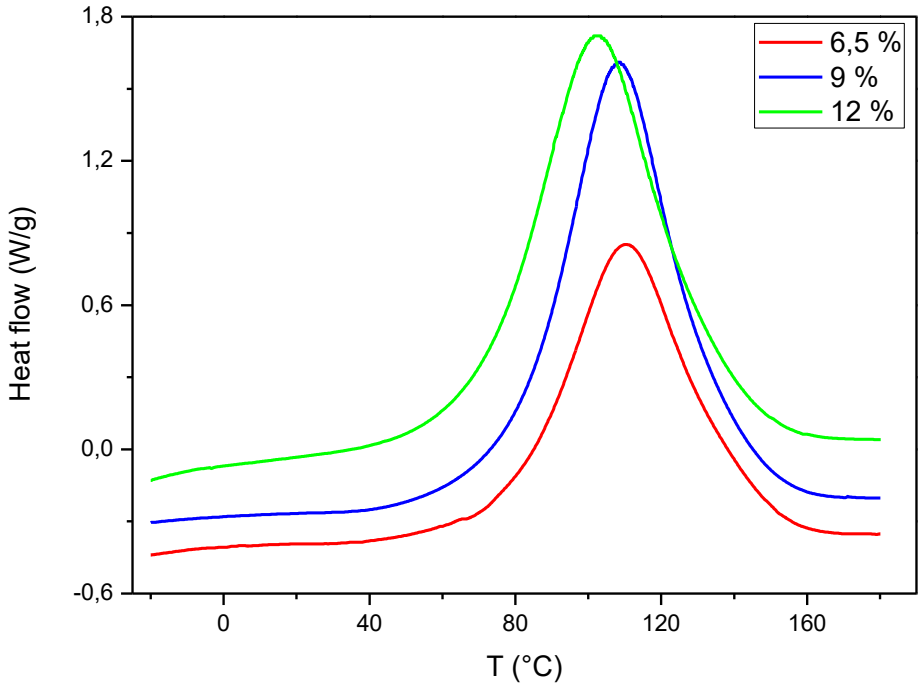

Figure 5: DSC thermogram of curing reaction with varying ratio DGEBA:DETA

As was expected, a higher amount of hardener leads to a higher amount of released heat of reaction, which means more formed bonds (Figure 5). Indeed, for the ratio 100:12 the amount of released energy is about 50 % higher than for the ratio 100:6,5. From this it can be assumed that the reaction is incomplete, because otherwise the energy increase would be 100 %. It can be explained by an increase in viscosity, which reduces the mobility of the reactive groups and thereby prevent completion of the reaction. However, even if the reaction is not complete, still more groups undergo the reaction than at lower selected ratios, leading to higher density networks. Specific values are given in the Table 3.

Table 3: Released heat reaction for different ratios DGEBA:DETA

DGEBA:DETA ratio	Released reaction heat (J/g)
100:6,5	309
100:9	436
100:12	464

7.2 Determination of curing temperature

For the preparation of the epoxy resin, the proper curing temperature selection is required. At high temperatures there is a danger of degradation, boiling of hardener or a large temperature gradient leading to uneven network. In contrast, low temperature leads to long reaction times (risk of sedimentation of silicone elastomer) and possible incompletion of the reaction. To determine the correct curing temperature and time several methods can be used: measurements of T_g, mechanical properties (hardness), residual heat of reaction, etc. [74]. For the simplicity, in the current work, measurement of the residual heat of reaction by DSC, which also reveal T_g. Thus, several compositions with selected ratio of epoxide and hardener have been prepared and casted into the moulds and then cured at different temperatures. After a sufficient time of curing small samples were taken for DSC measurements. The samples were cooled to -20 °C and then heated to 150 °C with a heating rate of 10 °C/min.

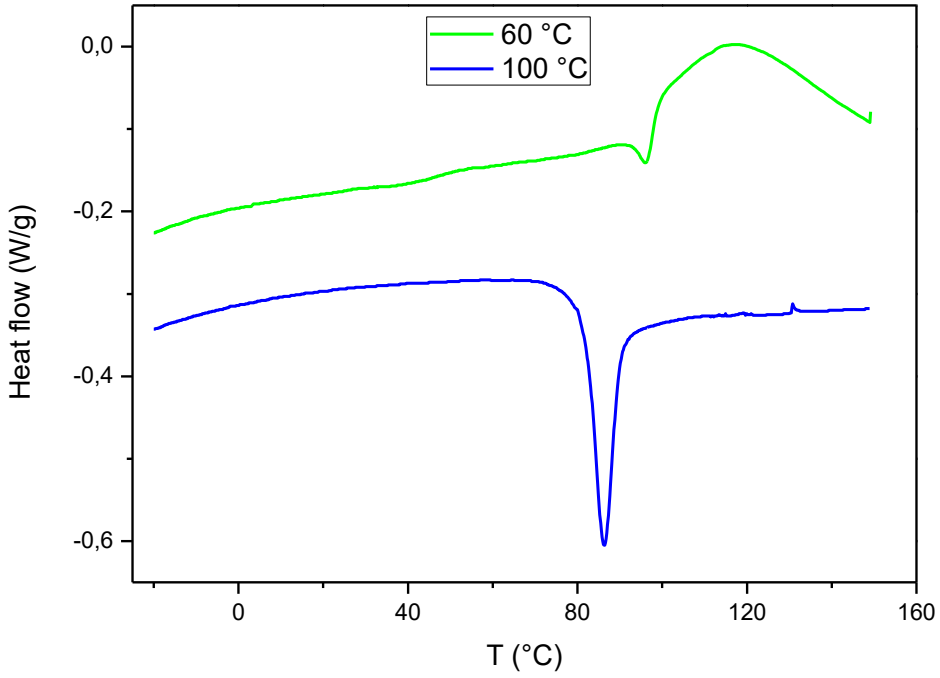

Figure 6: DSC thermogram of ER cured at different temperatures for DGEBA:DETA ratio 100:12

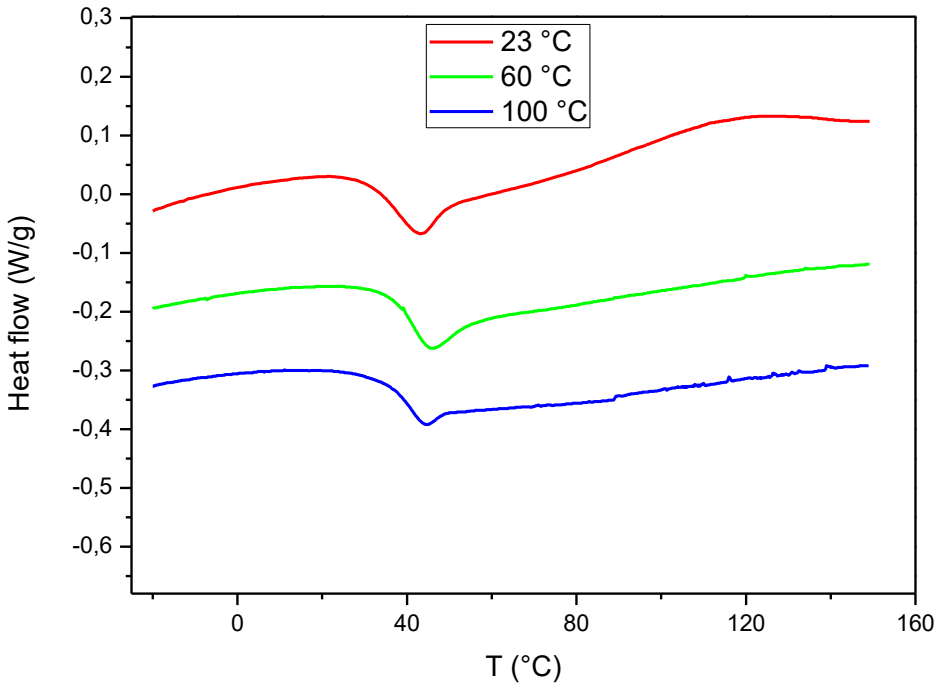

Figure 7: DSC thermogram of ER cured at different temperatures for DGEBA:DETA ratio 100:6,5

As seen from the Figure 6, the full cross-linking was reached in all selected temperatures when the epoxy resin:hardener ratio was 100:6,5, which is proved by the absence of any exothermic peak on the DSC thermogram. The only observed endothermic peak is between 45–50 °C where samples undergo a glass transition with an enthalpy relaxation. The situation is different for the epoxy resin:hardener ratio 100:12 (Figure 7). The crosslinking reaction at 100 °C resulted in the fully cross-linked system and only one noticeable heat process is identified for T_g with enthalpy relaxation between 80 and 90 °C. If the crosslinking temperature is lower than T_g (e.g. 60 °C), the reaction does not proceed completely, resulting in exothermic reactions when heated above T_g.

Based on the results obtained, the epoxy resin:hardener ratio 100:12 and the crosslinking temperature 100 °C has been selected.

8 RHEOLOGICAL MEASUREMENT

Rotational rheometer (Bohlin Gemini, Malvern Instrument, UK) was used to monitor the crosslinking reaction. The measurement was performed on plate geometry (d = 25 mm, h = 0,5 mm) in oscillatory mode at constant temperature. The aim was to find gelation point and the time-dependent viscosity. At single frequency test (f = 1 Hz, strain = 0,05) gelation point was found as a cross-section of storage and loss modulus. Although this method is generally accepted, the results are slightly imprecise. The reason is, that when stress is applied to system forming network, stress relaxation takes place. Therefore it is difficult to measure the frequency dependent modulus when the chemical crosslinking occurs as a function of time. However, tan δ is independent on frequency at the true gelation point and therefore if cross-linking is measured at several frequencies, all of them will pass through a single point. This unambiguously defined point is the instant at which the gel forms. This method, called multiwave test [75][76], was performed at frequencies (0,1; 0,2; 1; 4 and 16) Hz.

8.1 Gelation point

Single test measurement of D0 at 80 °C (Figure 8) shows the increase in both elastic and viscous modulus during the time of cross-linking reaction. It is evident that for the first 10 minutes of reaction, only small molecules are created and therefore the value of elastic moduli is low in the range G´ = (0,05; 0,2) Pa. However then exponential growth of elastic modulus starts and a cross-section of both modulus (effectively gelation point) appears at t = 913 s.

Multiwave test measurement of D0 at 60 °C (Figure 9) shows evolution of loss angle δ for different frequencies in the time of cross-linking reaction. Loss angle δ for all frequencies start at 90° and significant change appear around the time 1500 s. At this point starts the decrease of loss angle for the highest used frequency (16 Hz) successively followed by smaller frequencies (4; 1; 0,2 and 0,1) Hz. Their cross-section is found at t = 2047 s which is the true gelation point.

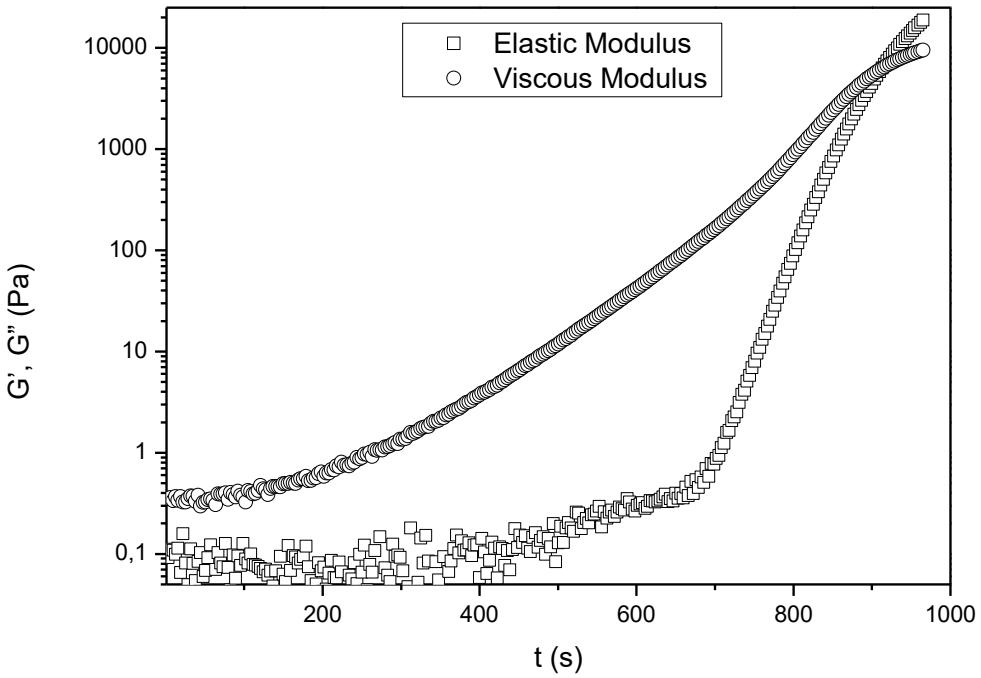

Figure 8: Example of gelation point determination from single frequency test (D0 – 80 °C)

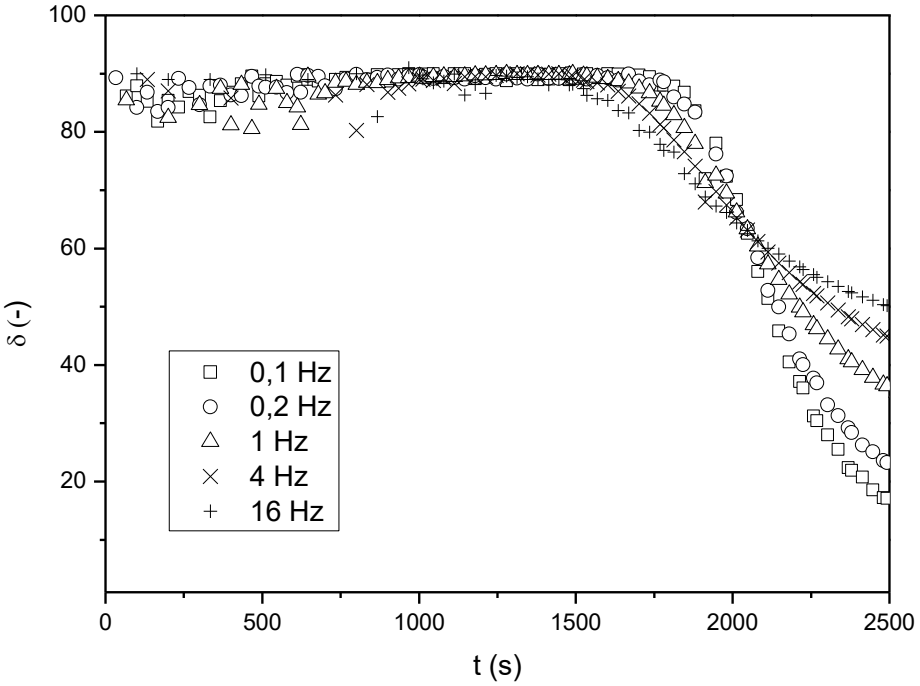

Figure 9: Example of gelation point determination from multiwave test (D0 – 60 °C)

The Table 4 shows that the addition of PDMS reduces the gelation time. This might be explained by the fact that the elastomer in the sample occupies some volume; thereby this volume is unavailable for growing macromolecule leading to formation an endless macromolecule penetrating whole sample sooner. On the other side, the addition of DCP should reduce the gelation time due to the creation of larger molecules in previous step. However this assumption was fully confirmed only at ER/V blend, for ER/S blend this remains unclear.

Table 4: Gelation points of polymer blends ER/PDMS

Samples	T	Single frequency test	Multiwave test
	(°C)	(s)	(s)
D0	60	2642	2047
D0	80	913	782
D0	100	279	210
DV5	80	695	700
DV10	80	660	570
DV15	80	632	420
DV10d2	80	612	449
DS5	80	850	500
DS10	80	815	453
DS15	80	665	367
DS10d2	80	690	500

8.2 Viscosity

The importance of gelation point of ER/PDMS blends is certainly indisputable, however the viscosity plays an important role also. After crossing some level of viscosity, the processing will become more difficult even if the gelation point will not be reached yet. On the other side, for a blend with low viscosity there is a threat of coalescence and sedimentation of particles. Therefore there is a processing window of viscosity for blend and particular process (casting).

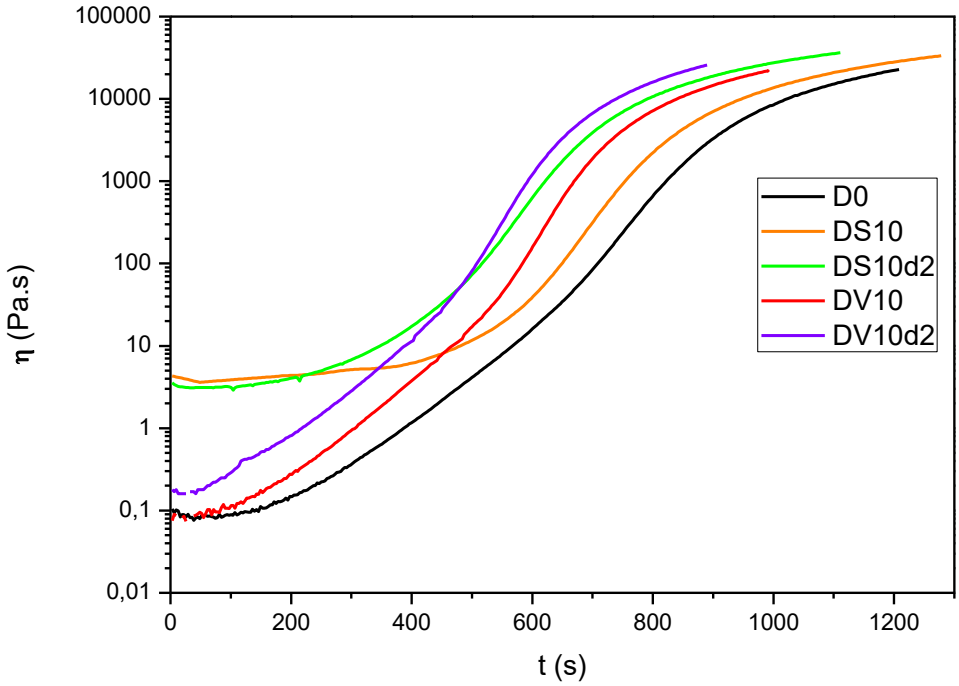

Figure 10: Evolution of viscosity in time during curing reaction of blends at 80 °C

The increase of viscosity during the reaction is shown in Figure 10. The effect of DCP on acceleration of curing is more evident than from gelation points. Polymer blends with DCP (DV10d2 and DS10d2) cross-links faster than polymer blends without DCP (DV10 and DS10). It might be concluded that during reactive blending, some DGEBA molecules are bonded with PDMS or with other DGEBA molecules, forming bigger molecules which cross-link faster and therefore viscosity increases more rapidly.

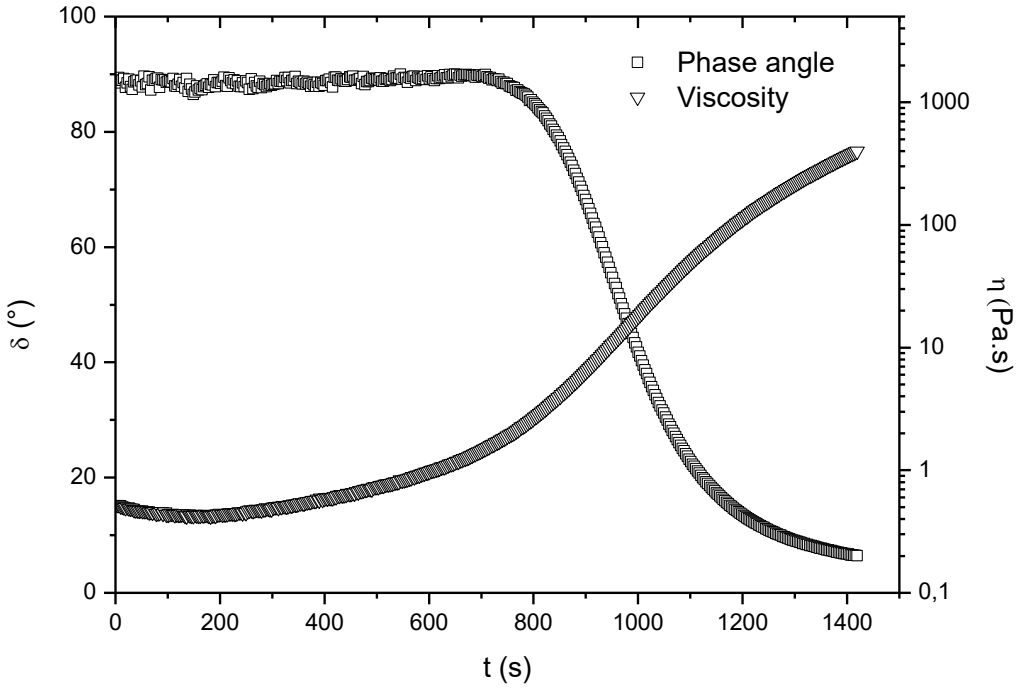

Figure 11: Time dependence of loss angle and complex viscosity during cross-linking reaction of PDMS-S by 2 wt.% DCP at 130 °C

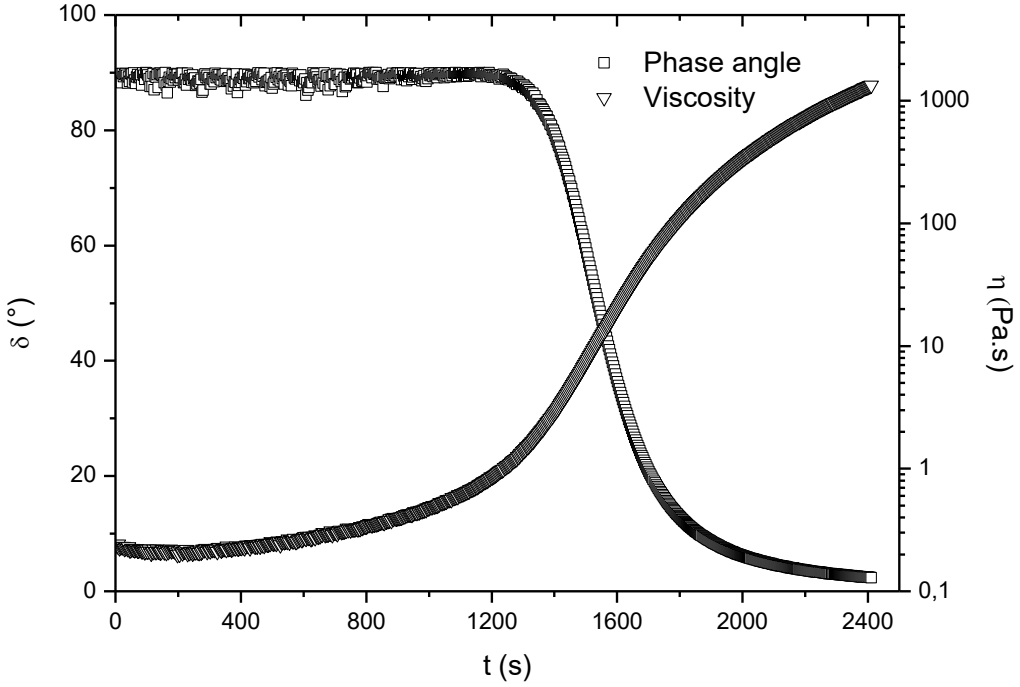

Figure 12: Time dependence of loss angle and complex viscosity during cross-linking reaction of PDMS-V by 2 wt.% DCP at 130 °C

Rheological measurements were performed for cross-linking of both PDMS (S and V) and gelation points were found to be 990 and 1560 s respectively. From Figure 11, 12 it is evident, that cross-linking of PDMS-S is faster than for PDMS-V, nevertheless the difference is negligible and thus it was decided to use the same technology for preparation of both blends containing PDMS (S and V).

Rheological measurements revealed the gelation points and increase of viscosity with reaction time of blends which could be used for adjustment of the preparation process. However, it was found that it is very complicated to use it, because of the fact that curing reaction behaves differently in small amount (1 ml) inside of the rotation rheometer with defined temperature and in big amount (30 ml) inside of the flask with temperature significantly rising due to chemical reaction. Nevertheless, it is important that curing times of all blends are within one relatively narrow time range indicating that prepolymerization phase of preparation can be same for all blends.

9 MORPHOLOGY OF POLYMER BLENDS

SEM (PhenomPro, BSED, USA) was used to observe the morphology of polymer blends. Samples for test were prepared by cooling in liquid nitrogen and fractured by mechanical force.

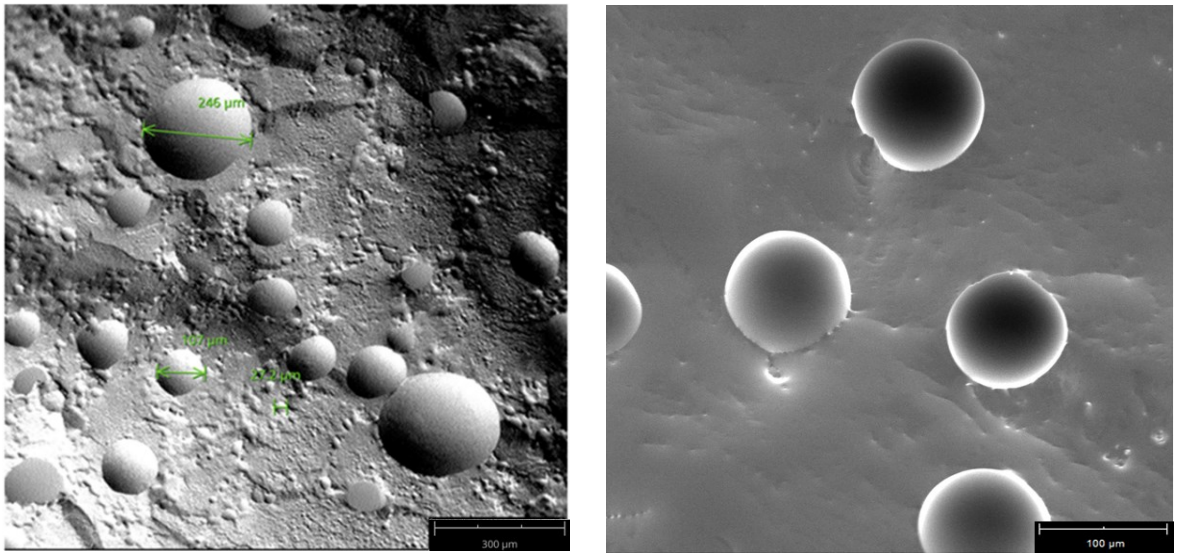

Figure 13: SEM micrographs for polymer blend DS15

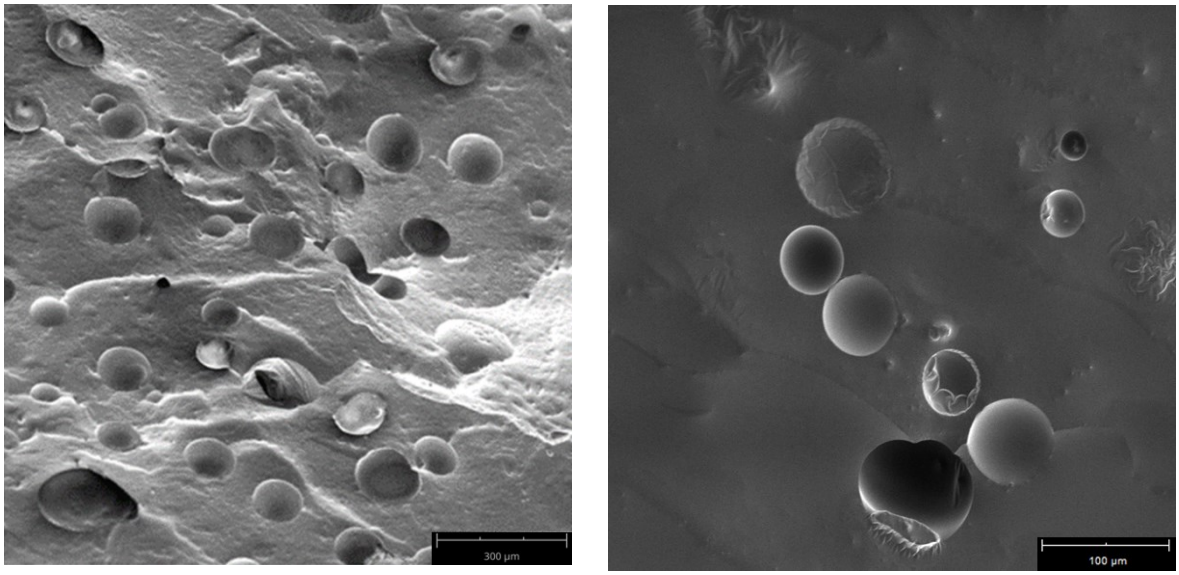

Figure 14: SEM micrographs for polymer blend DS15d2

In the polymer blend DS15 (Figure 13) can be seen relatively broader size distribution of PDMS spheres than in polymer blend DS15d2 (Figure 14). The difference in the shape of PDMS spheres is observed on the SEM images at high resolution: while PDMS in polymer blend DS15 are smooth, some of them are “wrinkled” in the polymer blend DS15d2. This might be caused by some interfacial bonding between ER and S created by DCP.

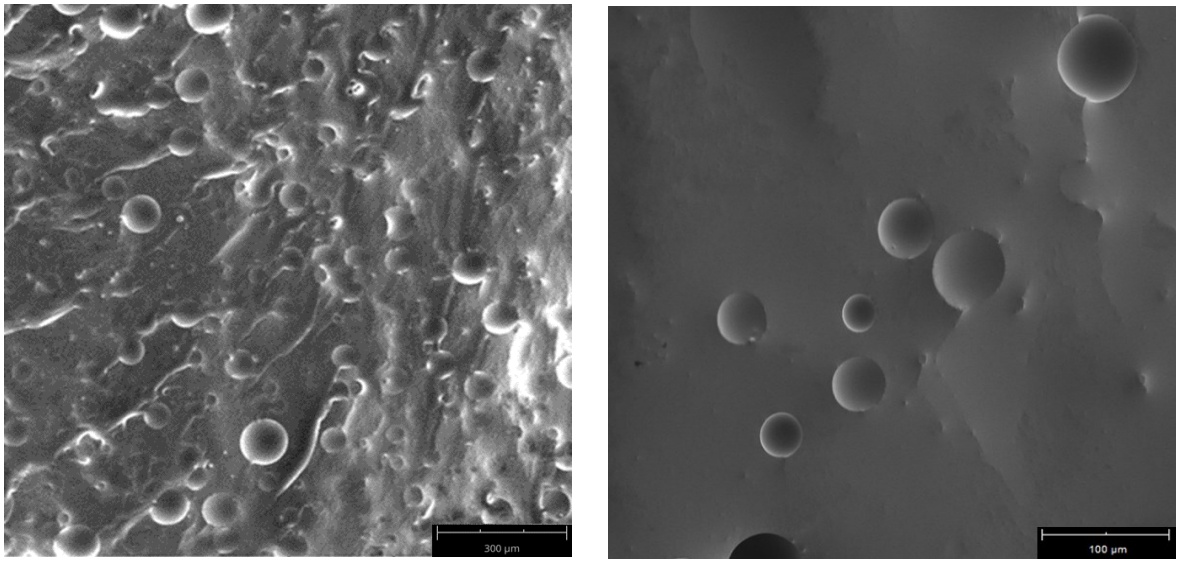

Figure 15: SEM micrographs for polymer blend DV15

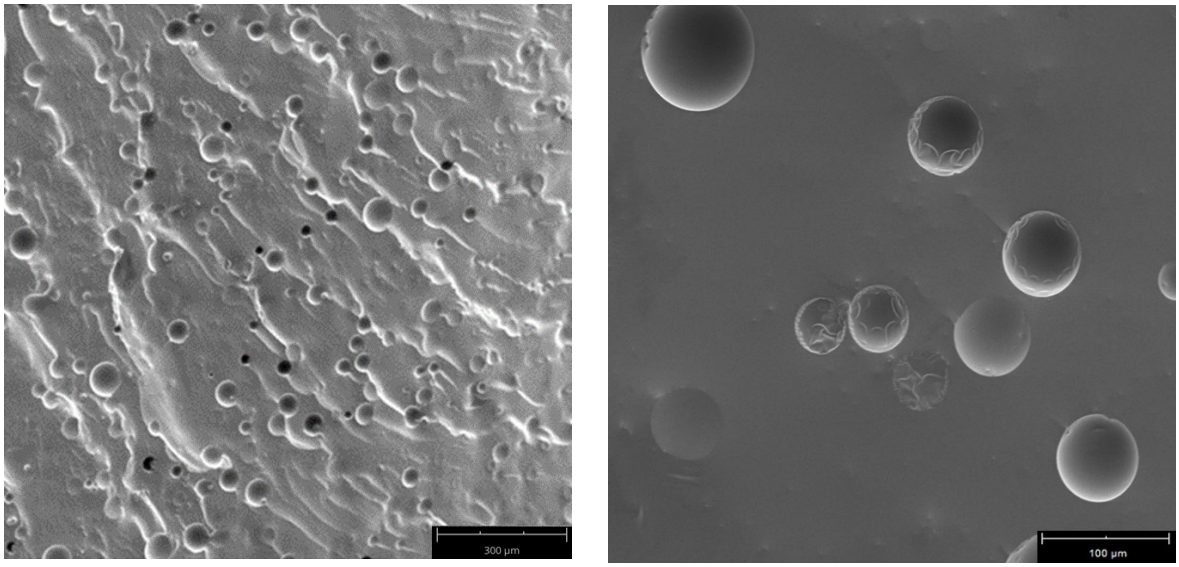

Figure 16: SEM micrographs for polymer blend DV15d2

In the polymer blend DV15 (Figure 15) can be seen similar size distribution of PDMS particles as in polymer blend DV15d2 (Figure 16). However, in higher resolution SEM images the difference in the shape of PDMS spheres can be seen, i.e. DV15d2 polymer blend (Figure 16) have also "wrinkled" PDMS spheres like DS15d2 (Figure 14).

Consequently, SEM images showed that using PDMS-V creates slightly smaller particles than PDMS-S and this difference retains even if DCP is used. Also the addition of DCP leads to "wrinkling" of the surface of some PDMS particles which might indicate the creation of some interface.

10 CHARPY IMPACT STRENGTH

Charpy impact tests were performed according to ISO 179 on unnotched izod specimens (80x10x4) mm using an impact tester (Zwick/Roell, Germany). Each polymer blend was measured on 10 specimens and some specimens might be excluded by Grubb's test for outliers.

Table 5: Toughness of polymer mixture ER/DCP

Samples	Impact strength (J/cm^2)
D0	1,04 ± 0,16
Dd1	1,04 ± 0,06
Dd2	1,02 ± 0,12
Dd3	1,00 ± 0,07

It was found that toughness of neat ER is 1 J/cm^2 (Table 5) and addition of PDMS generally improves this value. However, there are significant differences among the specimens as can be seen at table varying between 1 to 1,7 J/cm^2 as can be seen in Table 6.

Table 6: Toughness of polymer blends ER/PDMS

Samples	Impact strength (J/cm^2)	Samples	Impact strength (J/cm^2)
DV5	1,28 ± 0,08	DS5	1,33 ± 0,10
DV5d1	1,30 ± 0,10	DS5d1	1,18 ± 0,06
DV5d2	1,36 ± 0,15	DS5d2	1,42 ± 0,11
DV5d3	1,10 ± 0,06	DS5d3	1,30 ± 0,16
DV10	1,49 ± 0,15	DS10	1,28 ± 0,08
DV10d1	1,51 ± 0,07	DS10d1	1,15 ± 0,09
DV10d2	1,69 ± 0,12	DS10d2	1,46 ± 0,09
DV10d3	1,48 ± 0,12	DS10d3	1,20 ± 0,09
DV15	1,13 ± 0,09	DS15	1,02 ± 0,03
DV15d1	1,31 ± 0,12	DS15d1	1,06 ± 0,05
DV15d2	1,39 ± 0,11	DS15d2	1,07 ± 0,02
DV15d3	1,43 ± 0,14	DS15d3	0,99 ± 0,04

Based on the results obtained, the critical concentration of PDMS is 10 wt.% and efficient concentration of DCP is 2 wt.%. Therefore only samples D0, Dd2, DV5, DV10, DV10d2, DS5, DS10 and DS10d2 were chosen for further studies and tests.

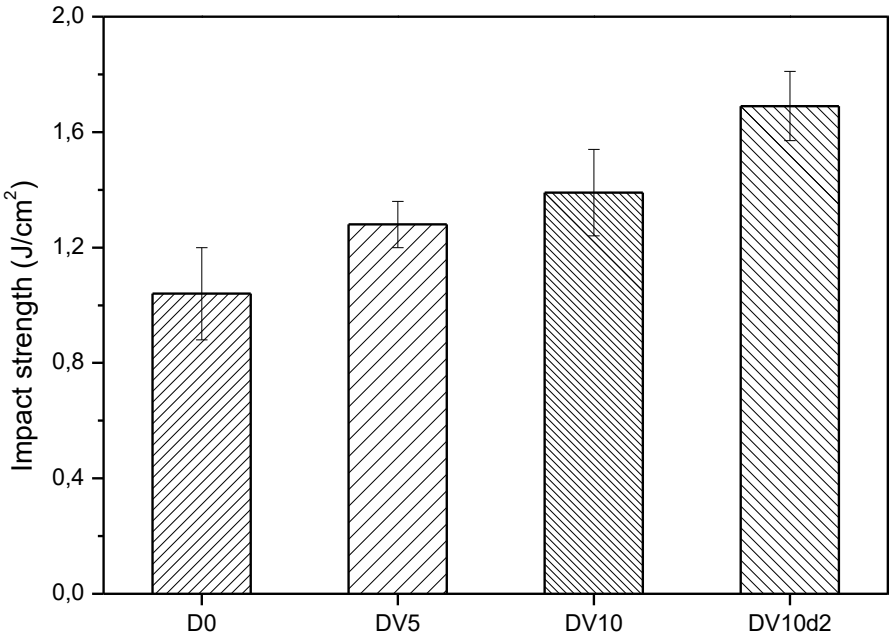

Figure 17: Impact strength of blends ER/V

Addition of PDMS-V has good influence on toughness of blend as can be seen from Figure 17. However the addition of DCP exhibit synergetic effect on phase-separated rubber-rich inclusion in brittle matrix as can be seen on SEM photos (Figure 16).

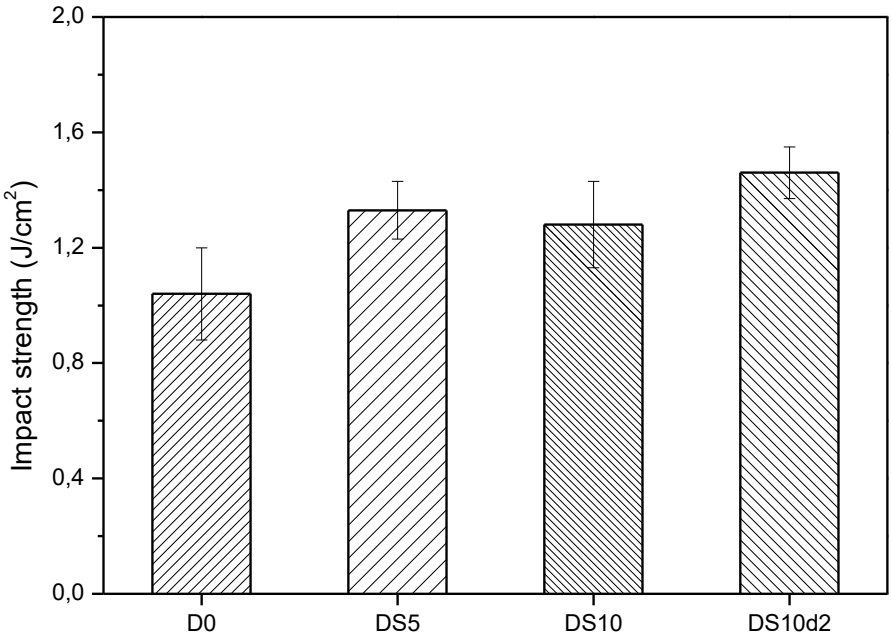

Figure 18: Impact strength of blends ER/S

Although the addition of PDMS-S also improves toughness of the blend, overall effect is smaller (Figure 18). From the decrease of toughness in blend DS10 in comparison with DS5, it can be concluded the poor compatibility of blended polymers. Also the effect of DCP is not so evident, some improvement of toughness was observed, however, considering standard deviation of the result obtained, the difference is very small.

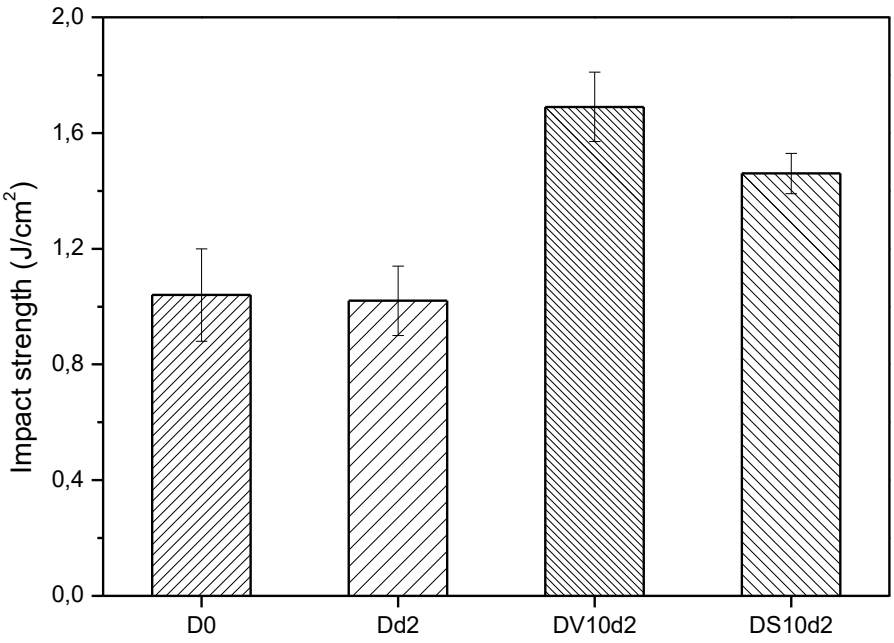

Figure 19: Impact strength of blends

Although both PDMS exhibit improvement of toughness by amplification of plastic deformation, the difference between DV10d2 and DS10d2 is clear: improvement of toughness by roughly 70 and 45 % respectively (Figure 19). Consequently, there is compatibility between ER/V than ER/S blends which is supported by SEM images.

11 DYNAMICAL MECHANICAL ANALYSIS

DMA was performed on specimens of dimensions (35x10x2,5) mm. Measurements were performed in dual cantilever mode at the temperature range from -120 to 180 °C with heating rate 3 °C. Before starting the actual measurement, the area of linearity was controlled and measuring force was determined as 2 N.

11.1 Comparison of stiffness of polymer blends at room temperature

The comparison of real part of complex elastic modulus of polymer blends at 30 °C is shown on Figure 20.

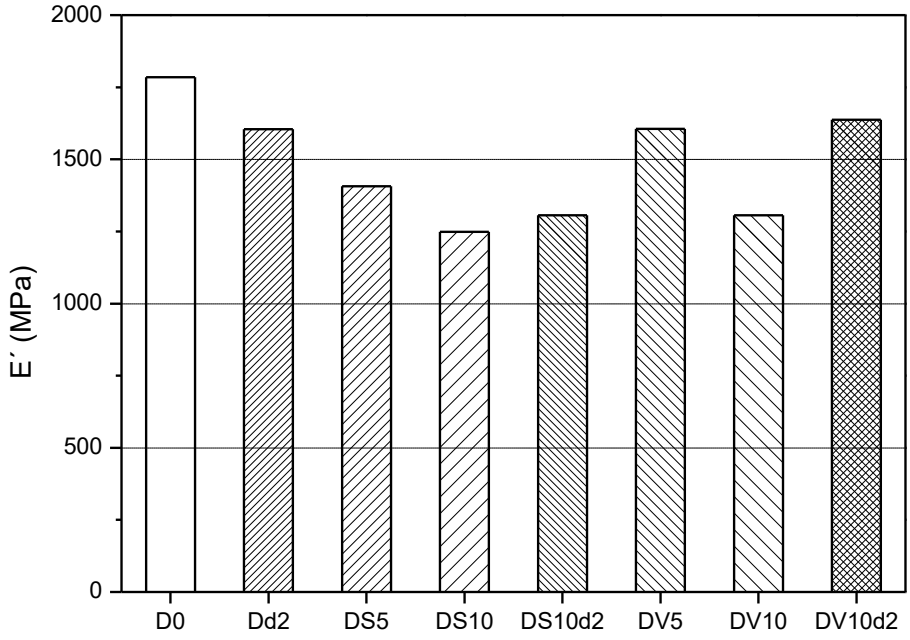

Figure 20: Stiffness of polymer blends at 30 °C

Although DMA is not suitable for accurate determination of the stiffness it can be used for comparison of the stiffness of similar polymers. As can be seen from the Figure 20, neat resin, exhibits the highest value of stiffness which decreases after addition of different types of PDMS. However, the stiffness of three other samples (Dd2, DV5 and DV10d2) decreased only about less than 10 %. For samples Dd2 and DV5 this is probably due to the small amount of addition. On the other side sample DV10d2 exhibits improved compatibility of blend ER/PDMS via DCP and therefore decrease of mechanical properties is lower in comparison with DV10. In contrary, the same effect of compatibility was achieved for the sample DS10d2 only partially. It is also important to note the difference between samples

DS5 and DV5 and in contrary a similarity of result for DS10 and DV10. However, at overall comparison of the PDMS additions (S and V), ER/V blends exhibits higher stiffness due to better compatibility.

11.2 Stiffness of polymer blends as a function of temperature

Real part of complex elastic modulus is plotted against temperature for polymer blends in following Figure 21–23. Generally, the gradual decrease of stiffness is observed with increasing temperature for all blends. However, the ER/PDMS blends should have three regions where the elastic modulus significantly changes at -120 °C, -50 °C, and 120 °C for the α transition of PDMS, γ transition of ER, and α transition of ER respectively. Although there was an effort, the T_g of PDMS was not found, probably because of the low concentration in samples.

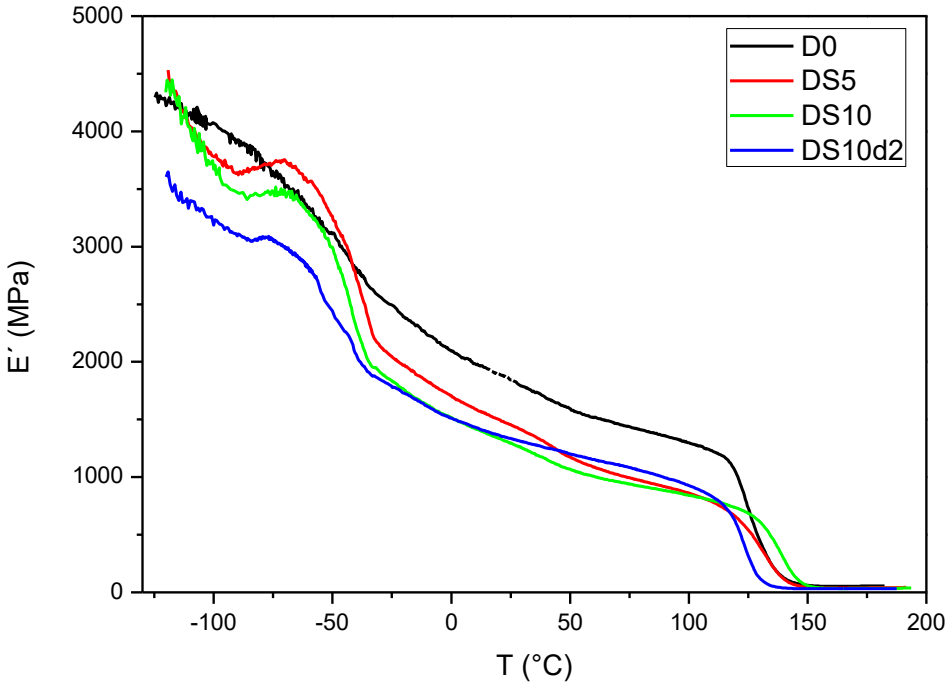

Figure 21: Temperature dependence of elastic moduli of ER/S blends

The Figure 21 shows that there is evident decrease in the stiffness of the blend with increasing amount of silicone. Besides, the effect of the DCP addition to S is not obvious. There is only small improvement of mechanical properties at positive temperatures. Another phenomenon is observed in the γ transition area around -50 °C, which is accentuated by the presence of silicone.

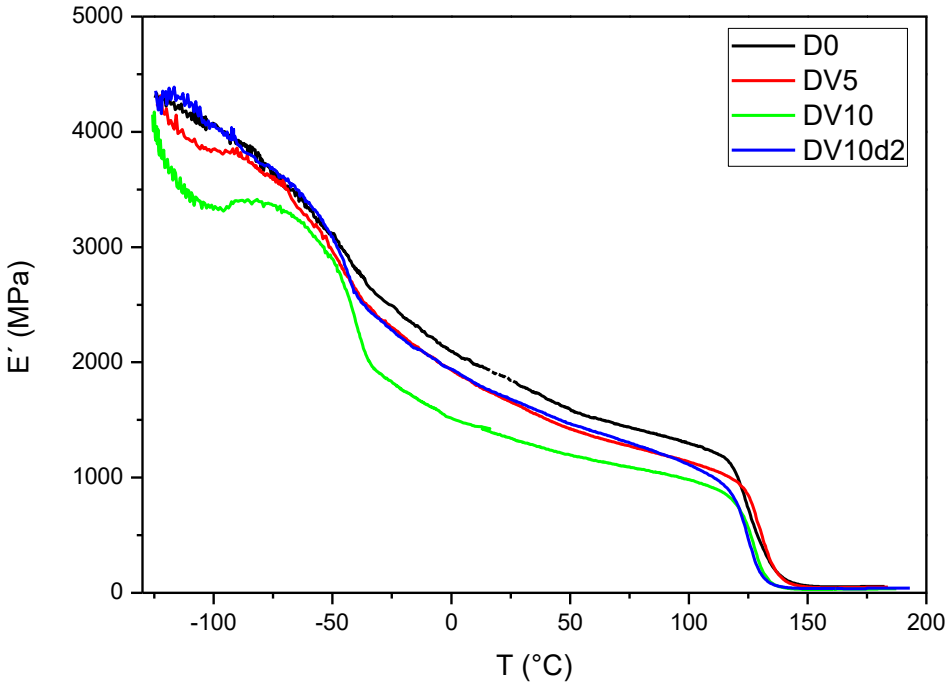

Figure 22: Temperature dependence of elastic moduli of ER/V blends

The blends ER/V (Figure 22) exhibit reduced stiffness likewise as ER/S blends. However, the effect of DCP addition is much clearer than for S: curve of DV10d2 follows the curve DV5 and both are clinging to D0. Another phenomenon is observed in the γ transition area around -50 °C, which is significant only for sample DV10. It can be clearly seen that DCP addition reduce the effect of γ transition.

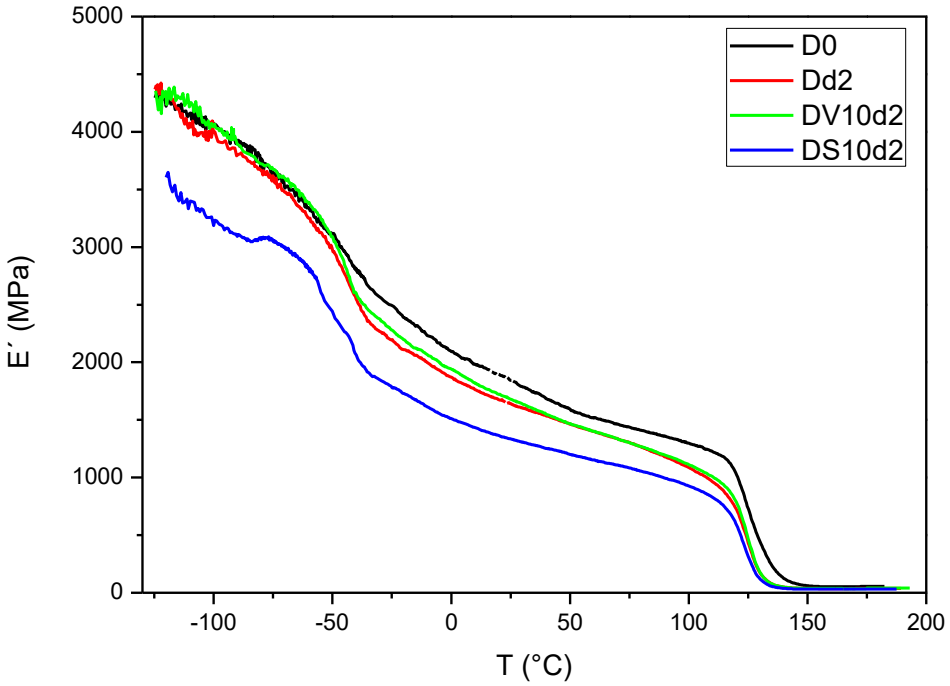

Figure 23: Temperature dependence of elastic moduli of blends

From the comparison of temperature dependence of elastic moduli (Figure 23), it is clear that the compatibility between ER/S is significantly lower than for ER/V. Despite the same amount of PDMS, ER/V blends exhibits much better mechanical properties.

11.3 Tg δ as a function of temperature for polymer blends

Evolution of tangent of loss angle δ is plotted against temperature for polymer blends in Figure 24–26. Generally, the tg δ has very low value (around 0,05) and only if some losses appear in the system, tg δ peaks appear. The highest point of the peak is one of the options how to determine transition temperature.

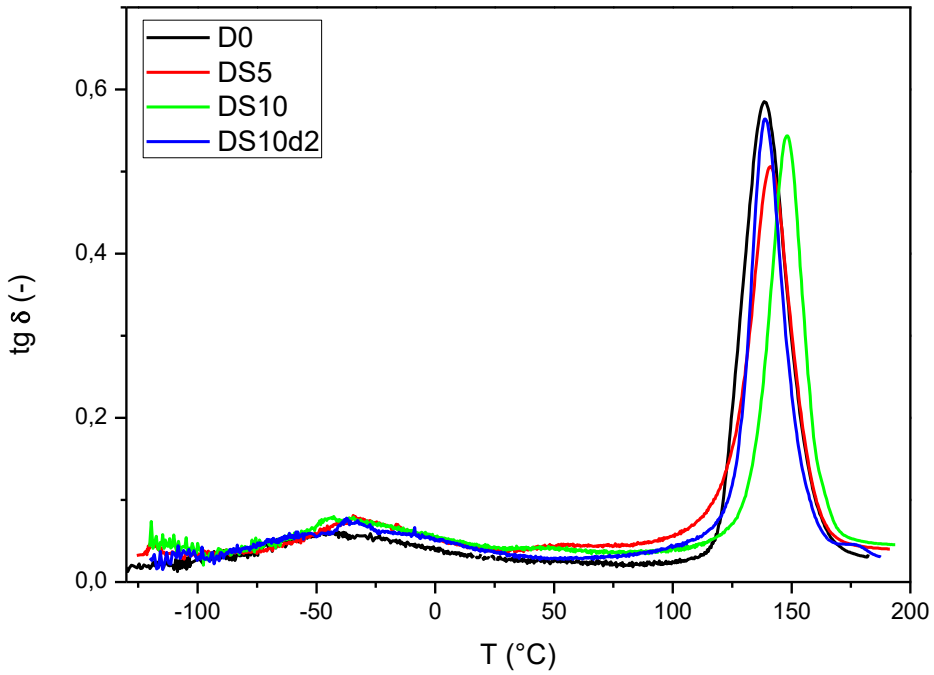

Figure 24: Temperature dependence of tg δ of ER/S blends

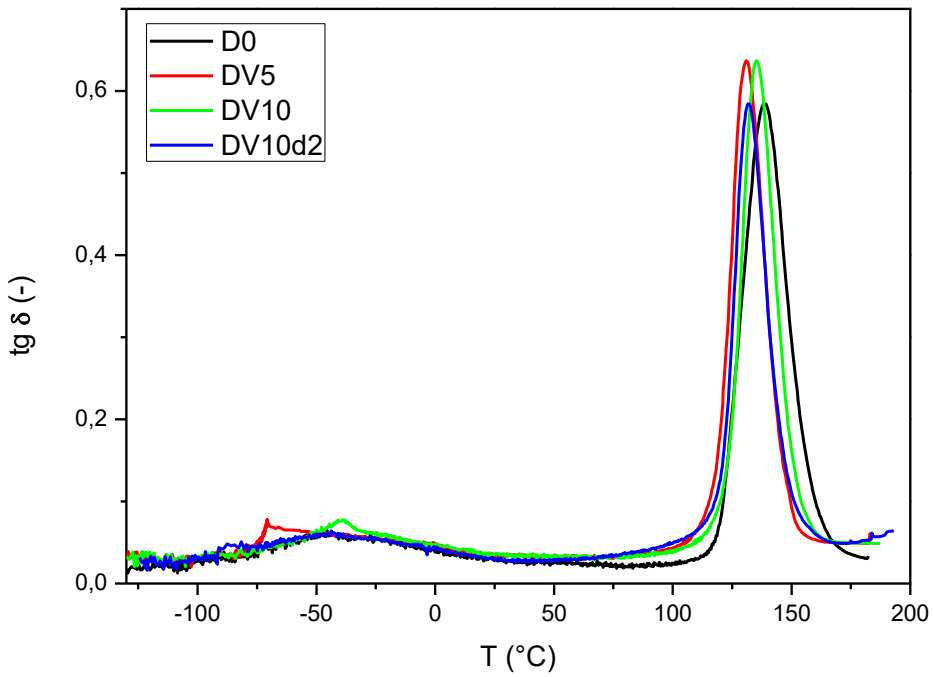

Figure 25: Temperature dependence of tg δ of ER/V blends

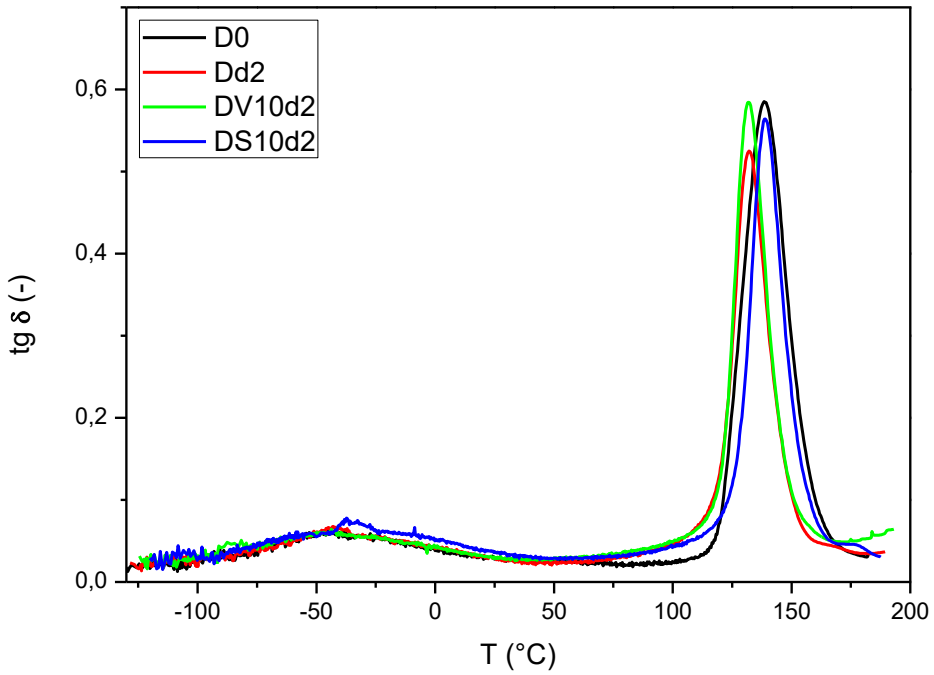

Figure 26: Temperature dependence of tg δ of polymer blends

From Figure 24–26 it is obvious that the highest influence on mechanical properties has T_g, i.e. α transition in region around 140 °C. However the existence of broad γ transition around -50 °C is not negligible. Transition temperatures of ER are shown in Table 7. It was found that the concentration of PDMS is too low to exhibit any difference detectable by DMA.

Table 7: Transition temperatures of prepared blends

Sample	α transition (°C)	γ transition (°C)	Sample	α transition (°C)	γ transition (°C)
D0	139	-46	Dd2	132	-43
DS5	141	-34	DV5	139	-48
DS10	148	-43	DV10	135	-39
DS10d2	139	-37	DV10d2	132	-44

While D0 and some other blends exhibit T_g around 140 °C, two other specimens, namely Dd2 and DV10d2 shown lower T_g. The addition of DCP (Dd2) it probably leads to some degradation of ER or it behaves as a plasticizer. However for blend DV10d2 might be suggested another explanation. Theory says that immiscible polymer blend will exhibit two glass transition temperatures that are equal to the respective polymers, while a complete

miscible blend will have one glass transition between the two polymers. Many polymer blends have partial solubility and will exhibit two glass transitions akin to respective polymers but shifted towards the centre. If this would be the case of DV10d2 blend, it would mean that there is partial miscibility between ER and PDMS. This explanation is supported by SEM images which show presence of an interphase.

The addition of PDMS to ER leads to reduction of stiffness of polymer blend. However, there are significant differences between the effect of PDMS-S and PDMS-V. While the stiffness of mixture ER/V exhibit clings to behaviour of pure resin, ER/S blends tend to have more significant decrease in stiffness. In other words, ER/V blends exhibit higher degree of compatibility than ER/S blends. Glass transitions of blends was observed around T = 140 °C and γ transitions in broad range between -70 °C and -20 °C with a peak around -45 °C.

12 PREPARATION OF POLYMER COMPOSITES

The second part of thesis is focused on preparation of polymer composites, which can be used as an antistatic coating and electromagnetic waves shielding materials. As a matrix of composites was used DV10d2 blend with good mechanical properties (impact strength 1,7 J/cm2) due to uniform distribution of PDMS particles in epoxy resin (SEM images, Figure 16). Three types of fillers were used: carbonyl iron particles with diameter 9 μm (SL type, BASF) labelled as Fe (CI-SL) and carbonyl nickel particles with diameter 3 μm labelled as Ni(3) and 45 μm as Ni(45). The main physical characteristics of fillers are listed in Table 8.

Table 8: Physical characteristics of used fillers [12][77]

Filler	Diameter of particles	Purity	Density	Resistivity
	μm	%	g/cm^3	μΩcm
Carbonyl Iron (SL)	9	99,5	7,9	9,6
Carbonyl Nickel	3-7	99,8	8,9	6,9
	45	99,5		

The major difference between two used fillers is the shape of particles. While carbonyl iron are smooth spheres (Figure 27a), nickel particles are hedhedog-like (Figure 27b).

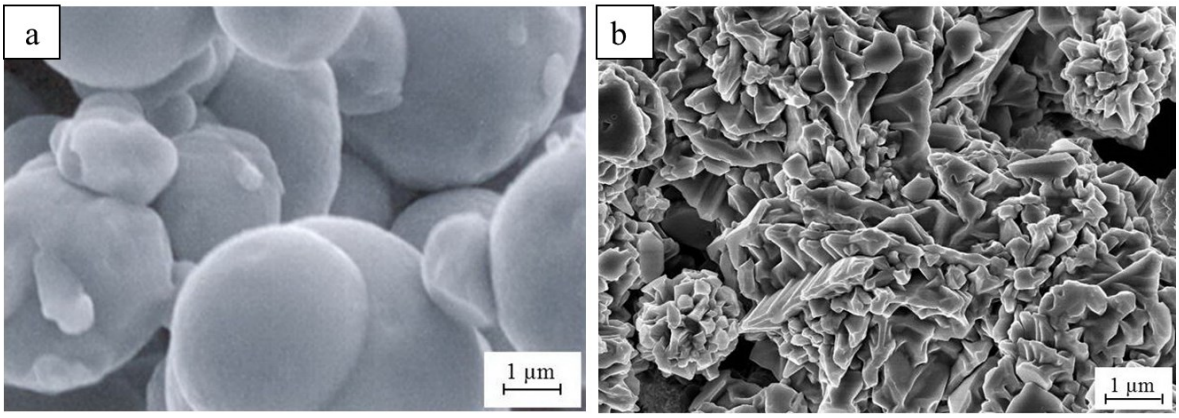

Figure 27: SEM micrographs of filler a) Fe b) Ni

Preparation of composites is based on blend preparation. DGEBA and DCP were put into the triple-neck round-bottom flask and stirred it half an hour at 80 °C. Than PDMS was added and stirred one hour at 130 °C. Afterward metallic filler was added to the blend and

stirred one hour at 80 °C. After cooling to 50 °C, DETA was added and the procedure was continued exactly as explained in the chapter 6 (Preparation of polymer blends).

Weight concentration of metallic fillers was gradually increasing from 10 wt.% up to 70 wt.%. Besides, the effect on electrical properties of different PDMS and DCP contents were studied for samples containing 50 wt.% of CI. List of polymer composites based on polymer blend DV10d2 filled by Fe, Ni(3) and Ni(45) with their composition and codes is listed in the Table 9. Polymer composites based on different matrixes are presented in Table 10.

Table 9: List of composites based on polymer blend DV10d2

Samples	DV10d2	Fe (CI-SL)	Ni(3)	Ni(45)
	(wt.%)	(wt.%)	(wt.%)	(wt.%)
DVdFe10	90	10	-	-
DVdFe20	80	20	-	-
DVdFe30	70	30	-	-
DVdFe40	60	40	-	-
DVdFe50	50	50	-	-
DVdFe60	40	60	-	-
DVdFe70	30	70	-	-
DVdNi(3)10	90	-	10	-
DVdNi(3)20	80	-	20	-
DVdNi(3)25	75	-	25	-
DVdNi(3)30	70	-	30	-
DVdNi(3)40	60	-	40	-
DVdNi(3)50	50	-	50	-
DVdNi(3)60	40	-	60	-
DVdNi(45)10	90	-	-	10
DVdNi(45)20	80	-	-	20
DVdNi(45)30	70	-	-	30
DVdNi(45)40	60	-	-	40
DVdNi(45)50	50	-	-	50
DVdNi(45)70	30	-	-	70

Table 10: List of composites with other polymer matrixes

Samples	DGEBA +DETA	PDMS-V	PDMS-S	DCP	Fe (CI-SL)	Ni(3)
	(wt.%)	(wt.%)	(wt.%)	(wt.%)	(wt.%)	(wt.%)
DFe10	90	-	-	-	10	-
DFe30	70	-	-	-	30	-
DFe50	50	-	-	-	50	-
DV10Fe50	45	5	-	-	50	-
DS10d2Fe50	44	-	5	1	50	-
DS10Fe50	45	-	5	-	50	-
DNi(3)20	80	-	-	-	-	20
DNi(3)30	70	-	-	-	-	30
DNi(3)40	60	-	-	-	-	40

13 MORFOLOGY OF POLYMER COMPOSITES

Morphologies of samples were investigated by scanning electron microscope NOVA NanoSEM 450 (FEI). Samples for test were prepared by cooling in liquid nitrogen and fractured by mechanical force.

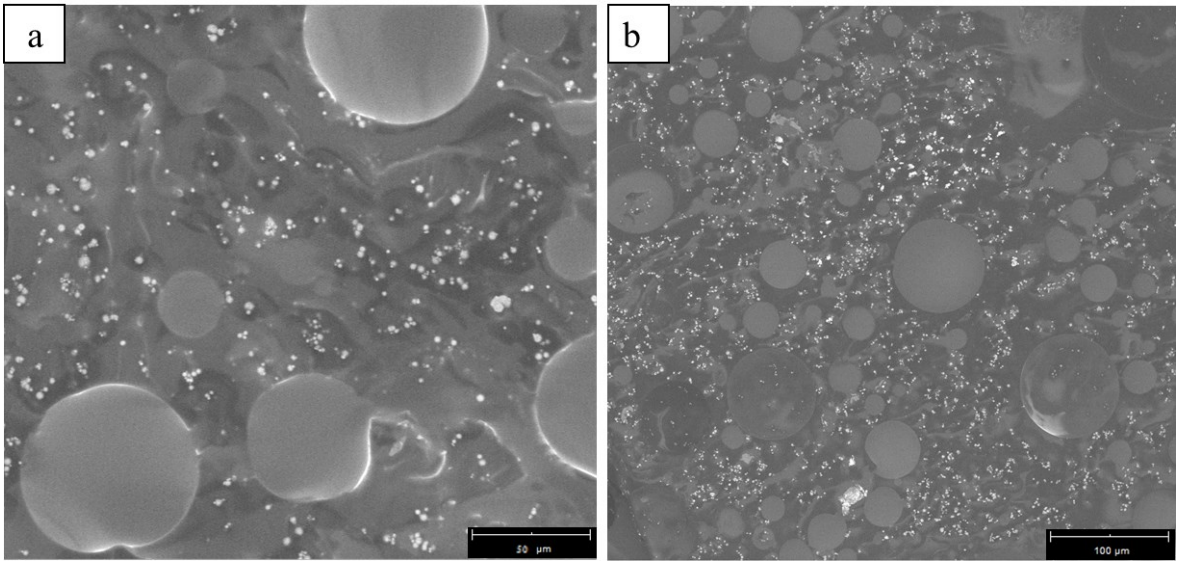

Figure 28: SEM micrographs for polymer composites based on polymer blend DV10d2 filled with 40 wt.% of a) 9 µm-sized carbonyl iron particles, b) 3 µm-sized carbonyl nickel particles

In Figure 28 we can observe the silicone phase (gray spheres) and the metal particles (white dots) dispersed in the continuous phase of the epoxy resin. Micrographs show that the metal filler is dispersed mostly within the epoxy phase. This occurred for both composites filled with carbonyl iron particles (Figure 28a) and composites filled with carbonyl nickel particles (Figure 28b). This can be caused by the fact that silicone particles are very well and preferably cross-linked by peroxides. Thus, for metal particles, the silicone phase becomes less available than the epoxy phase.

14 DC ELECTRICAL PROPERTIES

Polymer composites with low DC electrical conductivity (<10^{-8} S/cm) were measured by 2-point method by using programmable electrometer (KEITLEY 6517A, USA), which also served as a DC power source. While the samples with higher conductivity (>10^{-8} S/cm) were measured by 4-point method by using programmable electrometers (KEITLEY 6517B, 2410) and (KEITHLEY 7002 Switch system). From each composite (Table 9) were prepared three cylindrical specimens with a diameter of 1,5 cm and thickness of 2 mm. Specimens were measured under DC voltage (10 V). Mass concentration of filler was converted to the volume concentrations.

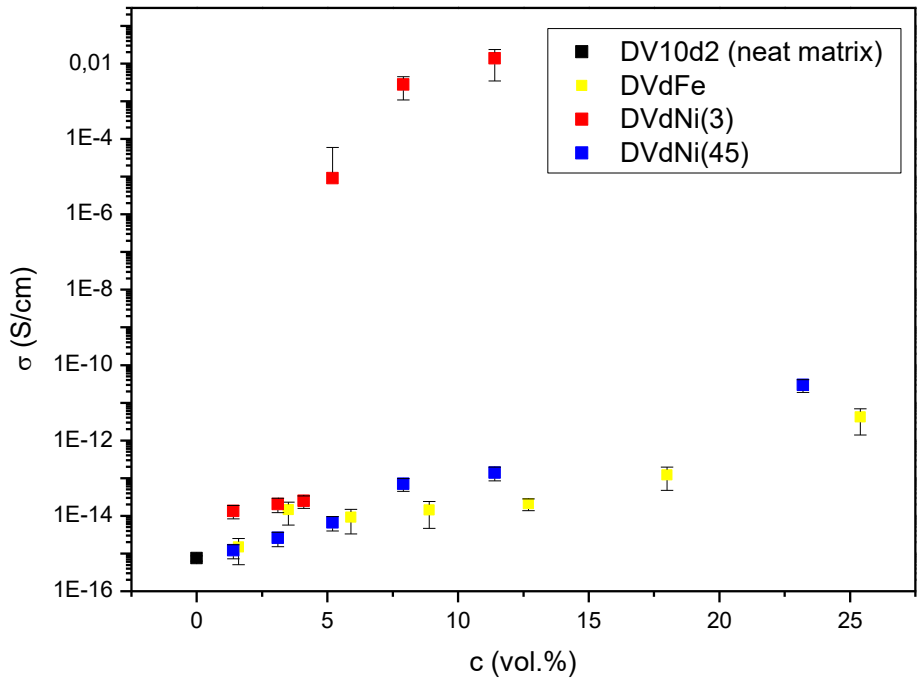

Figure 29: Comparison of DC conductivity for polymer composites based on DV10d2 matrix filled by Fe, Ni(3) and Ni(45) particles

DC Conductivity of composites based on DV10d2 matrix filled with carbonyl iron and carbonyl nickels are compared in Figure 29. Percolation threshold is observed only for hedgehog particles Ni(3) at relatively small concentration 5 vol.%. Increase of conductivity at percolation threshold is from 10^{-14} S/cm to 1a0^{-8} S/cm. According to the mathematical model as introduced by Schren-Zallen [78], the percolation limit was reached between (14–17) vol.% for randomly distributed conducting spheres. However, composites filled with Fe (CI-SL) particles (9 μm) with similar dimension as Ni(3) does not reach percolation

threshold even at five times higher concentration. It is caused by different shape of particles. While CI particles are smooth spheres, Ni particles are hedgehog-like with many protrusions. This significantly increases the probability that particles will be in touch and thus create a conductive path connecting both sides of the sample. On the other side, Ni(45) particles also did not reach percolation threshold even if they have similar shape. The reason is 15 times larger diameter of Ni(45) than for Ni(3). It means that there is roughly 3000 particles in Ni(3) for 1 particle of Ni(45) in same weight amount of filler, which significantly increases the chance that particles will form clusters and reach percolation threshold at much lower concentration.

15 DIELECTRIC SPECTROSCOPY

Dielectric spectroscopy of composites was measured by using impedance analyser Novocontrol (Concept 50, Germany). Samples with the same dimension as for DC conductivity measurement (chapter 14 DC electrical properties) were measured by AC voltage (2 V) in a frequency range (10^{-1}–10^{6}) Hz. As a result, frequency dependent AC conductivity, real and loss par of complex permittivity of composites were obtained.

15.1 Polymer composites filled with carbonyl iron particles

In this chapter was studied the influence of polymer matrix and amount of filler on dielectric behaviour of polymer composites filled with carbonyl iron.

15.1.1 Polymer composites filled with carbonyl iron based on blend DV10d2

In Figure 29 is presented AC conductivity in frequency dependence of polymer composites filled with carbonyl iron particles. The gradual increase in conductivity suggests that dielectric behaviour of polymer composites with CI is driven mostly by polarization process. Among the composites, only DVdFe70 exhibits DC plateau indicating free current availability.

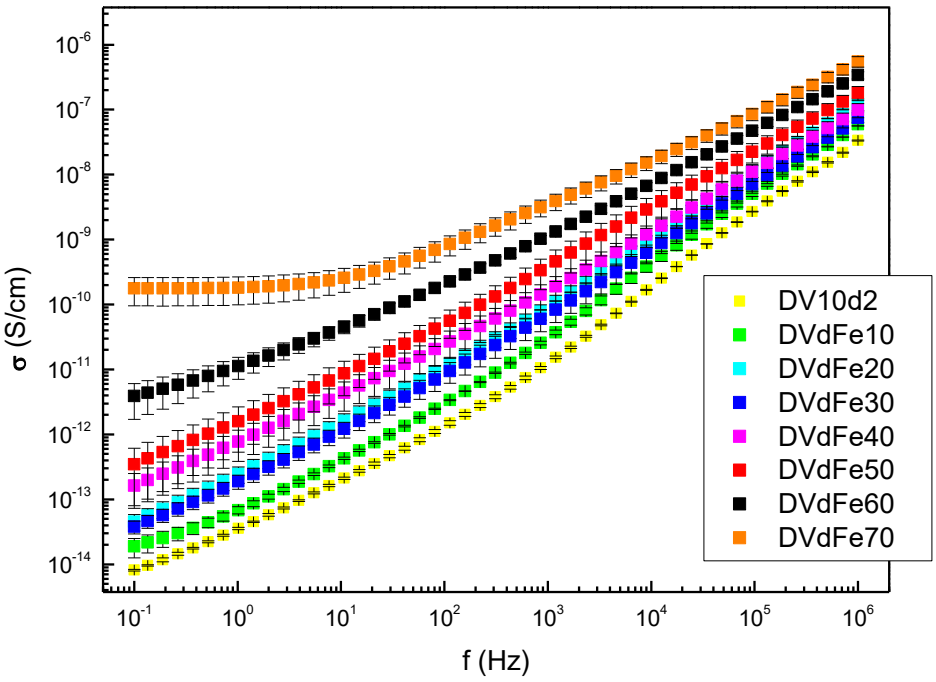

Figure 30: Frequency dependence of AC conductivity for composites based on DV10d2 matrix filled with Fe (CI-SL) particles

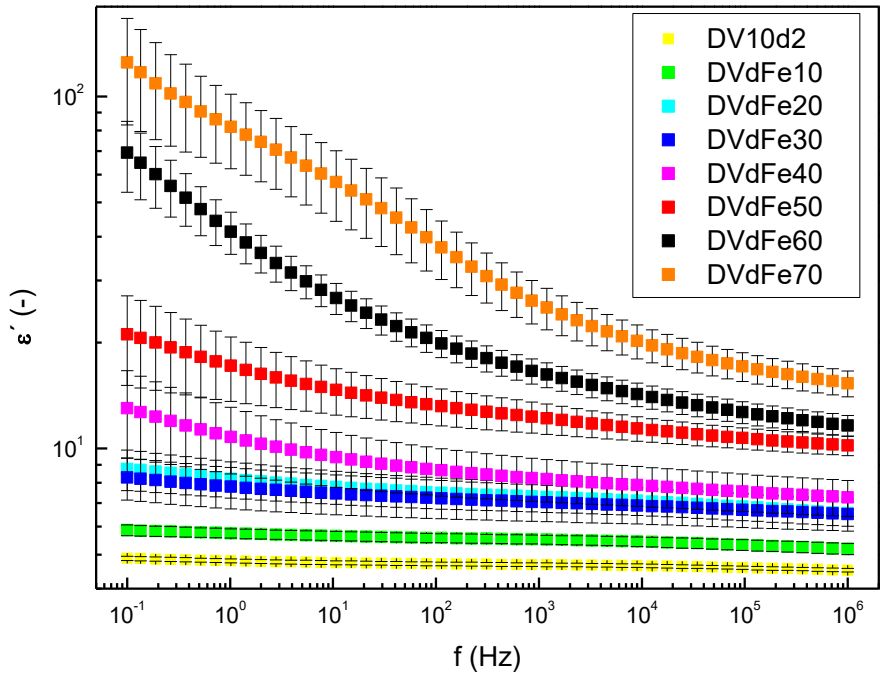

Figure 31: Frequency dependence of real part of complex permittivity for composites based on DV10d2 matrix filled with Fe (CI-SL) particles

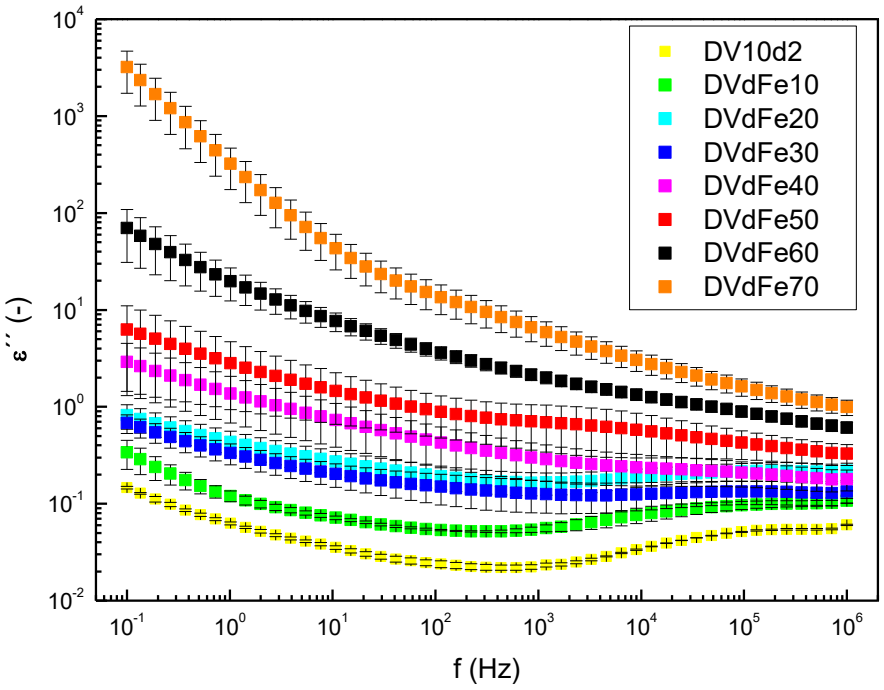

Figure 32: Frequency dependence of loss part of complex permittivity for composites based on DV10d2 matrix filled with Fe (CI-SL) particles

The blend DV10d2 exhibits dielectric behaviour. AC conductivity (Figure 30) is exponentially increasing with frequency, due to polarization current caused by the movement of electric dipole moments. This is typical for materials consisting of phases with different conductivities. Real part of the complex permittivity (Figure 31) of polymer blend has value 4,5 independent on frequency and only small changes (10^{-2}–10^{-1}) for low value of loss part of complex permittivity (Figure 32) can be observed. With addition of iron particles is observed gradual increase in all quantities, however the composites behave still as a dielectrics. At high concentrations of CI (>50 wt.%) interfacial polarizability leading to significant increase of both real and loss parts of complex permittivity at low frequencies. AC conductivity (Figure 30) of all composites is driven by polarization current, except DVdFe70 which exhibit DC plateau in the frequency range (10^{-1}–10^{1}) Hz, which indicates free current. However, the amount of filler was not sufficient enough to reach percolation threshold.

15.1.2 Influence of PDMS on dielectrical behaviour of composites with carbonyl iron particles

The effect of matrix with or without PDMS-V on electric properties of polymer composites filled with carbonyl iron were studied for (10, 30 and 50) wt.% concentration of CI.

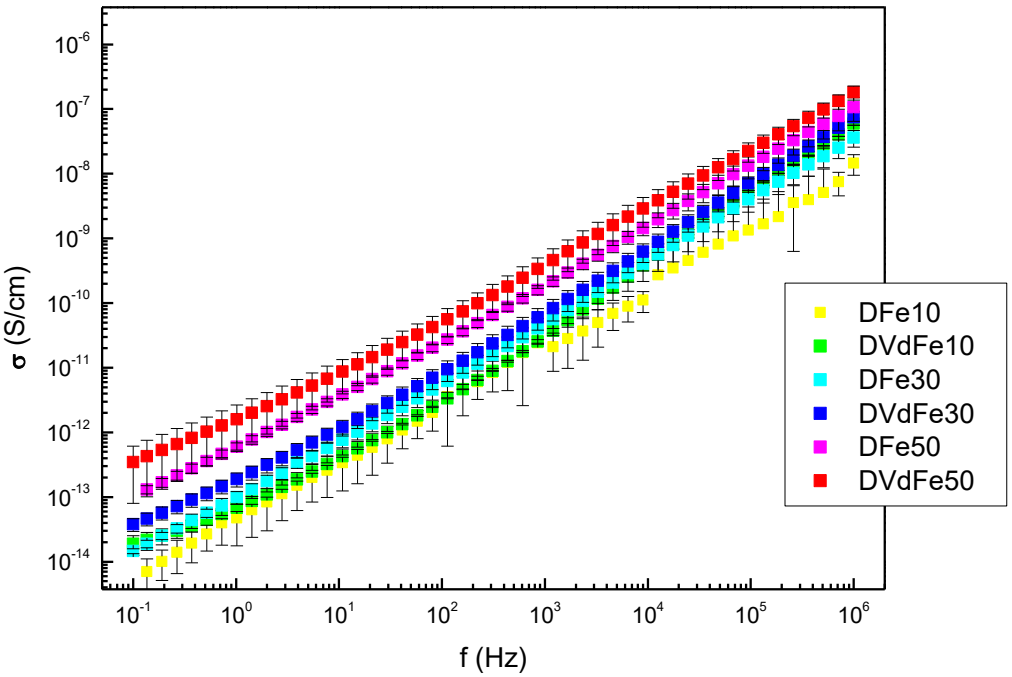

Figure 33: Frequency dependence of AC conductivity for polymer composites based on D0 and DV10d2 matrix filled with Fe (CI-SL) particles

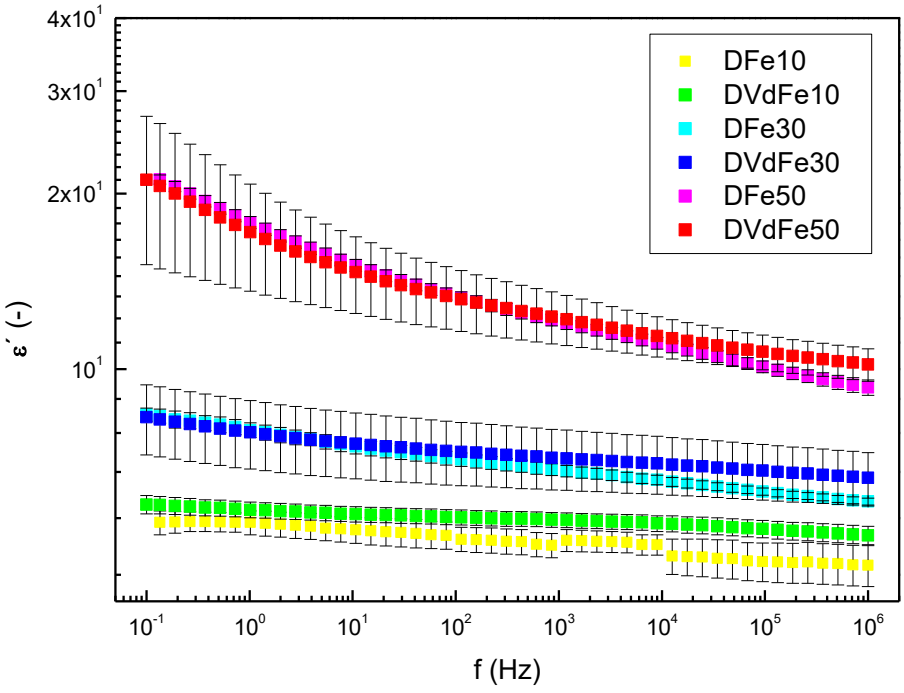

Figure 34: Frequency dependence of real part of complex permittivity for polymer composites based on D0 and DV10d2 matrix filled with Fe (CI-SL) particles

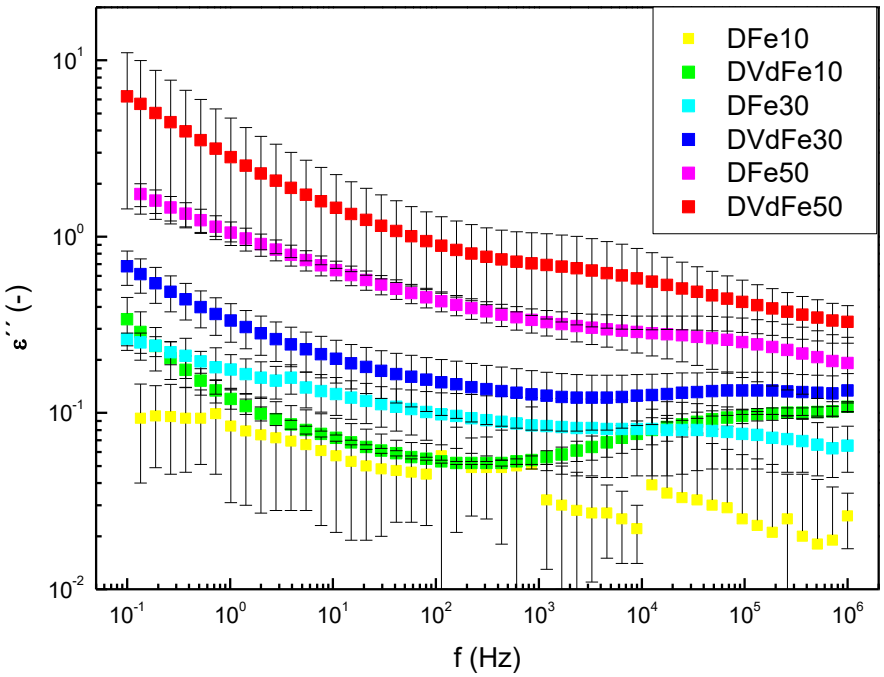

Figure 35: Frequency dependence of loss permittivity for polymer composites based on D0 and DV10d2 matrix filled with Fe (CI-SL) particles

From the comparison of conductivity of polymer composites based on epoxy matrix with and without PDMS (Figure 33) might someone think that there is not much difference, however, the increase of conductivity is (50–100) % as shown in Table 11. Real part of complex permittivity effectively (Figure 34) describes the ability of dipoles to rotate in AC field which is dominantly controlled by amount of filler and therefore there are negligible differences caused by different matrixes. However, the dielectric losses (Figure 35), which are connected with conductivity, exhibit increase if blends are used instead of neat ER.

Table 11: AC conductivity of polymer composites filled with carbonyl iron particles at f = 1200 Hz

Concentration of CI (wt. %)	AC conductivity at f = 1200 Hz (S/cm)	
	Matrix D0	Matrix DV10d2
10	$(2 \pm 1)\ 10^{-11}$	$(4 \pm 1)\ 10^{-11}$
30	$(6 \pm 3)\ 10^{-11}$	$(8 \pm 3)\ 10^{-11}$
50	$(2 \pm 1)\ 10^{-10}$	$(5 \pm 2)\ 10^{-10}$

The results obtained can be explained by the morphology of ER/V blend. Some volume of blend is filled by PDMS and therefore this volume is inaccessible to electrical filler which is in agreement with SEM (Figure 28). It means that carbonyl iron particles which are excluded from rubber particles are within the epoxy resin phase. Therefore the concentration of conductive filler in epoxy resin is higher, thus AC conductivity is also higher.

15.1.3 The effect of polymer matrixes on dielectric properties of composites filled with 50 wt.% of carbonyl iron

The effect of matrixes with cross-linked and uncross-linked particles of both elastomers on electrical properties were studied for polymer composites containing 50 wt.% of carbonyl iron particles.

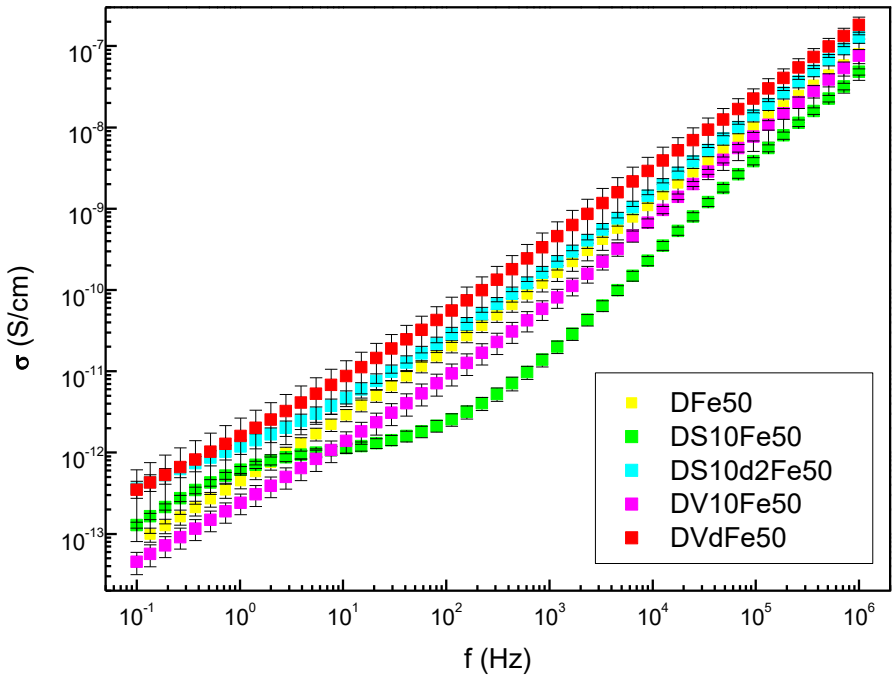

Figure 36: Frequency dependence of AC conductivity of composites based on different matrixes containing 50 wt.% of Fe (CI-SL) particles

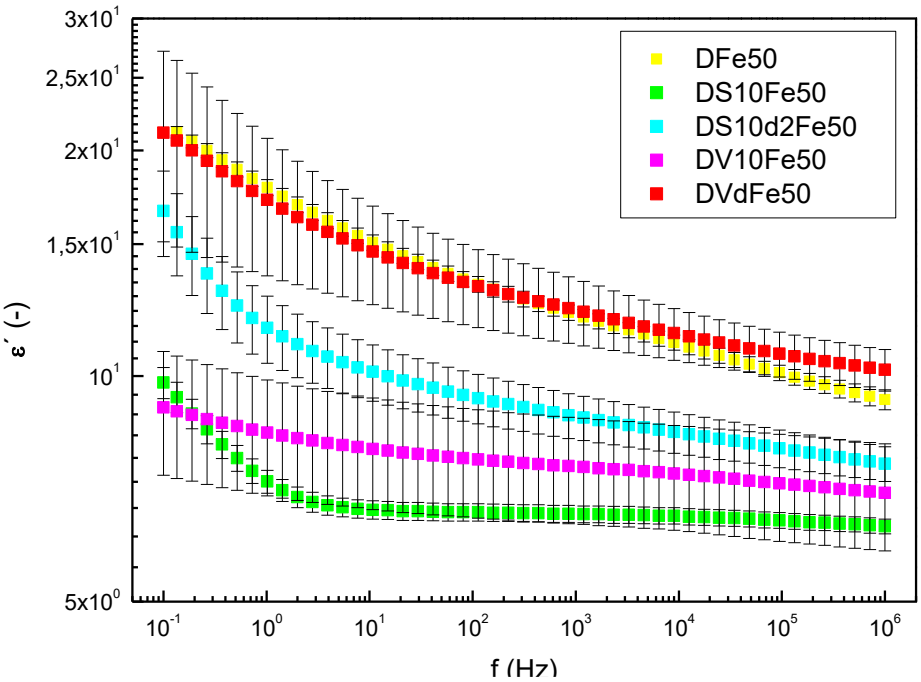

Figure 37: Frequency dependence of real part of complex permittivity of composites based on different matrixes containing 50 wt.% of Fe (CI-SL) particles

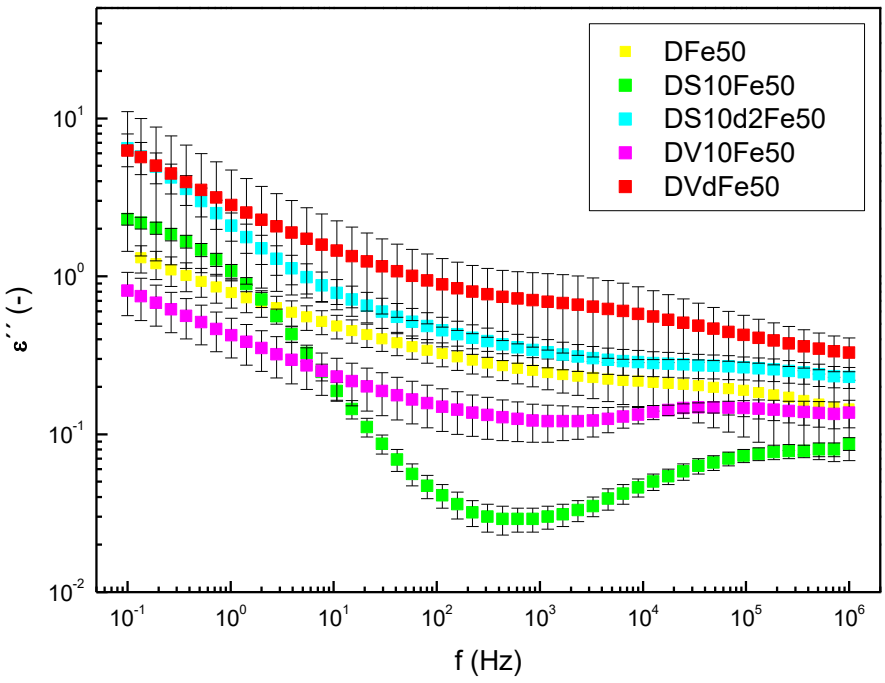

Figure 38: Frequency dependence of loss part of complex permittivity of composites based on different matrixes containing 50 wt.% of Fe (CI-SL) particles

It is clear from Figure 36 that usage of uncross-linked particles of PDMS (without DCP) leads to decrease of AC conductivity while crosslinked particles (with DCP) exhibit synergic effect on AC conductivity. This effect was found for both used elastomers (S and V). It might be caused by better affinity of iron particles to PDMS than to ER. Therefore some CI might be trap inside of rubber inclusions which are effectively isolated islands in continuous phase of epoxy resin.

Interestingly, it was found that usage of PDMS-S instead of PDMS-V leads to slight decrease of conductivity. This difference is even more obvious when real and loss pats of complex permittivity are compared (Figure 37, 38). This might be due to higher purity of PDMS-V than PDMS-S, which might lead to better dispersion of CI in polymer blend.

15.2 Polymer composites filled with carbonyl nickel particles

In this chapter was studied the influence of polymer matrix and amount of filler on dielectric behaviour of polymer composites filled with carbonyl nickel particles.

15.2.1 Polymer composites filled with Ni(45)

Frequency dependence of AC conductivity of polymer composites filled with 45 μm-sized nickel particles is shown in Figure 39. The gradual increase in conductivity of composites with filler concentration suggests that polymer composites with Ni(45) exhibit only polarization processes.

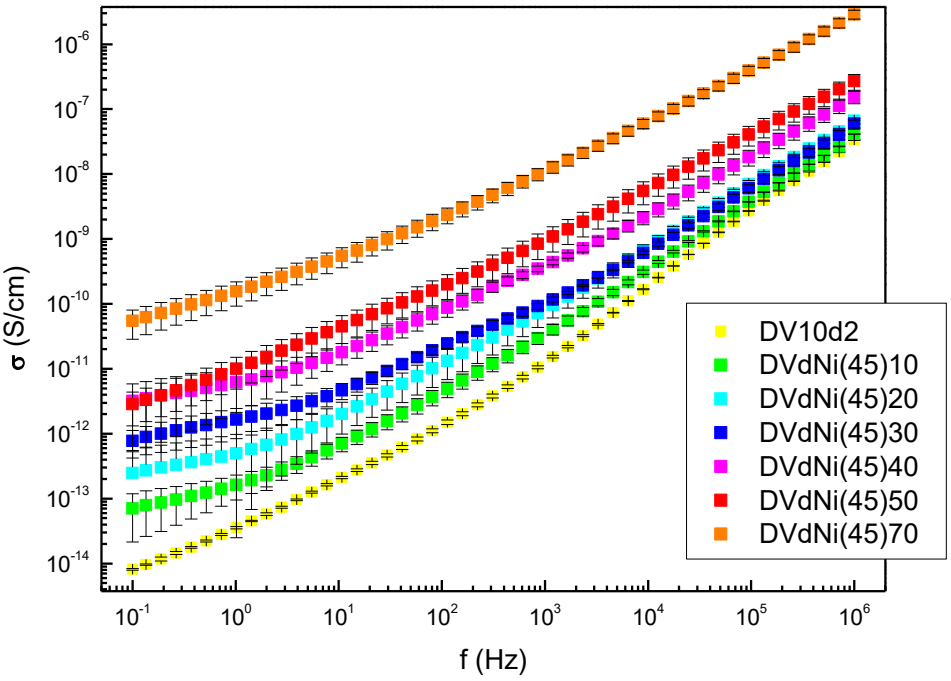

Figure 39: Frequency dependence of AC conductivity for polymer composites based on DV10d2 matrix filled with Ni(45) particles

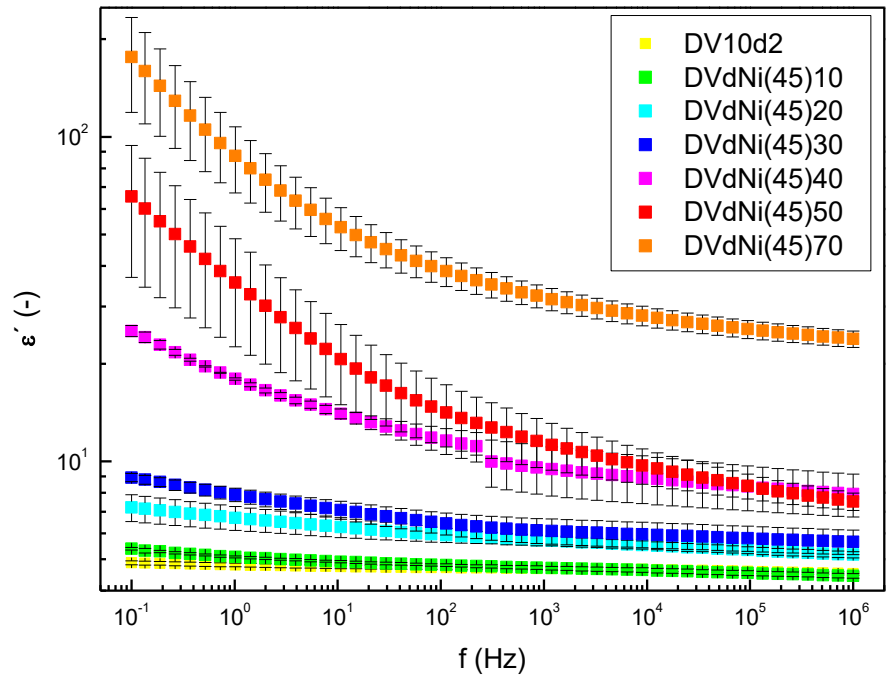

Figure 40: Frequency dependence of real part of complex permittivity for polymer composites based on DV10d2 matrix filled with Ni(45) particles

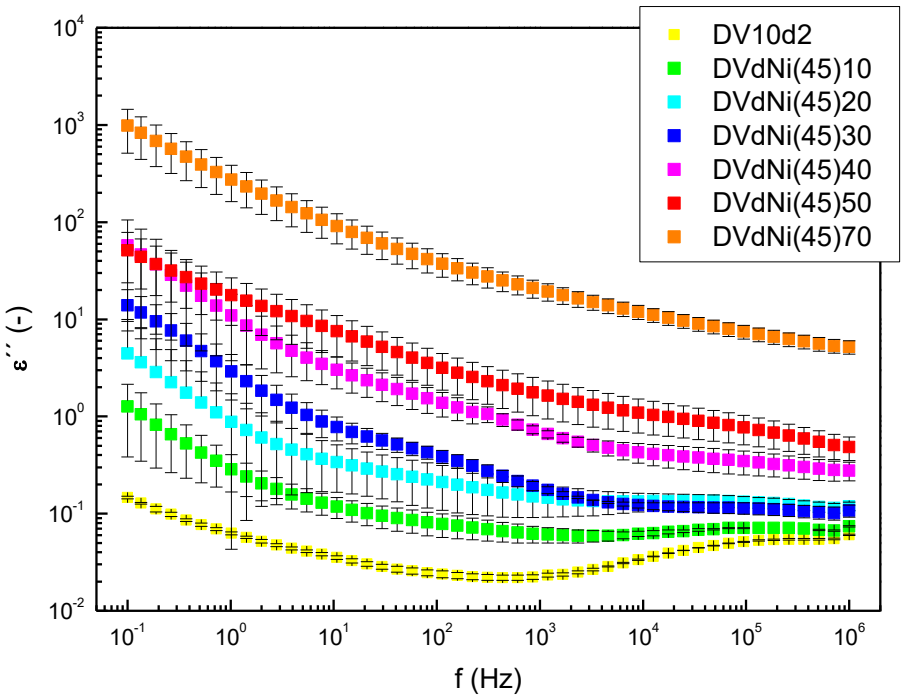

Figure 41: Frequency dependence of loss part of complex permittivity for polymer composites based on DV10d2 matrix filled with Ni(45) particles

The observed effect of nickel particles with diameter 45 μm on dielectric properties of composites is similar to what was observed for 9 μm-sized carbonyl iron particles filled composites, i.e. gradual increase of AC conductivity and complex permittivity with filler concentration. However the DC plateau was not observed for any composites (Figure 39). Indeed, the real part of permittivity increase from tens for low-filed composites (up to 30 wt.% of Ni(45) particles) to hundreds for composites with 70 wt. % (Figure 40).

15.2.2 Polymer composites filled with Ni(3)

The size of electroconductive particles significantly influence the behaviour of polymer composites in both, AC and DC electrical fields. Thus, the nickel particles with diameter 3 μm represent smaller particles if compared with nickel particles with diameter 45 μm. Therefore the number of charge carriers in polymer composites with Ni(3) is significantly higher and percolation threshold was reached at as low concentration as 30 wt.% (5,2 vol.%).

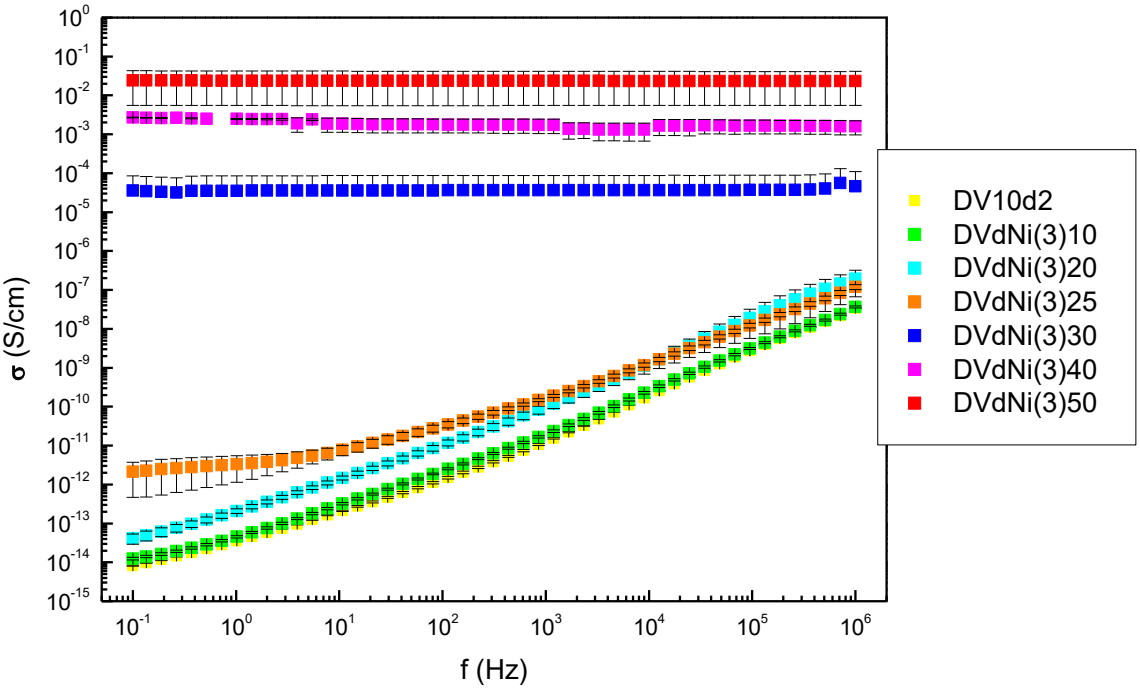

Figure 42: Frequency dependence of AC conductivity for composites based on DV10d2 matrix filled with Ni(3) particles

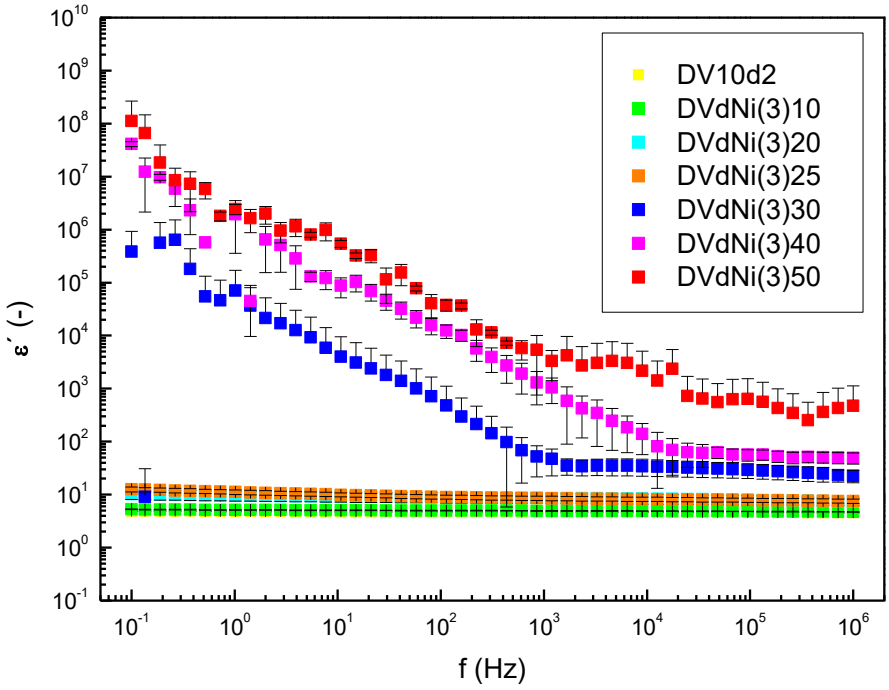

Figure 43: Frequency dependence of real part of complex permittivity for composites based on DV10d2 matrix filled with Ni(3) particles

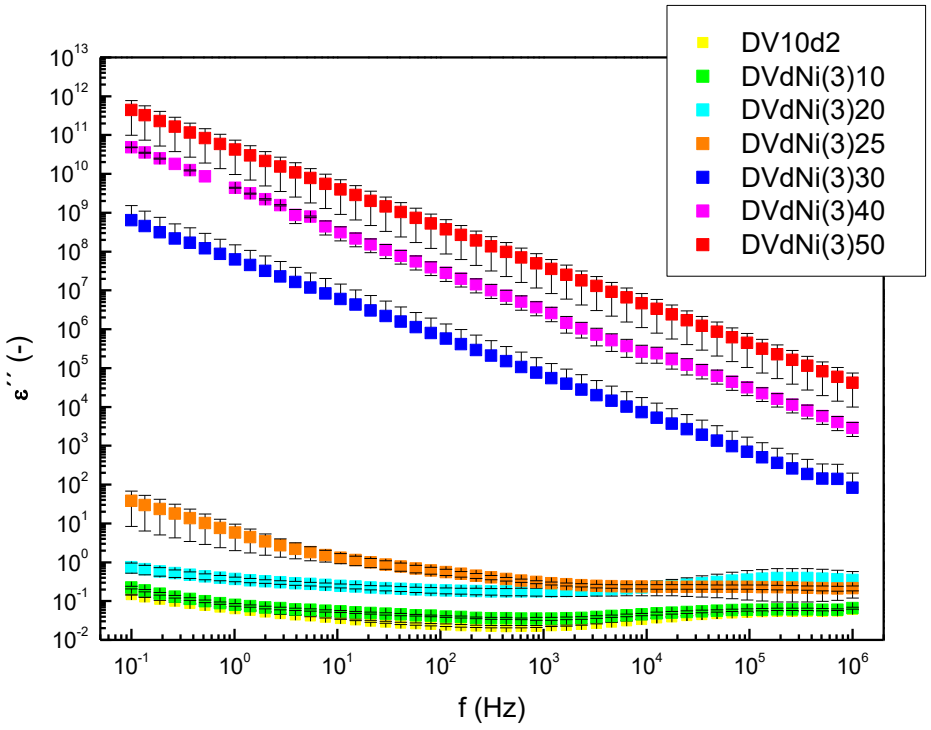

Figure 44: Frequency dependence of loss part of complex permittivity for composites based on DV10d2 matrix filled with Ni(3) particles

While Ni(3) composites (Figure 42) with low filling (up to 25 wt.%) behave as dielectrics with polarization dipolar conductivity, conductivity of composites with more than 30 wt.% of Ni(3) reached percolation threshold and exhibit only free conductivity. The standard deviation at the concentration 30 wt.% is enormous due to fact that while some samples at this concentration behave as a conductors, the other exhibit insulator behaviour. This is given by certain probability that particles will create a conductive path from one side of the specimen to the other side. At filler concentration above percolation threshold (>25 wt.%) is again observed exponential increase of conductivity and composites behave as conductors with frequency dispersion of complex permittivity (Figure 43, 44). Therefore is observed the decrease (5 orders of magnitude) of permittivity with increasing frequency. Also it is important to note that the values of loss part of complex permittivity $\varepsilon'' = (10^3–10^{12})$ are higher than real part of complex permittivity $\varepsilon' = (10^2–10^8)$ which is also sign of conductor behaviour.

15.2.3 Influence of PDMS on dielectric behaviour of composites filled with Ni(3)

The effect of matrix with or without PDMS-V on dielectric properties of polymer composites filled with nickel particles were studied for composites with (20, 30 and 40) wt.% of Ni(3).

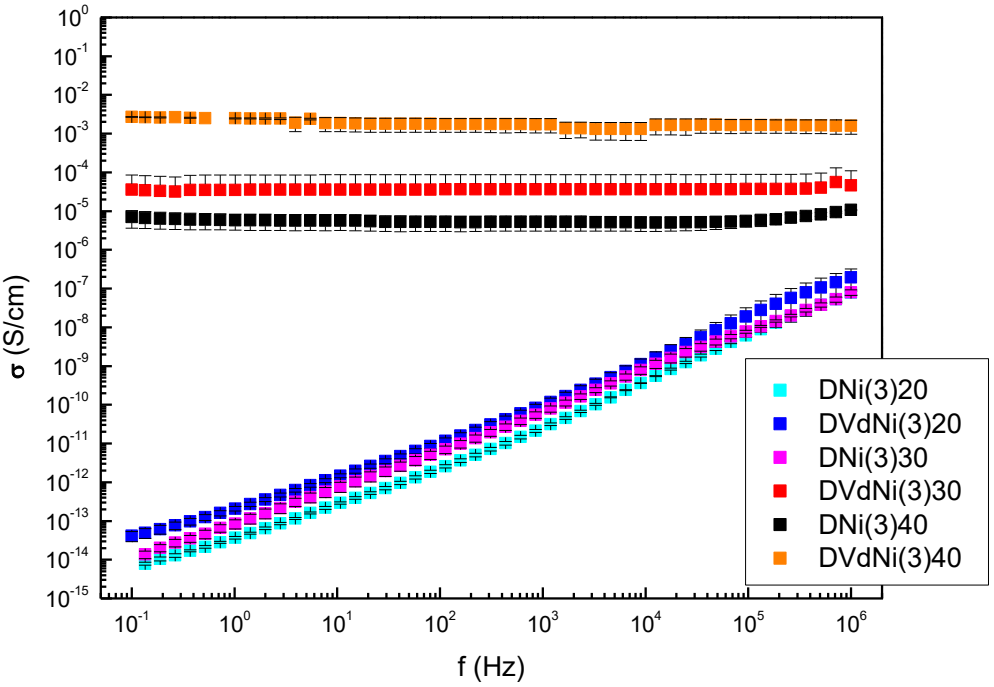

Figure 45: Frequency dependence of AC conductivity for composites based on D0 and DV10d2 matrix filled with Ni(3) particles

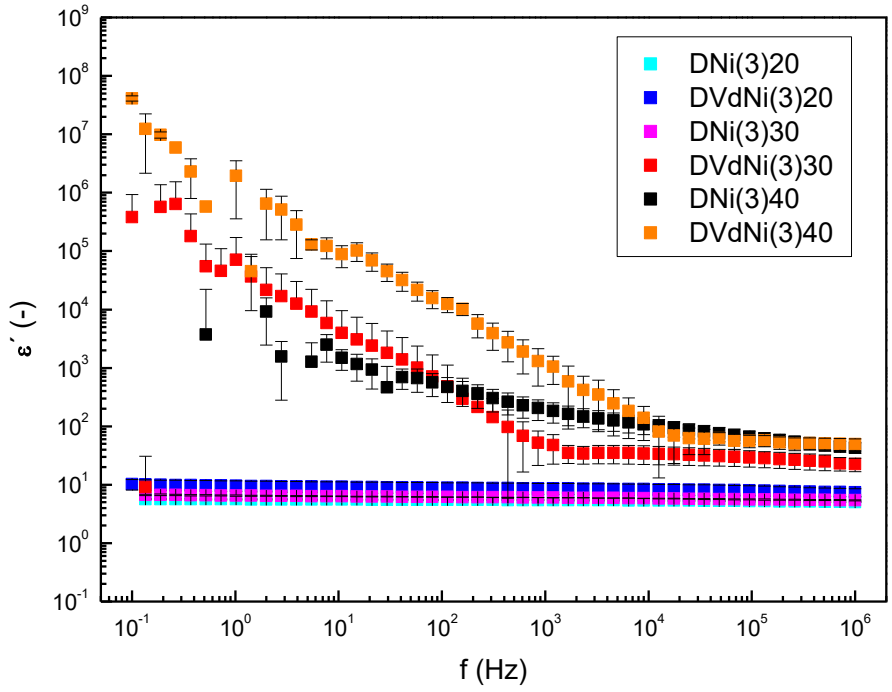

Figure 46: Frequency dependence of real part of complex permittivity for composites based on D0 and DV10d2 matrix filled with Ni(3) particles

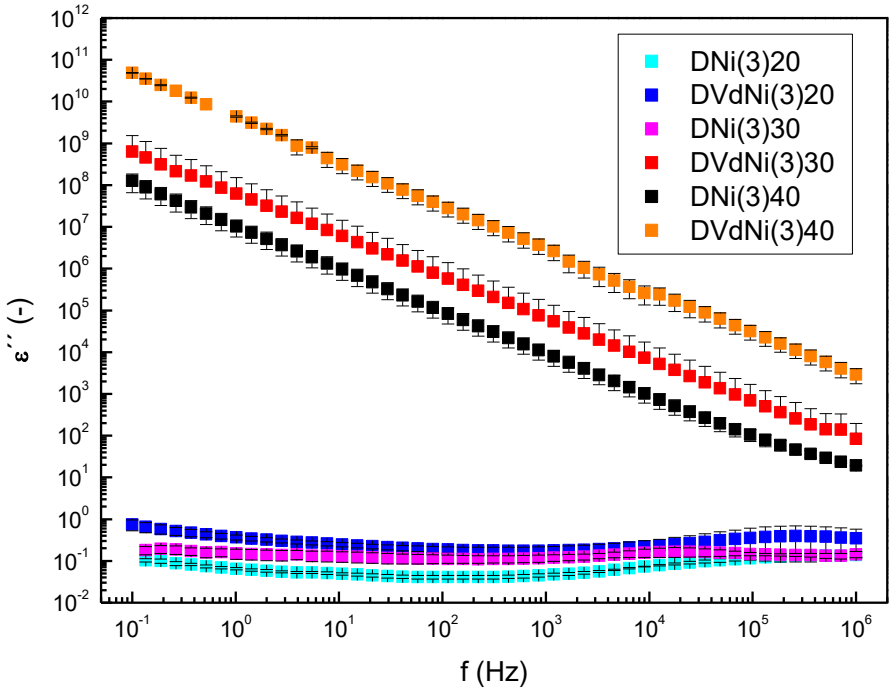

Figure 47: Frequency dependence of real part of complex permittivity for composites based on D0 and DV10d2 matrix filled with Ni(3) particles

The effect of PDMS on composites dielectric properties filled with nickel particles is more evident than for composites filled with carbonyl iron particles. According to the AC conductivity frequency dependence (Figure 45), the addition of PDMS to epoxy resin decreases the percolation threshold of composites filled with Ni(3) particles: the polymer composites with PDMS reach percolation threshold at 30 wt.% (5,2 vol.%) of Ni(3), whereas polymer composites without PDMS required 40 wt.% (7,9 vol.%) of Ni(3). This is caused by exclusion of metal particles from rubber phase as can be seen in Figure 28. Moreover, ER/PDMS composite filled with 40 wt.% of Ni(3) exhibits the AC conductivity of two orders of magnitude higher than ER composite filled with the same concentration of filler.

CONCLUSIONS

The diploma work is aimed at the investigation of the addition of polydimetylsiloxanes (PDMS) for processing of epoxy resin ER-PDMS blends with improved physical-mechanical properties. Such type of polymer matrix can be used for the preparation of antistatic coatings and the design of electromagnetic shielding materials.

To this end, the epoxy resin based on diglycidyl ether bispfenol A (DGEBA) has been modified by two types of PDMS: polydimethylsiloxane (PDMS) vinylterminated (V) and PDMS Sylgard 184 (S). The epoxy monomer was cured with diethylentriamine (DETA) as a hardener in the presence of dicumyl peroxide (DCP) as a crosslinking agent of PDMS.

The composite materials were prepared by addition of conducting filler (carbonyl iron and nickel particles) to the blends. The morphology, network structure, and the mechanical and fracture behaviour of modified epoxy resin and its composites with conducting fillers have been determined by SEM, DMA, Dielectric Spectroscopy, Charpy impact strength and Rheological studies.

The conducted investigations showed the following:

1) The addition of PDMS to ER gives rise to a phase-separated structure consisting of elastomer domains dispersed in the epoxy phase. Moreover, homogeneous distribution of elastomer inclusions in ER can be achieved by (i) introduction of DCP (2 wt. %) that plays a role of compatibilizer, and (ii) the use of PDMS-V rather than PDMS-S, since former reacts better with ER during the curing process.
2) The stiffness of the modified DGEBA decreases with increase of PDMS concentration.
3) According to the charpy impact test, the highest impact strength is recorded with samples with PDMS-V (10 wt.%) in the presence of DCP (2 wt.%) in ER due to the interfacial compatibility between PDMS and resin: the Charpy impact strength reached (1,7 ± 0,1 J/cm2), which equals to a 70 % improvement.
4) By electrical conductivity measurements, the cross-linked PDMS-V increased conductivity and shifted the percolation threshold from 8 vol.% to 5 vol.% for polymer composites filled with Ni particles.
5) The metallic filler's geometry in polymer composites leads to (i) increase of conductivity with decreasing size of filler and (ii) increase of conductivity with increased specific surface of filler particles.

BIBLIOGRAPHY

[1] Ratna, Debdatta. Handbook of thermoset resins. Shawbury: Smithers Rapra, 2009. ISBN 9781847354105

[2] EPOXY: *Tomorrow's technology today.* http://www.epoxy-europe.eu [online]. [cit. 2017-04-24]. Dostupné z: http://www.epoxy-europe.eu/en/applications/

[3] Jones, R.G., et. al. *Silicon-Containing Polymers The Science and Technology of Their Synthesis and Applications*. Dordrecht: Springer Netherlands, 2000. ISBN 9789401139397.

[4] J C Lötters et al., "The Mechanical Properties of the Rubber Elastic Polymer Polydimethylsiloxane for Sensor Applications," *Journal of Micromechanics and Microengineering* 7, no. 3 (1999): 145–47, doi:10.1088/0960-1317/7/3/017.

[5] Alvaro Mata, et. al."Characterization of Polydimethylsiloxane (PDMS) Properties for Biomedical Micro / Nanosystems Characterization of Polydimethylsiloxane (PDMS) Properties for Biomedical Micro / Nanosystems," *Springer* 2, no. April 2016 (2006): 281–93, doi:10.1007/s10544-005-6070-2.

[6] Denisov, E. T., et. al. *Handbook of free radical initiators*. Hoboken, N.J.: Wiley-Interscience, 2003. ISBN 9780471207535.

[7] *Process for the preparation of dicumyl peroxide*. USA. US 06/324,144. Uděleno 15.2.1983.

[8] Polymer Properties Database: INITIATOR HALF-LIFE. *Http://polymerdatabase.com* [online]. [cit. 2017-04-22]. Dostupné z: http://polymerdatabase.com/polymer%20chemistry/t-half2.html

[9] Nakamura T. Suyama S., Ishigaki H., Watanabe Y., " Crosslinking of Polyethylene by Dicumyl Peroxide in the Presence of 2,4-Diphenyl-4-methyl-1-pentene" *Polymer Journal* 27, no. 4 (1995): 371–75.

[10] Jacob Heiner, Bengt Stenberg, and Maria Persson, "Crosslinking of Siloxane Elastomers," *Polymer Testing* 22, no. 3 (2003): 253–57, doi:10.1016/S0142-9418(02)00081-8.

[11] Baoshan Zhang et al., "Microwave-Absorbing Properties of de-Aggregated Flake-Shaped Carbonyl-Iron Particle Composites at 2-18 GHz," *IEEE Transactions on Magnetics* 42, no. 7 (2006): 1778–81, doi:10.1109/TMAG.2006.874188.

[12] Lopatin, Alexander. Polymer magnetic composites for microwave absorbers: Polymerní magnetické kompozity pro mikrovlnné absorbéry : English doctoral thesis. Zlín: Tomas Bata University in Zlín, 2009. ISBN 9788073188443.

[13] Madina A. Abshinova et al., "Correlation between the Microstructure and the Electromagnetic Properties of Carbonyl Iron Filled Polymer Composites," *Composites Part A: Applied Science and Manufacturing* 38, no. 12 (2007): 2471–85, doi:10.1016/j.composites.2007.08.002.

[14] Y.a Tao et al., "Nickel-Cobalt Double Hydroxides Microspheres with Hollow Interior and Hedgehog-like Exterior Structures for Supercapacitors," *Journal of Materials Chemistry* 22, no. 44 (2012): 23587–92, doi:10.1039/c2jm35263j.

[15] Neikov, O. D., et al. (2009). Handbook of non-ferrous metal powders: technologies and applications, Elsevier. ISBN: 978-1-85617-422-0.

[16] Sperling, L. H. *Introduction to physical polymer science*. 4th ed. Hoboken, N.J.: Wiley, 2006. ISBN 978-0-471-70606-9.

[17] Utracki, Leszek A. a C. A. Wilkie, ed. *Polymer blends handbook*. 2nd ed. New York: Springer, 2014. ISBN 978-94-007-6063-9.
[18] Inoue, T. a S. Kobayashi. A super impact-absorbing polymer alloy by reactive blending of nylon with poly(ethylene-co-glycidyl methacrylate*). Recent Res. Devel. Polymer Science*, 2012. ISBN 978-81-7895-538-4.
[19] M. W. Matsen and R. B. Thompson, "Equilibrium Behavior of Symmetric ABA Triblock Copolymer Melts," *The Journal of Chemical Physics* 111, no. 15 (October 15, 1999): 7139–46, doi:10.1063/1.480006.
[20] McGarry, F.J.; Willner, A.M. Toughening of an epoxy resin by an elastomer second phase, R 68-8, MIT, 1968.
[21] Sultan, J. N.; McGarry, F. J. "Effect of rubber particle size on deformation mechanisms in glassy epoxy", *Polymer Engineering Science* 1973, *13* (1), 29–34.
[22] Eugene B. Caldona et al., "A Review on Rubber-Enhanced Polymeric Materials," *Polymer Reviews* 57, no. 2 (2016): 1–28, doi:10.1080/15583724.2016.1247102.
[23] A. Ozturk, C. Kaynak, and T. Tincer, "Effects of Liquid Rubber Modification on the Behaviour of Epoxy Resin," *European Polymer Journal* 37, no. 12 (2001): 2353–63, doi:10.1016/S0014-3057(01)00158-6.
[24] Raju Thomas et al., "Miscibility, Morphology, Thermal, and Mechanical Properties of a DGEBA Based Epoxy Resin Toughened with a Liquid Rubber," *Polymer* 49, no. 1 (2008): 278–94, doi:10.1016/j.polymer.2007.11.030.
[25] Raju Thomas et al., "Cure Kinetics, Morphology and Miscibility of Modified DGEBA-Based Epoxy Resin - Effects of a Liquid Rubber Inclusion," *Polymer* 48, no. 6 (2007): 1695–1710, doi:10.1016/j.polymer.2007.01.018.
[26] P.P. Vijayan et al., "Effect of Organically Modified Nanoclay on the Miscibility, Rheology, Morphology and Properties of Epoxy/carboxyl-Terminated (Butadiene-Co- Acrylonitrile) Blend," *Soft Matter* 9, no. 10 (2013): 2899–2911, doi:10.1039/c2sm27386a.
[27] Makoto Imanaka, Satoshi Motohashi, and Kazuaki Nishi, "Fracture Behavior of Epoxy Resins Modified with Liquid Rubber and Cross-Linked Rubber Particles under Mode I Loading," *Polymers & Polymer Composites* 29, no. 6 (2009): 45–55, doi:10.1016/j.ijadhadh.2007.11.004.
[28] Stephan Sprenger, "Epoxy Resins Modified with Elastomers and Surface-Modified Silica Nanoparticles," *Journal of Materials Science* 49, no. 6 (2014): 2391–2402, doi:10.1007/s10853-013-7963-8.
[29] Lian Wang et al., "Investigations on the Morphologies and Properties of Epoxy/acrylic Rubber/nanoclay Nanocomposites for Adhesive Films," *Composites Science and Technology* 93, no. 1 (2014): 46–53, doi:10.1016/j.compscitech.2013.12.023.
[30] Viju Susan Mathew et al., "High Performance HTLNR/epoxy Blend-Phase Morphology and Thermo-Mechanical Properties," *Journal of Applied Polymer Science* 125, no. 1 (2012): 804–11, doi:10.1002/app.35446.
[31] Viju Susan Mathew et al., "Epoxy Resin/liquid Natural Rubber System: Secondary Phase Separation and Its Impact on Mechanical Properties," *Journal of Materials Science* 45, no. 7 (2010): 1769–81, doi:10.1007/s10853-009-4154-8.

[32] Hamidreza Ali-Asgari Dehaghi et al., "Thermal and Morphological Characteristics of Solution Blended epoxy/NBR Compound," *Journal of Thermal Analysis and Calorimetry* 114, no. 1 (2013): 185–94, doi:10.1007/s10973-012-2920-3.

[33] Soo Jin Park et al., "Synthesis of a Novel Siloxane-Containing Diamine for Increasing Flexibility of Epoxy Resins," *Materials Science and Engineering A* 399, no. 1–2 (2005): 377–81, doi:10.1016/j.msea.2005.04.020.

[34] Sarah Sobhani, Ali Jannesari, and Saeed Bastani, "Effect of Molecular Weight and Content of PDMS on Morphology and Properties of Silicone-Modified Epoxy Resin," *Journal of Applied Polymer Science* 123, no. 1 (January 5, 2012): 162–78, doi:10.1002/app.34435.

[35] Jyotishkumar Parameswaranpillai et al., "Micro Phase Separated Epoxy/poly(ε-Caprolactone)-Block-Poly(dimethyl Siloxane)-Block-Poly(ε-caprolactone)/4,4′-Diaminodiphenylsulfone Systems: Morphology, Viscoelasticity, Thermo-Mechanical Properties and Surface Hydrophobicity," *Polymer Testing* 55, no. 8 (2016): 115–22, doi:10.1016/j.polymertesting.2016.08.016.

[36] St Lin and Sk Huang, "Thermal Degradation Study of Siloxane-DGEBA Epoxy Copolymers," *European Polymer Journal* 33, no. 3 (1997): 365–373, http://www.sciencedirect.com/science/article/pii/S0014305796001759.

[37] J. Chen et al., "The Mechanical Properties and Toughening Mechanisms of an Epoxy Polymer Modified with Polysiloxane-Based Core-Shell Particles," *Polymer (United Kingdom)* 54, no. 16 (2013): 4276–89, doi:10.1016/j.polymer.2013.06.009.

[38] Erich D. Bain et al., "Failure Processes Governing High-Rate Impact Resistance of Epoxy Resins Filled with Core-shell Rubber Nanoparticles," *Journal of Materials Science* 51, no. 5 (2016): 2347–70, doi:10.1007/s10853-015-9544-5.

[39] Sayed Rasoul Mousavi and Iraj Amiri Amraei, "Toughening of Dicyandiamide-Cured DGEBA-Based Epoxy Resin Using MBS Core-Shell Rubber Particles," *Journal of Composite Materials* 49, no. 19 (2014): 2357–63, doi:10.1177/0021998314545338.

[40] Y. Rostamiyan and A. B. Fereidoon, "Preparation, Modeling, and Optimization of Mechanical Properties of epoxy/HIPS/silica Hybrid Nanocomposite Using Combination of Central Composite Design and Genetic Algorithm. Part 1. Study of Damping and Tensile Strengths," *Strength of Materials* 45, no. 5 (2013): 619–34, doi:10.1007/s11223-013-9499-1.

[41] Amir Bahrami et al., "Synergistic Local Toughening of High Performance Epoxy-Matrix Composites Using Blended Block Copolymer-Thermoplastic Thin Films," *Composites Part A: Applied Science and Manufacturing* 91, no. 9 (2016): 398–405, doi:10.1016/j.compositesa.2016.08.038.

[42] Bejoy Francis et al., "Cure Kinetics, Morphological and Dynamic Mechanical Analysis of Diglycidyl Ether of Bisphenol-A Epoxy Resin Modified with Hydroxyl Terminated Poly(ether Ether Ketone) Containing Pendent Tertiary Butyl Groups," *Polymer* 47, no. 15 (2006): 5411–19, doi:10.1016/j.polymer.2006.05.029.

[43] Mohammad T. Bashar, Uttandaraman Sundararaj, and Pierre Mertiny, "Morphology and Mechanical Properties of Nanostructured Acrylic Tri-Block-Copolymer Modified Epoxy," *Polymer Engineering & Science* 54, no. 5 (May 2014): 1047–55, doi:10.1002/pen.23648.

[44] M Miwa et al., "Volume Fraction and Temperature Dependence of Mechanical Properties of Silicone Rubber Particulate/epoxy Blends," *Composites* 26, no. 5 (1995): 371–77, doi:10.1016/S0010-4361(06)80136-9.

[45] Tao Wang et al., "Acrylate Copolymers as Impact Modifier for Epoxy Resin," *Journal Wuhan University of Technology, Materials Science Edition* 30, no. 6 (2015): 1210–14, doi:10.1007/s11595-015-1297-0.

[46] P. Van Velthem et al., "Morphology and Fracture Properties of Toughened Highly Crosslinked Epoxy Composites: A Comparative Study between High and Low Tg Tougheners," *Composites Part B: Engineering* 101, no. 7 (2016): 14–20, doi:10.1016/j.compositesb.2016.06.076. *Composites Part B: Engineering* 101, no.7 (2016): 10.1016/j.compositesb.2016.06.076

[47] M. Gonzalez et al., "Crosslinking of Epoxy-Polysiloxane System by Reactive Blending," *Polymer* 45, no. 16 (2004): 5533–41, doi:10.1016/j.polymer.2004.05.059.

[48] Huai-Ping Cong et al., "Flexible Graphene–polyaniline Composite Paper for High-Performance Supercapacitor," *Energy & Environmental Science* 6, no. 4 (2013): 1185, doi:10.1039/c2ee24203f.

[49] Tianyu Liu et al., "Polyaniline and Polypyrrole Pseudocapacitor Electrodes with Excellent Cycling Stability," *Nano Letters* 14, no. 5 (May 14, 2014): 2522–27, doi:10.1021/nl500255v.

[50] Hongjie Tang et al., "Growth of Polypyrrole Ultrathin Films on MoS 2 Monolayers as High-Performance Supercapacitor Electrodes," *Advanced Materials* 27, no. 6 (February 2015): 1117–23, doi:10.1002/adma.201404622.

[51] J. Vilčáková et al., "'Switching Effect' in Pressure Deformation of Silicone Rubber/polypyrrole Composites," *Synthetic Metals* 146, no. 2 (2004): 121–26, doi:10.1016/j.synthmet.2004.04.028.

[52] Teahoon Park et al., "Flexible PEDOT Electrodes with Large Thermoelectric Power Factors to Generate Electricity by the Touch of Fingertips," *Energy & Environmental Science* 6, no. 3 (2013): 788, doi:10.1039/c3ee23729j.

[53] Gul, V.E. *Structure and Properties of Conducting Polymer Composites*. Utrecht: VSP, 1996. ISBN 9067642045.

[54] Ye.P. Mamunya et al., "Electrical and Thermal Conductivity of Polymers Filled with Metal Powders," *European Polymer Journal* 38, no. 9 (September 2002): 1887–97, doi:10.1016/S0014-3057(02)00064-2.

[55] Burmistr M. V. et al., 2005; Structure, thermal properties and ionic conductivity of polymeric quarternary ammonium salts (polyionenes) containing ethylene oxid and aliphatic chain fragments; *Solid State Ionics*; 176, no. 1 (2005): 1787-1792.

[56] Katz, Harry S. a John V. Milewski. *Handbook of fillers for plastics*. New York: Van Nostrand Reinhold Co., 1987. ISBN 0442260245.

[57] Zweifel, Hans, et. al. *Plastics additives handbook*. 6th ed. /. Cincinnati, Ohio: Hanser Publications, c2009. ISBN 978-1569904305.

[58] Shante, Vinod K.S. a Scott Kirkpatrick. An introduction to percolation theory. *Advances in Physics* [online]. 2006, **20**(85), 325-357 [cit. 2017-05-09]. DOI: 10.1080/00018737100101261

[59] Kazantseva, N.E., et. al. Promising materials for microwave absorbers. *Journal of Communications Technology and Electronics*, 2003, vol. 48, no. 2, p. 173-184.

[60] Lopatin, A.V., et.al. The efficiency of application of magnetic polymer composites as radio-absorbing materials. *Journal of Communications Technology and Electronics*, 2008, vol. 53, no. 5, p. 487-496.

[61] Natalia Kazantseva et al.: Tenký širokopásmoý radioabsorbér, Patentové číslo 305 905, Úřad patentového vlastnictví, CZ, 2016.

[62] Gamini P. Mendis et al., "Enhanced Dispersion of Lignin in Epoxy Composites through Hydration and Mannich Functionalization," *Journal of Applied Polymer Science* 132, no. 1 (2014): 1–8, doi:10.1002/app.41263.

[63] S. Montserrat, "Physical Aging Studies in Epoxy Resins. I. Kinetics of the Enthalpy Relaxation Process in a Fully Cured Epoxy Resin," *Journal of Polymer Science Part B: Polymer Physics* 32, no. 3 (1994): 509–22, doi:10.1002/polb.1994.090320312.

[64] Nicolas Causse et al., "Enthalpy Relaxation Phenomena of Epoxy Adhesive in Operational Configuration: Thermal, Mechanical and Dielectric Analyses," *Journal of Non-Crystalline Solids* 387, no. 1 (2014): 57–61, doi:10.1016/j.jnoncrysol.2013.12.028.

[65] Gallagher, Patrick K., et.al. Handbook of thermal analysis and calorimetry. New York: Elsevier, 2003. ISBN 978-0-444-51286-4.

[66] Brown, Roger. Handbook of polymer testing: physical methods. New York: Marcel Dekker, c1999. Plastics engineering (Marcel Dekker, Inc.), 50. ISBN 0-8247-0171-2.

[67] Menard, Kevin P. Dynamic mechanical analysis: a practical introduction. Boca Raton, FL: CRC Press, c2008. ISBN 9781420053128.

[68] Barnes, Howard A. at. al. *An introduction to rheology*. New York: Distributors for the U.S. and Canada, Elsevier Science Pub. Co., 1989. Rheology series, 3. ISBN 0444871403.

[69] Goldstein, Joseph. Scanning electron microscopy and x-ray microanalysis. 3rd ed. New York: Kluwer Academic/Plenum Publishers, c2003. ISBN 978-0-306-47292-3.

[70] Bhattacharya, S. K. a A. C. D. Chaklader. Review on Metal-Filled Plastics. Part1. Electrical Conductivity. *Polymer-Plastics Technology and Engineering* [online]. 2006, **19**(1), 21-51. DOI: 10.1080/03602558208067726.

[71] Van der Pauw, "A Method of Measuring Specific Resistivity and Hall Effect of Discs of Arbitrary Shape," *Philips Res. Rep.* 13, no. 1 (1958): 1–9.

[72] Electronics World: Frequency Dependence: Dielectric Constant and Dielectric Loss. *Electronics World* [online]. [cit. 2017-05-09]. Dostupné z: http://elektroarsenal.net/frequency-dependence-dielectric-constant-and-dielectric-loss.html

[73] Hedvig, Péter. Dielectric spectroscopy of polymers. New York: Wiley, 1977. ISBN 0470367474.

[74] Ehrenstein, Gottfried W. Polymerní kompozitní materiály. V ČR 1. vyd. Praha: Scientia, 2009. ISBN 978-80-86960-29-6.

[75] Sang-Young Kim, Dae-Geun Choi, and Seung-Man Yang, "Rheological Analysis of the Gelation Behavior of Tetraethylorthosilane/ Vinyltriethoxysilane Hybrid Solutions," *Korean Journal of Chemical Engineering* 19, no. 1 (2002): 190–96, doi:10.1007/BF02706894.

[76] Yang Jiao et al., "A Rheological Study of Biodegradable Injectable PEGMC/HA Composite Scaffolds," *Soft Matter* 8, no. 5 (2012): 1499–1507, doi:10.1039/C1SM05786C.
[77] Goodfellow: Catalogue. Goodfellow [online]. [cit. 2017-05-09]. Dostupné z: http://www.goodfellow.com
[78] Harvey Scher and Richard Zallen, "Critical Density in Percolation Processes," *The Journal of Chemical Physics* 53, no. 9 (1970): 3759, doi:10.1063/1.1674565.

LIST OF ABBREVIATIONS

ER	epoxy resin
DGEBA	diglycidyl ether bispenol A
DETA	diethylenetriamine
LED	light-emitting diode
PDMS	polydimethylsiloxane
M_n	number average molar mass
PDI	polydispersity index
DCP	dicumyl peroxide
UV	ultraviolet light
CI	carbonyl iron
$Fe(CO)_5$	iron pentacarbonyl
$Ni(CO)_4$	nickel tetracarbonyl
LCST	lower critical solution temperature
ΔG_m	change of the Gibbs energy of mixing
ΔH_m	change of the enthalpy of mixing
T	temperature
ΔS_m	change of the entropy of mixing
z	lattice coordinate number
N	number of macromolecules
r_1	number of segments in polymer
v_2	volume fraction
ω_{12}	change of internal energy
χ_{12}	mixing parameter
k	Boltzmann constant

Ω	number of possible configurations
V_1	molar volume
δ	solubility parameter
β	lattice constant of entropic origin
ΔE	cohesive energy
V	molar volume of the material
S_{th}	thickness of the surface
b	statistical segment length
γ	surface tension
ΔQ	change of energy
ΔA	change of surface
γ_D	dispersive part of the surface tension
γ_P	polar part of the surface tension
CTBN	carboxyl-terminated acrylonitrile–butadiene rubber
PANI	polyaniline
Ppy	polypyrrol
PEDOT	poly(3,4-ethylenedioxythiophene
σ	conductivity of composite
σ_m	conductivity of matrix
v_c	critical volume concentration of filler
v	volume concentration of filler
q	geometrical constant
σ_0	conductivity of filler
t	geometrical constant
EWA	electromagnetic wave absorbers
FSS	frequency selective surface

DSC	differential scanning calorimetry
E_{k1}	kinetic energy of hammer before impact
E_{k2}	kinetic energy of hammer after impact
E_f	energy needed for fracture
E_{ks}	kinetic energy of pieces of specimen after impact
Q	heat given by impact and friction of pendulum
E_{p1}	potential energy of hammer at the start of test
E_{p2}	potential energy of hammer
ΔE_p	difference between potential energies
A	area of sample
DMA	dynamic mechanical analysis
delta	loss angle
E′	storage modulus
E′′	loss modulus
E*	complex modulus
i	imaginary unit
τ	shear stress
c_1	geometrical constant
M	torque
$\dot{\gamma}$	shear rate
c_2	geometrical constant
ω	angular velocity
SEM	scanning electron microscopy
DCP	direct current
AC	alternating current
G	conductivity

I	electrical current
U	voltage
σ	specific conductance
l	length of conductor
DSC	dielectric spectroscopy
ε*	complex permittivity
ε′	real part of permittivity
ε′′	imaginary part of permittivity
ΔE	dielectric loss angle
T_g	glass transition temperature
PDMS-V	vinyl-terminated polydimethylsiloxane
PDMS-S	polydimethylsiloxane Sylgard 184
n_E	number of epoxy groups
n_H	number of active hydrogens in curing agent
z_E	quantity of epoxy groups in molecule of epoxy resin
m_E	weight of epoxy resin
M_E	molar mass of epoxy resin
z_H	quantity of active hydrogens in molecul of curing agent
m_H	weight of used curing agent
M_H	molar mass of curing agent
ISO	International Organization for Standardization
ER/V	blend of epoxy resin and vinyl-terminated polydimethylsiloxane
ER/S	blend of epoxy resin and polydimethylsiloxane Sylgard 184
Ni(3)	carbonyl nickel particles with diameter 3 μm
Ni(45)	carbonyl nickel particles with diameter 45 μm
f	frequency

LIST OF FIGURES

LIST OF TABLES

LIST OF SCHEMES